Biomechanics of ascending aortic aneurysms: An investigation into 2D strain echocardiography and tensile mechanics to identify at-risk patients

Alexander Emmott

Department of Chemical Engineering

McGill University

Montreal, Québec, Canada

April 2018

A thesis submitted to McGill University in partial fulfillment of the requirements of the degree of Doctor of Philosophy

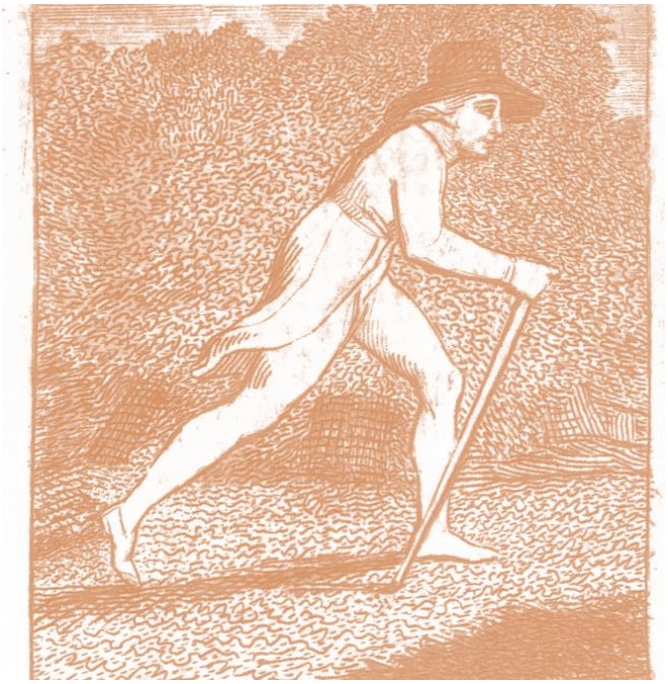

The Traveller hasteth in the Evening.
-William Blake

Acknowledgements

I would like to sincerely thank my supervisor Prof. Richard Leask and my *de facto* co-supervisor Dr. Kevin Lachapelle for their support and encouragement throughout the project. I would also like to thank Dr. Ismail El-Hamamsy for his collaboration with the project, as well as all the members of the Leask Lab.

I've had the privilege of sharing the hallowed halls of McGill with good friends whose patience and support have helped me meet this challenge: Leron Vandsburger, Adamo Petosa, Paul Jonak, Scott Cooper, Karli McDonald, Avital Horowitz and many others.

To my friends back in BC, Allan Corrigal and Michael Turner: thank you both for your support and friendship over the years.

To my parents, Janet and Neil, sister Jen and her husband Tristan: you've always offered me love, patience and support which gives me the confidence to push myself. Thank you.

Finally, to Vanessa: it was with your love and encouragement that I met this challenge.

Funding: The work presented in this thesis was supported by grants from Heart and Stroke Canada and the Canadian Institutes of Health Research (CIHR). I would like to thank the McGill Engineering Doctoral Award (MEDA) and the generous support of Lorne Trottier through the Lorne Trottier Engineering Graduate Fellowship.

Abstract

The aorta is the largest artery in the body and serves as the conduit for systemic blood flow from the heart. Its central property is its passive elastic behaviour that converts fluid energy to elastic potential during systole and subsequently returns that stored potential to maintain systemic circulation during diastole. With disease the pathological remodelling of the wall can result in an impairment of its elastic function, particularly in the case of an aortic aneurysm. If left unrepaired, aortic aneurysms carry significant risk of tearing and often result in death or serious disability. Clinical guidelines for surgical intervention are based on aortic diameter thresholds, but unfortunately these criteria are insufficient and an estimated 40% of dissection and rupture cases occur at diameters below the surgical guidelines. Aortic diameter criteria do not fully relay the risk that elastic impairment and pathological remodelling contribute to dissection or rupture. Herein, this thesis tested the hypothesis that the elastic or mechanical properties of the aortic wall can be used as a marker of ascending aortic dysfunction and contribute added information beyond size to identify at-risk patients.

In this work we used transesophageal echocardiography, an application of ultrasound imaging to the heart and great vessels, to assess the mechanical properties of the ascending aorta and subsequently validated this methodology with *ex vivo* tensile analysis on resected tissue. Specifically, we developed novel *in vivo* stiffness metrics termed the Cardiac Cycle Pressure Modulus (CCPM) and the Cardiac Cycle Stress Modulus (CCSM) that were compared with aortic wall histology and *ex vivo* stiffness and energy loss parameters that have been widely reported, previously. This approach was applied globally (*i.e.*, circumference averaged) and regionally at four distinct foci around the aortic circumference.

Global CCPM and CCSM were significantly predictive of *ex vivo* mechanical indices and histopathology and could be used to identify patients with adverse aortic remodelling who did not meet standard surgical criteria of ≥5.5 cm diameter. Regional analysis demonstrated that heterogeneity in CCPM and CCSM increased with medial degeneration creating uneven distribution of physiological stress in the aortic wall. Furthermore, both tensile and compressive strain patterns were observed simultaneously in neighbouring regions of some patients suggesting a more complex physio-mechanical environment than had previously been appreciated. Ultimately, this work proposes a novel assessment technique to follow patients with ascending aortic aneurysms that may provide a crucial added dimension to surgical management of patients.

Résumé

L’aorte est la plus grosse artère du corps et sert de conduit pour le flux sanguin systémique du cœur. Elle est caractérisée principalement par son comportement élastique passif, au cours de la systole, qui permet de convertir l’énergie des fluides en un potentiel élastique. Lors de la diastole, ce potentiel emmagasiné est utilisé afin de maintenir la circulation systémique. En condition pathologique, la paroi vasculaire subit un remodelage qui peut entraîner une altération de sa fonction élastique telle qu’observée dans les cas d’anévrismes aortiques. Sans traitement, les anévrismes aortiques comportent un risque important de rupture pouvant mener à une invalidité grave ou à la mort. Les lignes directrices cliniques pour l'intervention chirurgicale sont basées sur des seuils de diamètre aortique. Malheureusement, ces critères d’intervention sont de faibles prédicteurs d’incidents puisque environ 40% des cas de dissection et de rupture se produisent à des diamètres inférieurs aux lignes directrices chirurgicales. Le diamètre de l’aorte est un critère insuffisant pour établir la détérioration élastique et le remodelage pathologique du vaisseau contribuant à la dissection et la rupture. Dans le cadre de la présente thèse, nous avons testé l'hypothèse que les propriétés élastiques ou mécaniques de la paroi aortique peuvent être utilisées comme un marqueur de la dysfonction aortique ascendante et contribuer à titre de valeur ajoutée au critère de diamètre afin d’identifier les patients à risque.

Dans le cadre de la présente thèse, nous avons utilisé l'échocardiographie trans-œsophagienne, une technique qui nous permet d’évaluer les propriétés mécaniques de l'aorte ascendante via l'imagerie ultrasonore du cœur et des grands vaisseaux. Nous avons ensuite validé cette méthodologie avec un essai de traction *ex vivo* sur tissu réséqué. Plus

précisément, nous avons développé de nouvelles mesures de rigidité *in vivo* appelées le «Cardiac Cycle Pressure Modulus» (CCPM) et le «Cardiac Cycle Stress Modulus» (CCSM). Ces nouvelles mesures ont été comparées avec différentes techniques bien établies dans la littérature telles que l'histologie, les paramètres de rigidité et les paramètres de perte d'énergie *ex vivo* de la paroi aortique. Cette approche a été appliquée de façon globale (c'est-à-dire, la moyenne de la circonférence) et de façon régionale, soit à quatre foyers distincts de la circonférence aortique. Le CCPM global et le CCSM global ont été significativement prédictifs des indices mécaniques *ex vivo* et de l'histopathologie. Ces mesures pourraient être utilisées pour identifier les patients ayant un remodelage aortique défavorable et qui ne répondraient pas aux critères chirurgicaux standard de ≥5,5 cm de diamètre. L'analyse régionale a démontré que l'hétérogénéité dans le CCPM et le CCSM augmente avec la dégénérescence médiale créant une distribution inégale du stress physiologique dans la paroi aortique. De plus, des profils de déformation à la traction et à la compression ont été observés de façon simultanée dans des régions avoisinantes de l'aorte de certains patients, ce qui suggère un environnement physio-mécanique plus complexe que ce qui a été précédemment signalé. Finalement, la présente thèse propose une nouvelle technique d'évaluation des patients ayant un anévrisme de l'aorte ascendante. Cette technique peut fournir une dimension supplémentaire et cruciale à la gestion chirurgicale des patients.

Table of Contents

List of Figures

Chapter 5

Appendix A

Appendix B

List of Tables

List of Abbreviations

2DSE	**Two-Dimensional Strain Echocardiography**
AA	**Ascending Aorta**
AL	**Anterolateral**
Ao	**Aorta**
BAV	**Bicuspid Aortic Valve**
CCPM	**Cardiac Cycle Pressure Modulus**
CCSM	**Cardiac Cycle Stress Modulus**
CIRC	**Circumferential**
D	**Diameter**
IC	**Inner Curvature**
L	**Current Segment Length**
L_0	**Reference Segment Length (*i.e.*, length at end-diastole)**
LAX	**Longitudinal Axis**
LONG	**Longitudinal**
Max ΔCCPM	**Maximum Nearest-Neighbour Regional Difference in CCPM**
Max ΔCCSM	**Maximum Nearest-Neighbour Regional Difference in CCSM**
MMP	**Matrix Metalloproteinase**
MPa	**Megapascal (1 MPa=1×10^6 Pascals)**
OC	**Outer Curvature**
P	**Pressure**
PL	**Posterolateral**

RAD	**Radial**
SAX	**Short Axis (*i.e.*, transverse axis)**
SEM	**Standard Error of the Mean**
TAV	**Tricuspid Aortic Valve**
TEE	**Transesophageal Echocardiography**
TTE	**Transthoracic Echocardiography**
β	**Stiffness Index**
ε	**Strain**
λ	**Stretch**
σ	**Stress**
τ	**Wall thickness**
φ	**Phase Shift (Blood Pressure Wave)**

Contribution of Authors

In this section the contributions of each author are described for the four manuscripts presented in this thesis.

Article 1 (Chapter 3) - Biomechanics of the ascending thoracic aorta: a clinical perspective on engineering data

Contributions:

Alexander Emmott – researched and wrote the review, prepared figures and contributed to the response to reviewers.

Justine Garcia – contributed to the research and writing as well as the preparation of figures.

Jennifer Chung – contributed to editing the manuscript, provided clinical feedback.

Kevin Lachapelle – helped plan the manuscript and contributed to editing the manuscript, provided clinical feedback.

Ismail El-Hamamsy – contributed to editing the manuscript, provided clinical feedback.

Rosaire Mongrain – contributed to editing the manuscript.

Raymond Cartier – contributed to editing the manuscript, provided clinical feedback.

Richard L. Leask – funded the work, helped plan the manuscript and contributed to editing the manuscript as well as the response to reviewers.

Article 2 (Chapter 5) - Transesophageal echocardiographic strain imaging predicts aortic biomechanics: Beyond diameter

Contributions:

Alexander Emmott – performed the experiments, analyzed and interpreted the data, wrote and edited the manuscript and completed the response to reviewers.

Haitham Alzahrani – contributed to obtaining patient consent, assisted with experiments and reviewed the manuscript.

Mohammed Alreshidan – contributed to consenting the patients, reviewed the manuscript.

Judith Therrien – reviewed and edited the manuscript.

Richard L. Leask – co-directed the research, provided funding and contributed to editing and revising the manuscript.

Kevin Lachapelle – surgeon, co-directed the research, provided funding and contributed to editing and revising the manuscript.

Article 3 (Chapter 6) – Measuring non-uniform wall motion and regional biomechanics of the ascending aorta using transesophageal echocardiography

Contributions:

Alexander Emmott – performed the experiments, analyzed and interpreted the data, wrote and edited the manuscript and completed the response to reviewers.

Haitham Alzahrani – contributed to obtaining patient consent, assisted with experiments and reviewed the manuscript.

Judith Therrien – reviewed and edited the manuscript.

Kevin Lachapelle – surgeon, co-directed the research, provided funding and contributed to editing and revising the manuscript.

Richard L. Leask – co-directed the research, provided funding and contributed to editing and revising the manuscript.

Article 4 (Appendix A) – Histopathological and biomechanical properties of the aortic wall in 2 cases with chronic Type A aortic dissection.

Contributions:

Alexander Emmott – performed the experiments, analyzed and interpreted the data, wrote and edited the manuscript and completed the response to reviewers.

Ismail El-Hamamsy – surgeon, provided clinical notes, contributed to editing and revising the manuscript.

Richard L. Leask– directed the research, provided funding and contributed to editing and revising the manuscript.

Publications

Manuscripts published in refereed journal

As first author

1. Emmott, A., Alzahrani, H., Alreshidan M., Therrien, J., Leask, R.L., Lachapelle, K. Transesophageal echocardiographic strain imaging predicts aortic biomechanics: Beyond diameter. *Journal of thoracic and cardiovascular surgery.* 2018 (In press)
2. Emmott, A., El-Hamamsy, I., Leask, R.L. Histopathological and biomechanical properties of the aortic wall in 2 cases with chronic Type A aortic dissection. *Cardiovascular pathology*. 2017;29:48-52. doi: 10.1016/j.carpath.2017.05.006.
3. Emmott, A., Garcia, J., Chung, J., Lachapelle, K., El-Hamamsy, I., Mongrain, R., Cartier, R., Leask, R.L. Biomechanics of the ascending thoracic aorta: a clinical perspective on engineering data. *Canadian journal of cardiology*. 2016;32(1):35-47. doi: 10.1016/j.cjca.2015.10.015.

As co-author

4. Alreshidan, M., Shahmansouri, N., Chung, J., Lash, V., Emmott, A., Leask, R.L., Lachapelle, K. Obtaining the biomechanical behavior of ascending aortic aneurysm via the use of novel speckle tracking echocardiography. *Journal of thoracic and cardiovascular surgery.* 2017;153(4):781-788. doi: 10.1016/j.jtcvs.2016.11.056.
5. Shahmansouri, N., Alresidan, M., Emmott, A., Lachapelle, K., Cartier, R., Leask, R.L., Mongrain, R. Evaluating ascending aortic aneurysm tissue toughness: dependence on

collagen and elastin contents. *Journal of mechanical behavior of biomedical materials*. 2016;64:262-71. doi: 10.1016/j.jmbbm.2016.08.006.

6. Shahmansouri, N., Alresidan, M., Emmott, A., Lachapelle, K., El-Hamamsy, I., Cartier, R., Leask, R.L., Mongrain, R. Investigation on the regional loss factor and its anisotropy for aortic aneurysms. *Materials (Basel)*. 2016;9(11). pii: E867. doi: 10.3390/ma9110867.
7. Mort, J.S., Beaudry, F., Théroux, K, Emmott, A., Richard, H., Fisher, W., Lee, E.R., Poole, A.R., Laverty, S. Early cathepsin K degradation of type II collagen in vitro and in vivo in articular cartilage. *Osteoarthritis and cartilage*. 2016;24(8):1461-9. doi: 10.1016/j.joca.2016.03.016.
8. Dionne, P.O., Wener, E., Emmott, A., Cartier, R., Mongrain, R., Leask, R.L., El-Hamamsy, I. The Ross procedure: biomechanical properties of the pulmonary artery according to aortic valve phenotype. *Interactive Cardiovascular Thoracic Surgery*. 2016;23(3):371-6. doi: 10.1093/icvts/ivw148.

Manuscript submitted to refereed journal

1. Emmott, A., Alzahrani, H., Therrien, J., Lachapelle, K., Leask, R.L. Measuring non-uniform wall motion and regional biomechanics of the ascending aorta using transesophageal echocardiography. *Journal of thoracic and cardiovascular surgery*. (submitted April 2018)

Chapter 1: Introduction

Aneurysm of the ascending aorta (AA) is an insidious disease that often is asymptomatic prior to catastrophic failure. It is estimated that AA aneurysms effect ~10 persons per 100,000 person-years[1]. Approximately 60% of thoracic aortic aneurysms involve the aortic root and/or AA[2, 3]. When identified, prophylactic replacement of the AA is undertaken to prevent dissection or rupture of the aortic wall which would otherwise result in haemorrhage, tamponade and death. The current guidelines recommend replacement for AA diameters exceeding 5.5 cm[4-6]. In this regard, aortic diameter is used as a surrogate of the overall mechanical properties of the vessel. This is a very simplistic and fundamentally ignores the well-documented remodelling of the vessel microstructure that occurs[7-9]. In fact, AA dissections−localized acute tearing of the vessel wall−often occur below the surgical threshold of 5.5cm suggesting that size alone is insufficient to describe the mechanical integrity of the tissue[10-12].

Ex vivo mechanical testing of resected aortic tissues has been used to directly identify mechanical dysfunction of the vessel wall, including tensile strength, stiffness and energy loss. These *ex vivo* tensile measurements are reproducible, yet they are inappropriate for patient management since mechanical dysfunction can only be identified retrospectively. *In vivo* methods using clinical imaging modalities could allow these measurements to be pivoted from a postoperative to a preoperative assessment by measuring local physiological strain in the clinic. Echocardiography has shown considerable potential due to its low scan time and excellent temporal resolution without the need to expose patients to contrast dyes or radiation. Several studies have used echo-based stiffness parameters to estimate the elastic

properties of the AA[13-17]; however, these methodologies have not been validated against *ex vivo* tensile data or prospectively tested to improve patient outcome. Furthermore, these estimates have ignored the heterogeneity in local *in vivo* strain profiles which may be fundamental to the mechanical risk criteria of the aorta.

With the potential of applying mechanical criteria to clinical assessment of aortopathy, it is of significant interest to further develop echo-based estimates of biomechanical function. A robust and repeatable methodology is central to this process. Validating these methods against *ex vivo* data and current size criteria is necessary to better understand future clinical implementations of echo-based strain estimates or aortic biomechanics.

Chapter 2: Objectives

The underlying research question of this thesis asks if echocardiography-based mechanical measures of the ascending aorta can aid in clinical patient management. The central hypothesis is that echocardiography-based biomechanical metrics are reliable *in vivo* surrogates of the mechanical properties of the ascending aorta. To test this hypothesis, transesophageal echo and blood pressure tracing of patients undergoing elective aortic replacement were used to generate global and regional *in vivo* stiffness moduli. *Ex vivo* mechanical testing and histological analysis was used as a standard to compare these measurements. The hypothesis was tested through the following objectives:

Objective 1: Using clinically available echocardiographic strain imaging and blood pressure tracing, develop robust metrics (*i.e.*, stiffness moduli) that estimate ascending aortic mechanical properties *in vivo*.

Objective 2: Evaluate the echocardiographic-derived metrics in a cohort of patients with a range of clinical ascending aortic aneurysm severity (by aortic diameter) to compare their effectiveness at identifying mechanical dysfunction and pathological tissue remodelling defined by *ex vivo* analysis of the surgically removed tissue.

Objective 3: Evaluate the regional variation in echo-derived metrics (around the aortic circumference) to identify mechanics/deformation heterogeneity *in vivo* and compare these estimates with regional *ex vivo* mechanics and histopathology.

Chapter 3: Biomechanics of the Ascending Thoracic Aorta: A Clinical Perspective on Engineering Data

3.1 Preface

This chapter was published as an invited review article in The Canadian Journal of Cardiology (2016) on the topic of biomechanics of the ascending aorta. The objective of this review was to present a comprehensive overview of *i*) the structural properties of the ascending aorta, *ii*) methodological concepts in tensile analysis, and *iii*) the evolution of the tensile properties in states of disease. With a primary CJC readership of cardiac surgeons and cardiologists, this review aimed to present these concepts in a clinical context.

With respect to the research presented in this thesis, this review introduces concepts in aortic structure and anatomy that provide insight into histological interpretation of aortic specimens. Furthermore, this chapter reviews important findings that substantiate the paradigm that mechanical properties−including energy loss and stiffness−are altered in states of disease (*e.g.*, degenerative aneurysm) and can be reliably measured by tensile testing of the vessel wall. Finally, this chapter introduces concepts in medical strain imaging. However, concepts pertaining to strain imaging using echocardiography were limited to a general discussion and therefore are elaborated in the proceeding chapter (Chapter 4).

3.2 Article

Biomechanics of the Ascending Thoracic Aorta: A Clinical Perspective on Engineering Data

Alexander Emmott[a,c], Justine Garcia[b,c], Jennifer Chung[d], Kevin Lachapelle[d], Ismaïl El-Hamamsy[c], Rosaire Mongrain[b,c], Raymond Cartier[c] and Richard L. Leask[a,c]

[a]Department of Chemical Engineering, McGill University, Montreal, QC

[b]Department of Mechanical Engineering, McGill University, Montreal, QC

[c]Montreal Heart Institute, Montreal, QC

[d]Department of Surgery, Royal Victoria Hospital, Montreal, QC

Address of corresponding author

Richard L. Leask, PhD, PEng, Department of Chemical Engineering, McGill University, 3610 University St., Montreal, Quebec H3A 0C5, Tel: 1-514-398-4270, Fax: 1-514-398-6678, E-mail: richard.leask@mcgill.ca

3.3 Abstract

Aneurysms of the ascending thoracic aorta often require prophylactic surgical intervention to resect and replace the aortic wall with a synthetic graft to avoid the risk of dissection or rupture. The main criterion for surgical intervention is the size of the aneurysm, with elective surgery recommended above a maximal aortic diameter of 4.2-5.5 cm depending on valve type and other patient risk factors. Although the risk of dissection and rupture increases with the size of aneurysm, different pathologies, including aortic valve phenotype and connective tissue disorders uniquely influence the mechanical dysfunction of the aortic wall. Dissection and rupture are mechanical modes of failure caused by an inability of the tissue to withstand local tissue stresses. Tensile testing of aortic tissues, therefore, has been used to reveal the mechanical parameters of diseased and healthy tissues to better characterize the mechanical function of aortic tissues in different patient groups. In this review, we highlight the principles and methods of *ex vivo* tensile analysis as well as the composition and structural properties that contribute to the mechanical behaviour of the ascending aorta. We also present a clinically oriented description of mechanical testing along with insight into the characterization of aneurysm. Finally, we highlight recent advances in echocardiography, CT and MRI that have the potential to measure biomechanical properties non-invasively and therefore help select aortas at risk.

3.4 Introduction

Aneurysms of the thoracic aorta have an incidence of approximately 10.4 per 100,000 person-years [1]. Aneurysms are often asymptomatic until they undergo dissection or rupture resulting in catastrophic haemorrhage, tamponade and death. For those patients lucky enough to make it to a hospital after a dissection or rupture, the in-hospital mortality (41%) is bleak [18]. Such non-elective ascending aorta replacements have an operative mortality of 15-24% while elective replacement is much safer with an estimated operative mortality of 3.4% [19, 20]. It is therefore not surprising that the number of prophylactic ascending thoracic aorta replacements has risen significantly in the past decade. The number of aortic replacements will continue to increase due to our aging population and improved cardiac imaging [21].

Approximately 60% of thoracic aortic aneurysm (TAA) involve the aortic root and/or ascending aorta [2, 3]. Elective aortic resection and replacement by a synthetic graft is recommended at maximum ascending aortic diameters ranging from 4.2-5.5 cm, depending on etiology and need for concomitant cardiac surgery [4-6]. This metric of aortic size is derived from population studies demonstrating a hinge point rise in rates of complications above a diameter of 6 cm [22]. The underlying biomechanical principle inferred is Laplace's Law which states that the mechanical stresses increase in the vessel wall in proportion to the vessel diameter. This is very simplistic and fundamentally ignores the well documented remodelling of the vessel microstructure that occurs [7-9]. In fact, ascending TAA dissections often occur below the surgical threshold diameters suggesting that size alone is insufficient to describe the mechanical integrity of the tissue [10-12]. Recent reports have suggested the diameter cutoffs may be an overly aggressive approach and are almost certainly putting some patients

unnecessarily at risk of operative and early morbidity [23, 24,25]. Understanding aortic biomechanics of TAA is key not only to better patient stratification for surgery but also to elucidating the mechanobiology of this deadly pathology [26].

Ultimately, the cause of dissection or rupture in the ascending TAA is a mechanical failure of the vessel wall where the local stresses in the tissue exceed the mechanical integrity of the vessel. Mechanical testing of human tissue allows one to categorize and understand human tissues using the same engineering parameters that allow us to understand the mechanical behaviours of materials. In this article, we present the structural components and changes of the thoracic aorta, mechanical principles behind current surgical guidelines and testing methods that are currently used to characterize aortic tissues. We then review the state of our understanding of the structural and tensile properties of the ascending thoracic aorta (see the article addenda for a comprehensive list of values, **Table 3.S.1**) and currently available *in vivo* estimates of TAA biomechanics. In doing so, we hope to provide insight into the behaviour of normal and abnormal aortic tissue mechanics, which may provide a better framework than size alone in selecting patients for surgery.

3.5 Mechanical Structure of the Ascending Aorta

3.5.1 Normal Structure of the Ascending Aorta

The ascending aorta is the primary conduit for blood flow and the largest artery in the body. The ascending aorta contains three tissue layers: the intima, lined by a single layer of endothelial cells, the elastic media and the largely collagenous adventitia. The elastic media dominates the mechanical response of the ascending aorta, accounting for ~80% of the vessel thickness in normal ascending aortas. The media is comprised of alternating concentric layers of fenestrated elastic sheets, *lamellae*, and smooth muscle cells (SMCs) [27], **Figure 3.1-A**. Within these sheets are interspersed collagens (types I, III, IV and V), mucopolysaccharides and an abundance of fibrillar matrix proteins [27, 28]. The elastic lamellae and collagen fibrils define the passive elastic behaviour and largely the tensile strength of the tissue, respectively [29]. A mechanically normal ascending aorta, characterized by its distension and recoil, allows the vessel to store energy from systole and redistribute it during diastole by elastic recoil to provide forward flow—this is known as the *Windkessel effect* [30] and is vital to maintaining normal pulse pressure.

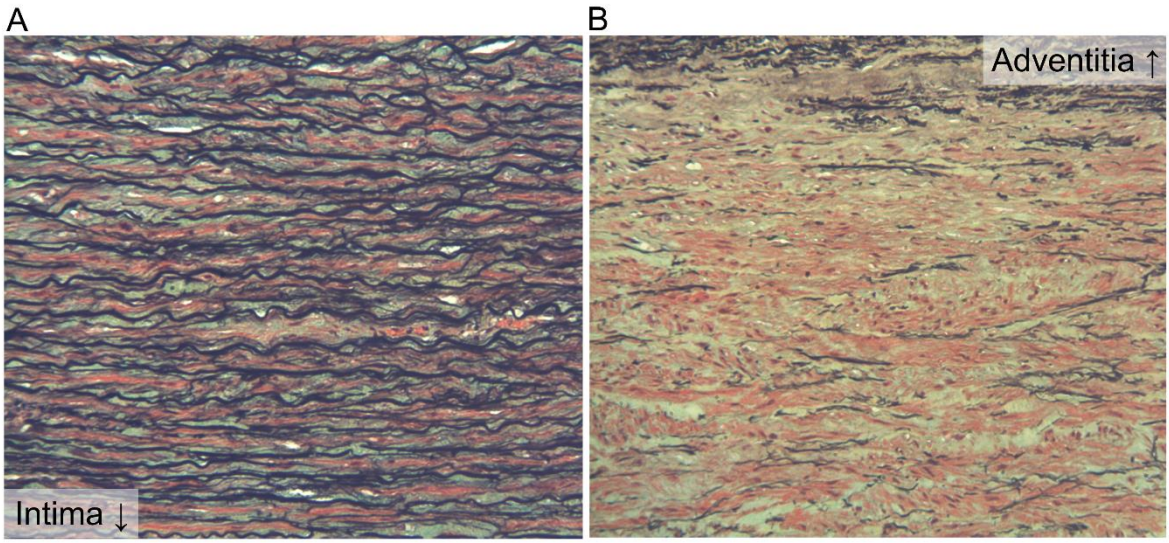

Figure 3.1. Histopathology of the ascending aorta using Movat pentachrome staining in A) a 52 year old male with a non-dilated ascending aorta and B) a 51 year old male with a 5.8 cm dilated ascending TAA. Black – elastin, Red/Purple – smooth muscle cells, Blue – mucopolysaccharides and, Yellow – collagens.

The aortic wall is a dynamic composite structure consisting of matrix macromolecules and vascular cells. Each component has a role in defining the structure of the tissue and, therefore, a disruption of these components may change the mechanical behaviour of the vessel wall. Here, we highlight the mechanical role of the components whose relative amounts and organization are believed to have the greatest influence on the degenerative pathology of ascending TAAs.

3.5.2 Component Mechanical Properties

Role of Elastin

Elastic fibres are highly extensible networks of cross-linked elastin that provide elastic-energy storage in tissues [31]. The compliant behaviour of elastic fibres is largely derived from the random-coil conformation that can unravel when stretched. In vascular tissue, soluble tropoelastin molecules are secreted by SMCs and assembled into covalently cross-linked elastic sheets that are highly hydrophobic. Elastin molecules have a relatively low stiffness (*i.e.*, elastic modulus) and large extensibility of approximately 1.1 MPa and 150%, respectively [31]. In the aorta, elastin behaviour defines the compliance of the tissue under low and moderate levels of strain [32].

Role of Collagens

Collagen types I and III represent over 80% of the total collagen found in the aorta [28] and are the primary load-bearing fibrils of the ascending aorta. Type IV and V collagens are also present in the basement membranes of endothelial cells and SMCs in the aortic wall. Collagens have a large stiffness modulus of approximately 1,200 MPa (approximately 1,000x greater than elastin) and a low extensibility of 13% [31]. Collagens have a distributed circumferential alignment [33], which results in increased maximum tissue stiffness in the circumferential direction over the longitudinal axis. However, collagens are believed to be mechanically engaged only at large strain due to their crimped nature and contribute to the large non-linear increase in tissue stiffness. As a result, it is believed that collagen's role is to reinforce and provide strength to the wall to avoid rupture of the comparatively weak

elastic fibres [31]. A study considering the stress-strain response of collagenase-treated thoracic aortas demonstrated marked tissue softening only above moderate stretch ratios ($\lambda \approx 1.3$) [32].

Role of Smooth Muscle Cells

SMCs are the main resident cell type of the aortic elastic media and have a dynamic phenotype with both contractile and secretory properties. SMCs express both matrix proteins (including elastin and collagens) as well as enzymes involved in ECM catabolism, such as matrix-metalloproteinases (MMPs), in response to cyclic strain [34-36] and cytokines like transforming growth factor-β1 (TGF- β1) [37, 38]. SMCs are generally aligned circumferentially [39]; however, the angle of orientation can change in response to tension forces in the vascular wall and, by measuring the contractile behaviour of SMCs in the ascending aorta, the regional orientation may change up to 20-30° from the circumferential axis [40].

A recent hypothesis suggests that a disruption in the contractile apparatus within SMCs may alter aortic wall homeostasis and contribute to inheritable thoracic aortic aneurysm and dissection (TAAD) [37, 41]. In particular, mutations have been identified in the genes that encode for cytoskeletal α-actin and β–myosin (ACTA-2 and MYH11, respectively), which form the intracellular assembly of the cytoskeleton-receptor-ECM complex [37, 41].

Role of Mucopolysaccharides

Focal pooling of mucopolysaccharides (also termed glycosaminoglycans) is characteristic of medial degeneration of the aorta. It is believed that mucopolysaccharide accumulation in the medial layer can cause increased tissue swelling that ultimately decouples the elastic fibres

from their collagen support (delamination) [42]. This disruption of the lamellae is believed to lead to increased levels of tissue dissection.

3.5.3 Tissue Remodelling of the Ascending Aorta with Age and Disease

The Aging Aorta

The aorta naturally dilates over time at a rate of approximately 0.15 mm/year [43, 44]. The effect of age on aortic wall thickness is less clear as it has been reported to either increase [45] or remain constant [44] over time. However, even preserved thickness with dilation requires an increase in total aortic tissue mass. As a result, the concentration of aortic elastin decreases by approximately one third over eight decades of life [46, 47]. The total mass of elastin likely remains constant in the ascending aorta and the decrease in concentration can be explained by increased collagen deposition [27]. Age-related fragmentation of the elastic lamellae and increased medial fibrosis have also been noted in normal, non-aneurysmal aortas making it difficult to distinguish the histopathology of aneurysmal tissue from age-matched normal tissue [27, 48-51].

The Effect of Disease

While abdominal aortic aneurysms are generally associated with atherosclerosis, ascending TAAs develop in response to dysfunctional changes in the elastic media of the artery. Classically, aneurysms have been attributed to medial degeneration (formerly termed *cystic medial necrosis* or *cystic medial degeneration* [52]), a non-inflammatory loss of SMCs and fragmentation of the elastic fibres [49, 52], **Figure 3.1-B**. Medial degeneration leading to aneurysm is believed to be an imbalance in the synthesis and degradation of the medial matrix

proteins but, currently, the cause of medial degeneration is still poorly understood. What is clear is that, as the ascending aorta dilates, it continues to lay down new tissue and tries to preserve its thickness which would otherwise decrease with increasing diameter [53, 54]. Although medial thickness may decrease with idiopathic aneurysm [54], total wall thickness usually remains constant [53, 55]. Increasing ECM thickness is likely a response of SMCs to try and maintain mechanical homeostasis [26]. Ascending TAAs may present with some regional variation in aortic wall thickness [53] and in the relative severity of medial degeneration [56, 57].

The cause of ascending TAAs is often considered idiopathic, however several pathological features have been suggested. In certain cases, an imbalance in the medial expression of MMPs, specifically the gelatinases (MMP-2 and MMP-9) and their inhibitors (TIMP-2 and TIMP-1) are believed to result in accelerated proteolytic degradation of elastin and collagen fibres [58]. It is important to note that MMP-2 and -9 are known to have elastolytic and collagenolytic properties [59]. Furthermore, defects in fibrillin-1, a protein found in elastic fibre-associated microfibrils, have been strongly implicated in familial thoracic aortic aneurysm and dissection (TAAD) and is the defining mutation in patients with Marfan Syndrome (MFS) [60]. Also central to MFS (and fibrillin-1 mutations), and other syndromic forms of ascending TAA (mainly Loeys-Dietz syndrome (LDS)), is an increase in TGF-β activity within the ECM, as well as its signalling cascade within the SMCs [37]. Disruption of TGF- β activity is believed to lead to medial fibrosis [61].

Bicuspid Aortic Valve

Bicuspid aortic valve (BAV) is the most common congenital heart defect that affects 1-2% of the population [62] with a male-to-female ratio of approximately 3:1 [63]. The increased incidence of aortic dilatation in BAV patients (estimated at approximately 40% [64]) has led to the hypothesis that there is a common genetic link relating valve phenotype to a weakening of the aortic wall [65]. Studies have found that some BAV patients have a reduced expression of fibrillin-1 [8] and mutations in the FBN1 gene encoding the protein [66], however no consistent genetic link has been discovered to explain the increased prevalence of ascending TAAs in BAV patients.

Aneurysm formation in BAV patients has also been hypothesized to be a result of an altered hemodynamic profile as blood passes through the aortic valve [67]. Bauer *et al.* observed that patients with BAV had significantly greater hemodynamic stresses on the anterolateral wall of the ascending aorta [68] and Hope *et al.* noted that BAV gave rise to eccentric helical hemodynamic flow patterns in the ascending aorta that were not observed with tricuspid aortic valve (TAV) patients [69].

Whether driven by genetics, hemodynamics, or more likely a combination of the two, medial ECM structural proteins and local enzyme expression is distinct in patients with BAV. In particular, elastin and collagen fibres in the ascending aorta are highly aligned in the BAV patients when compared to TAV [70]. Distinct tissue remodelling in BAV patients is characterized by markedly higher expression of medial MMP-2 [8, 70-73] which may explain reported decreases in collagen [70, 74].

Connective Tissue Disorders

Several classes of connective tissue disorders can lead to aneurysms by a disruption of ECM fibril or scaffold proteins. In MFS, an autosomal dominant disorder affecting 2-3 persons per 10,000, there is an identified mutation in the gene encoding fibrillin-1 [75]. Fibrillin-1 is central in elastic fibre assembly as it provides the necessary microfibril scaffold for aggregation and cross-linking of tropoelastin by lysyl oxidase [76, 77]. In addition to its structural role, it is rather its functional role that mainly leads to aneurysm formation. Fibrillin-1 sequesters TGF-β in a latent state in the ECM. Mutations in fibrillin-1 lead to an increase in TGF-β activity, which is the common pathway in LDS [37]. Non-syndromic mutations of fibrillin-1 have been identified in patients with ascending TAAs and may be familial [78, 79]. Similarly, EDS syndrome is a connective tissue disorder that results in aneurysm in response to a mutation in type III collagen [80].

The mechanical dysfunction that results in aneurysm is a result of remodelling of the aortic wall. Maximal aortic diameter is the only epidemiologically derived surrogate of the gross mechanical properties of the vessel. However, diseases of the aorta manifest with notable differences in the underlying wall pathologies. As has been previously described, this is somewhat reflected in the variety of size thresholds used to evaluate intervention but is limited in assuming that aortas of the same size are subjected to the same physiological forces and have the same structural properties. We believe that a more thorough mechanical analysis of human aortas may, in the future, derive more robust mechanical metrics for intervention.

3.6 Ascending Aortic Biomechanics

3.6.1 Aortic Size as a Predictor of Mechanical Stability

Maximal aortic diameter is the primary criterion for surgical resection of the aorta and replacement with a prophylactic graft. It is important to acknowledge that this measure is not a mechanical property, but instead acts as a surrogate for tissue circumferential stress (σ_θ). This mechanical interpretation follows Laplace's law (**Figure 3.2**) which states that the circumferential stress in a vessel simplified by a cylinder with a defined thin wall thickness (τ) is a function of the aortic radius (r) and the pressure exerted on the vessel wall (P) by the following relation:

$$\sigma_\theta = Pr/\tau \qquad 3.1$$

This simple model of tissue stress fundamentally assumes the vessel material is linearly elastic (see next section) and has no directional dependency in its mechanical properties (isotropic). It also assumes the vessel is a uniform, straight cylinder with no other applied stresses other than blood pressure.

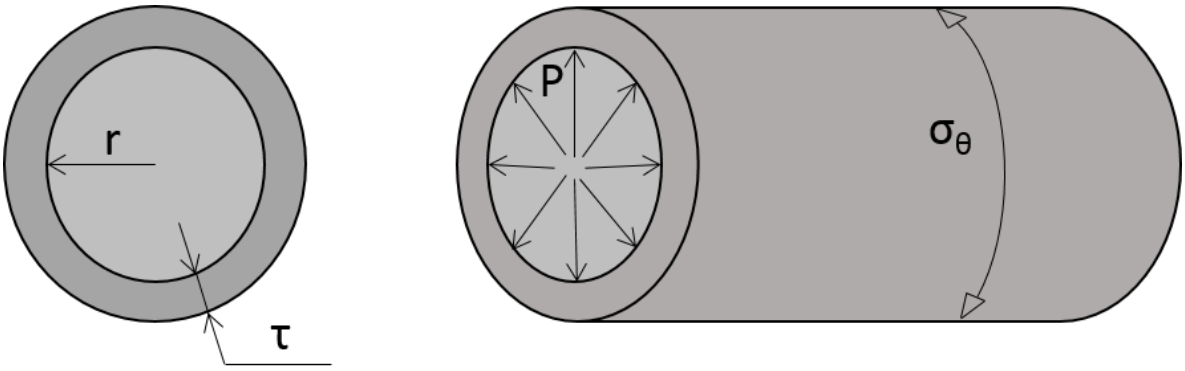

Figure 3.2. Illustration of Laplace's law: Wall tensions (T) in the vessel (simplified by a cylinder with a radius (r) larger than a wall thickness (τ)) when pressure (P) is exerted by the aortic blood flow. P is assumed evenly distributed over the wall.

By this model, the circumferential stress in the vessel wall is then proportional to the size of the aneurysm alone if the tissue thickness and blood pressure remain constant. This suggests that, at exceedingly large aortic diameters the circumferential stress may exceed the ultimate tensile strength of the tissue and rupture may occur. Setting a threshold diameter limit implicitly assumes that all thoracic aortas have the same ultimate strength, thickness and blood pressure.

The thoracic aorta is not a uniform cylinder and the vessel wall thickness, radius and composition are heterogeneous [53, 81] even within the same thoracic aorta. Moreover, the composition changes significantly over time for a given aorta as it remodels and expands in size, changing its mechanical properties and ultimate tensile strength. The nature of the remodelling may vary significantly depending on the disease process, thus the composition, thickness and ultimate tensile strength may be vastly different between aortas of the same

size. Importantly, the equation neglects the significant longitudinal force on the tissue created by the motion of the heart and biaxial coupling between the circumferential and longitudinal direction. As well, it also neglects uneven hemodynamic load that can exist for patients with aortic valve stenosis or BAV [82]. These limitations help explain why up to 50% of ascending aorta dissections occur well below the threshold of intervention [10-12]. To move beyond diameter for patient stratification therefore requires a better understanding of the mechanical properties of TAA tissue.

Linear Elastic (Hookean) Model

The derivation of Laplace's law assumes that the stress-strain relationship is linear, and related by a constant tissue stiffness modulus, also known as the Young's or elastic modulus (E). Although aortic tissue is nonlinear and hyperelastic (see next section), the linear elastic model can describe tissue deformation for small changes in strain. The equation for linear stress-strain is presented as follows:

$$\sigma = E\varepsilon \qquad 3.2$$

where σ and ε are the material stress and strain, respectively. It is well known that vessel stiffness (E) is variable from patient to patient and generally increases with age [83, 84] and with aneurysm [53, 85]. In a stiff rather than a compliant vessel, it is intuitive that wall stress will increase at a much faster rate as the vessel expands. Even with the assumption of linear elasticity, solely using diameter neglects differences in tissue stiffness.

3.6.2 Measuring Aortic Biomechanics

Ex vivo mechanical testing of excised ascending aorta is the "gold standard" for assessing mechanical properties such as tissue stiffness. Healthy aortic tissue is acquired from transplant donors or from autopsy while ascending TAA specimens are acquired during elective surgical repair. Mechanical testing is done within 24-48h and specimens are kept mostly in a refrigerator (4°C) [53, 85-91], a freezer [92, 93] or on ice [94]. Freshness of the sample and techniques to keep the structure intact are major issues. To avoid tissue degeneration, aortas are often kept in saline or gauze at a low temperature. Before running the tests an equilibration at room temperature is required for the tissue. Ideally, due to the temperature dependence of material properties, tests are conducted at body temperature.

The passive biomechanical properties of the aorta are often evaluated by *ex vivo* tensile testing where a sample of aortic tissue is stretched and the corresponding tension in the wall is measured. By measuring this tension along with the amount of stretch (displacement), a stress-strain relationship curve is developed. Vascular tissues, like the ascending thoracic aorta, are hyperelastic materials characterized by a nonlinear relation between stress and strain, **Figure 3.3**. Moreover, vascular tissue is viscoelastic, which results in hysteresis in the tensile testing loop where the stress-strain relation follows different paths when applying load (loading) and removing load (unloading).

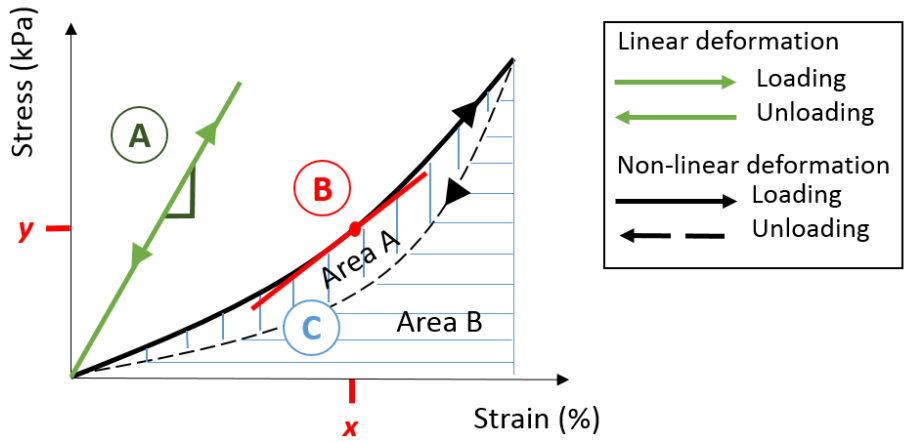

A E: Slope of the linear elastic deformation

B E_m: Slope of the loading curve defined by a red tangent line at ***x*** % strain or ***y*** kPa stress

C Energy loss: $\frac{Area\ A}{Area\ A + Area\ B}$

Figure 3.3. Typical shape of stress-strain curve for linear elastic (Green line) and viscoelastic response of biological tissue (black line). A) Elastic modulus of a linear elastic material, B) Incremental stiffness modulus (E_m) of a non-linear material and C) Energy loss.

These tensile tests can be conducted in a single direction, usually in either a circumferential or longitudinal orientation, and this is called uniaxial tensile testing; or tests can be conducted simultaneously in both the circumferential and longitudinal directions, and this is called biaxial tensile testing. For, uniaxial tensile testing, samples are often cut in rectangular shapes oriented along the desired axis and stretched lengthwise. Uniaxial testing generalizes the behaviour of the sample with two independent pieces, which may have unique structural imperfections and geometrical parameters (*e.g.*, thickness), and can increase analytical errors. It also neglects the transfer of stress from one direction to the other. Therefore biaxial

tensile testing, which considers the tensile properties in two axes simultaneously, is recommended. In this configuration, specimens are cut in squares allowing for testing in two perpendicular axes (**Figure 3.4-A**) and then stretched to obtain the tissue's stress-strain response (**Figure 3.4-B**). Equibiaxial tensile tests are biaxial tests where the tissue is stretched or loaded simultaneously and equally in both axes. This allows for the coupled response of the tissue in both directions to be measured.

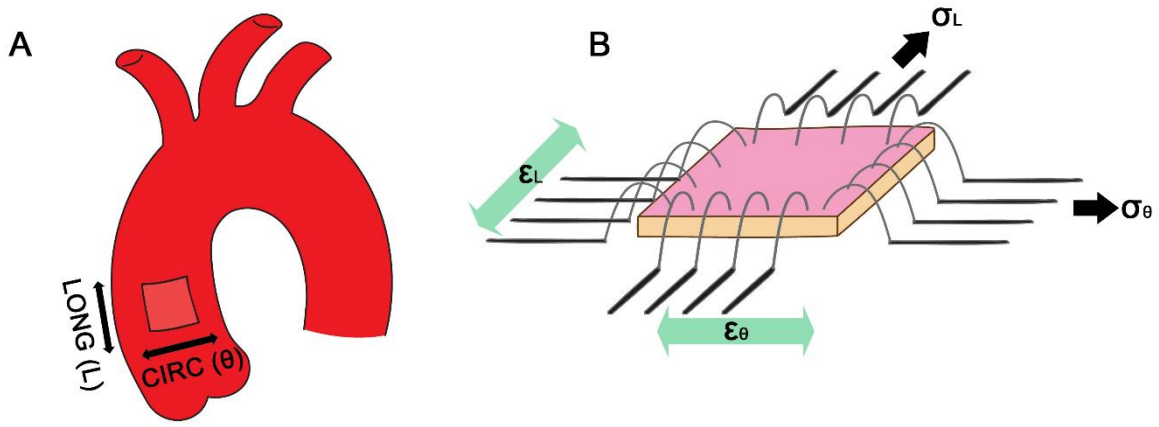

Figure 3.4. Sample isolation and biaxial tensile testing of ascending aortic tissue. A) The sample is obtained from the ascending aorta and prepared with the two testing axes in the circumferential (θ) and longitudinal (L) directions. B) The isolated sample is stretched in the two axes to determine the relation between stress (σ) and strain (ε).

3.6.3 Limitations of *Ex Vivo* Testing

Although *ex vivo* mechanical testing is rigorous and reproducible, there are important limitations. Most importantly, it is a postoperative or post-mortem analysis, as it requires the tissue to be removed from the patient. It is also labour-intensive, which translates to a limited

number of tissue samples in any given study. Thus, interpretations and the conclusions may not be representative of the larger patient population. As can be seen in the **Table 3.S.1**, the number of samples ranges between 6 and 40, which leaves very little room for patient sub-categorizing with any statistical power. Also, ascending TAA tissue is inhomogeneous with regional variations [53, 95, 96]. Most studies neglect this potential variability, especially when a small quantity of tissue is analyzed. Moreover, several tissue samples are sometimes extracted from the same subject, thus the diversity of the patient population and their tissue characteristics remain limited [89, 92]. This can be overcome by systematically sampling labelled quadrants of ascending aorta for each specimen [53, 97].

3.6.4 Tensile Testing Data and Derived Metrics

Currently, there are several families of testing protocols that are used to evaluate the mechanical state of vascular tissues. Here, we focus on the cumulative understanding of the mechanics of ascending aortic tissue using planar tensile testing; however, it is important to acknowledge that other metrics are needed for a holistic understanding of tissue biomechanics.

When interpreting published tensile test data, it is important to note there are multiple definitions of stress and strain or stretch that can be used. A discussion of these definitions is beyond the scope of this article. Notably, however, mechanical testing equipment will record force (F) and displacement. After measuring the tissue thickness and the distance between the grips or sutures, force and displacement can be converted to a variety of stress and strain definitions.

Data Fitting

Unique stress-strain curves composed of loading (stress added) and unloading (stress removed) curves can be generated (**Figure 3.2**). Raw data is generally smoothed for consistency or fitted by a strain energy function that corresponds to the energy stored while stress or stretch is imposed. Many different strain energy functions or constitutive models are used to describe tissue behaviour such as the Fung energy model [92, 98, 99].

Incremental Elastic Modulus (Stiffness)

The incremental elastic modulus (E_m) is the stiffness parameter of a non-Hookean material (*i.e.*, a material with a nonlinear stress-strain relation) and can be thought of as a material's resistance to deformation at a given strain or stress value. E_m, therefore, corresponds to the slope of the stress-strain curve under loading (**Figure 3.3**) and, as it is variable along the curve, must be defined at a specific strain or stress value. Table 1 highlights stiffness values from studies that consider the mechanics of ascending aortas and ascending TAAs. Although general trends can be derived from a study-to-study comparison (for instance, ascending TAAs are generally much stiffer than healthy ascending aortas), stiffness values cannot readily be compared unless they are reported with a similar definition of stress and strain and reported at the same point on the curve.

Table 3.1. Most common mechanical parameters in tensile testing

	References	N	Age (yr)	Size (cm)	Test	E_m (kPa)		Tensile strength (kPa)
Ascending thoracic aorta	[100]	7	51±18	2.4±0.4	**	Engineering strain: 40%	100±30	NA
	[98]	14	47±14	NA	**	Physiological Cauchy stress: 72.8kPa	Circumferential: 988.7±489.7, Axial: 952.1±479.1	NA
	[101]	14	51±6	3.3±0.2	*	Maximum elastic modulus	Circumferential: 3250±630, Axial: 2610±260	Circumferential: 1800±240, Axial: 1710±140
Aneurysm control	[100]	34	64±12	5.2±0.7	**	Engineering strain: 40 %	150±30	NA
	[89]	13	13-75	5.42±0.732	*	Maximum elastic modulus	Circumferential: E_m(G. curv.):8780, E_m(L. curv.):9190, Axial: E_m(G. curv.):5890, E_m(L. curv.):3130	NA
	[99]	6	25±2	NA	*	NA	Loading: 285±164, Unloading: 542±221	NA
	[101]	14	51±6	3.3±0.2	*	Maximum elastic modulus	Circumferential: 4670±420,Axial: 4480±590	Circumferential: 1180±120, Axial: 1210±90
	[88]	15^{TAV} 23^{BAV}	66±11 TAV 54±4 BAV	5.7±1.4 TAV 5.0±0.5 BAV	*	Maximum elastic modulus	Circumferential: 3351±222,Axial: 2207±203 Circumferential: 3504±160,Axial: 1916±96	Circumferential: 961±61,Axial: 540±37 Circumferential: 1656±98,Axial: 698±31

TAV: Tricuspid aortic valve with aneurysm, BAV: Bicuspid aortic valve with aneurysm, G. curv.: Great curvature, L. curv.:Lesser curvature, N: Number of specimens, *: Uniaxial tensile test, **: Biaxial tensile test

Anisotropy

Material mechanical properties (*e.g*. stiffness, etc.) can be identical in all directions (isotropic) or different (anisotropic). For this reason, directional dependence is evaluated with either *i*) the anisotropic index [53, 92, 102] or *ii*) the degree of anisotropy [93]. Both metrics usually use stiffness values from the two principal axes (*i.e.*, the circumferential axis and the longitudinal axis) and, like stiffness, change at different stress/strain values.

$$\text{Anisotropic Index} = 2[E_{m,L} - E_{m,C}]/[E_{m,L} + E_{m,C}] \quad (3.3)$$

$$\text{Degree of Anisotropy} = E_{m,L}/E_{m,C} \quad (3.4)$$

Energy Loss

Energy loss is a recently proposed biomechanical parameter. It has the advantage of being an integral metric of the mechanical response to both loading and unloading and is self-normalizing, making it less susceptible to strain and stress definitions and testing variables. It is a measure of the relative amount of energy loss of the loading cycles during tensile testing [94] (**Figure 3.2**). This reflects the aorta's natural physiologic function in absorbing energy during systole and returning a proportion during diastole. Increasing levels of energy loss indicate poor efficiency in performing this function. Higher energy loss has been found to be associated with aortic size and to reflect the underlying histopathology [94].

Ultimate Tensile Strength

The ultimate tensile strength (or simply *tensile strength*) is the peak stress a material can withstand before failing and is usually measured by uniaxial tensile testing. This intensive property cannot simply be translated to a pressure value due to the nonlinear hyperelastic

behaviour of vessel wall. Several studies have reported the ultimate tensile strength ascending aortas [83, 85, 91, 95, 103] and, intuitively, ascending TAAs are less strong than non-dilated aortas [85].

3.6.5 Characterization of Ascending TAAs by Tensile Testing

Tensile testing allows us to describe tissue stress-strain relationships and, when stretched to failure, the ultimate tensile strength of the tissue. Comparison of these parameter values in the literature is complex and often impracticable. As described, many factors influence tensile analysis and several definitions of material properties are encountered when reviewing studies of the ascending aorta. Reported stiffness and strength values for the ascending aorta in health and disease (ascending TAA, ascending TAA-TAV, ascending TAA-BAV and Dissecting Aneurysm (DA)) are provided in **Table 3.1**. This is an abridged form of **Table 3.S.1** which provides a more exhaustive list of tensile parameters of the ascending aorta.

Although reported values vary from study to study, depending on testing protocol and definition of stress and strain, general trends remain similar. Aneurysmal tissue is stiffer [85, 91, 92, 94] and weaker [85] than healthy ascending aortic tissues. Energy loss, similarly, is increased in ascending TAA tissues over healthy tissues and scales with aortic diameter and age [94]. However, outliers do occur demonstrating the inability of diameter and age alone to predict mechanical function. Advanced medial degeneration and increased collagen content is often seen in TAV patients; however, the degeneration associated with BAV is less evident and likely linked to microstructural disruption not visible by

histopathology and the younger age of BAV patients. As a result, mechanical analysis of ascending TAAs is often distinct in patients with BAV. Ascending TAA tissue has been found to be stronger for BAV patients than TAV patients [93, 103]. Yet, it has also been noted that the average aortic wall thickness is decreased [53, 93] and the delamination strength (*i.e.*, the strength required to propagate a tear through the medial layer of the artery) is significantly lower for BAV patients [104], which may explain an increased propensity for aortic dissection with BAV [105].

Aging increases the collagen-elastin ratio and, therefore alters the mechanical properties of the aortic wall. Younger ascending aortic tissue is known to have a greater extensibility (the stretch ratio at failure), tensile strength and less longitudinal wall stress at systolic blood pressure [83, 84]. The younger age of presentation for patients with BAV is an often neglected but critical factor when interpreting biomechanical data.

These measures represent the global tissue properties and, while the potential for an ascending TAA to rupture or dissect is indeed influenced by these properties, tissue failure is a result of localized phenomena like micro-fractures. Moreover, rupture potential, which may be predicted from biomechanics, may be distinct from dissection, where tissue dysfunction is more nuanced.

3.6.6 Ascending Aortic Dissection

A dissection of the ascending aorta often manifests as an intimal tear in the aorta's transverse (circumferential) axis [52] and tends to follow the greater curvature of the artery [106]. The transverse tear is perhaps explained by a failure of the tissue in the long axis of the ascending aorta [107, 108], which is weaker (*i.e.*, lower tensile strength) than the circumferential axis [95, 103] and subjected to added strain caused by the downward motion of the heart [107]. Studies that examine the regional strength of the aorta are limited; however, Iliopoulos *et al*. found that the anterior and posterior walls of ascending TAAs had lower longitudinal strength than either of the walls of the lesser or greater curvature [95]. Initiation and propagation of an aortic dissection may not be wholly described by tensile strength and may be more influenced by a regional increase in hemodynamic load and/or decreased delamination strength of the aortic wall [104].

Although *ex vivo* testing is rigorous and descriptive, the results have not yet been translated to clinical parameters and guidelines. Beyond size, *in vivo* measurements of aortic wall motion, thickness and local hemodynamics will likely be needed to assess the mechanical stability of the artery, which may provide clinical insight into aortic wall pathology on a patient-by-patient basis. However, *in vivo* strain imaging is unable to provide direct information on tissue stresses. *Ex vivo* mechanical testing's role in this story, therefore, will likely be to establish the criteria by which we can assess *in vivo* mechanics.

3.7 Non-invasive *In Vivo* Methods for Assessing Aortic Biomechanics

Clinical imaging modalities are the current standard for assessing the degree of aortic dilation in cases of suspected aneurysm and aortic valve dysfunction. As a result, these methods have been adapted to infer the *in vivo* biomechanical properties of the aortic wall in a preoperative and minimally invasive way. O'Rourke *et al.* provides a comprehensive summary of the metrics used for *in vivo* mechanical imaging [109].

Echocardiography

In most cases, a patient with suspected aortic disease will undergo echo imaging to observe valve function and phenotype and to measure the dimensions of the vessel. Echo Doppler measurements have the added benefit of visualizing hemodynamics in the ascending aorta, including the jet/wall interaction during systole. 2D m-mode echo measurements in tandem with an aortic pressure line can be used to determine a pressure-diameter relation (often only in the circumferential direction), which can reveal the level of aortic distensibility and estimate stiffness. Using diameter change, when observing the long-axis of the aorta, Baumgartner *et al.* demonstrated that young patients with MFS had significantly stiffer aortas compared to controls [13]. Similar work has been used to reveal the *in vivo* stiffening behaviour of the ascending aorta in response to chronic hypertension [16]. Recalling Hook's law (equation 2), strain alone is insufficient to estimate the stress in the tissue and requires *a priori* knowledge of the tissue material properties.

Transverse (or short-axis) imaging of the aorta using 2D echo with speckle tracking, a process that tracks the movement of natural acoustic markers ("speckles") that move with

the wall, can better account for circumferential diameter change. Using this method, which is well established for left ventricle strain assessment [110], the full circumference of the aorta can be imaged, which accounts for non-uniform wall motion [15]. New developments in 4D echo (3D reconstruction with temporal resolution) will likely provide a more robust analytical tool for *in vivo* mechanical measurements, allowing for simultaneous strain assessment in both the circumferential and longitudinal aortic axes.

Again, for such *in vivo* strain imaging to be used to estimate tissue stress requires knowledge of the tissue's mechanical properties. Strain imaging will require extensive population analysis and comparison with *ex vivo* mechanical properties to become a reliable tool for patient stratification.

Computer Tomographic Angiography (CTA) and Magnetic Resonance Angiography (MRA)

CTA and MRA are attractive imaging modalities for *in vivo* analysis due to their high spatial resolutions. Where echo visualization is obstructed by local anatomy and probe angle (*e.g.*, the distal ascending aorta and aortic arch), CTA and MRA have no such limitations and therefore can better identify wall properties of the full thoracic aorta. These techniques have been used in concert to generate patient-specific ECG-gated geometric meshes of ascending TAAs (CTA) and then to visualize cyclic strain in the vessel wall (MRA), allowing for the calculation of stress concentration [111].

Some compelling evidence for a causal role of hemodynamic load in ascending TAA has come from recent 4D MRA studies. In BAV patients the valve opening orientation and competence has been associated with the rate of AA dilation [112, 113]. den Reijer *et al.* showed a correlation of left ventricle jet flow angle with ascending aortic dilation in pediatric BAV patients [114]. The localized severity of the hemodynamic stress on the ascending aortic wall, caused by the jet, is proposed as the stimulus for hemodynamic remodelling. Similarly Bissell *et al.* have found that flow abnormalities linked to valve fusion type may better predict risk in BAV patients [115]. Della Corte *et al.* used time-resolved MRI and computational fluid mechanics modeling to demonstrate restricted cusp opening in BAV patients to be independently predictive of ascending TAA diameter and growth rate [116]. Hope *et al.* used 4D MRI and estimated a significant increase in wall shear stress (WSS) of the outer-anterior ascending aortic wall with eccentric flow [117]. Mahadevia *et al.* most recently showed the presence and type of BAV fusion causes significant changes in regional WSS distribution on the ascending TAA wall due to eccentric jet flow [118]. Taken together this work suggests a causal link between BAV aortopathy and eccentric jet flow, however, no study has shown a correlation of this increased hemodynamic load with tissue mechanical property changes.

With recent improvements in spatial and temporal resolution, clinical imaging techniques are becoming a useful way to assess mechanical dysfunction. That said, there are limitations in interpretation, namely that pressure forces are not equivalent to stresses felt by the tissue. To date, no comprehensive studies have compared the *ex vivo* mechanical

properties of tissues with preoperative *in vivo* strain imaging which may be a useful next step to establish biomechanics-derived intervention criteria.

3.8 Comment

Current clinical practice views ascending TAA as a mechanical dysfunction of the vessel wall that can be inferred by size. In reality, this metric cannot account for the complexity, variation and dynamic nature of aortic diseases, which, on a mechanical and physiological level, are still not fully understood. Moving beyond aortic size alone, tensile testing of ascending aortic tissue in health and disease is central in defining and validating new metrics for identifying the pathology and assessing the risk of aneurysm. Here, we provide a point source for the reported understanding of ascending aortic and ascending TAA tensile properties **(Table 3.S.1**).

Indeed, the number values of reported stiffness and strength are often difficult to compare between studies with the high degree of variability in testing protocols. To our research colleagues, we advocate for consensus in testing and reporting standards with the aim of better comparing studies from lab to lab. Furthermore, age, sex and existing co-morbidities are important factors that must be reported alongside the mechanical data in order to ensure a proper contextual interpretation**.** This includes several classes of medications which have the potential to influence the microstructure of the aortic wall, its function and material properties, including statins, beta-blockers, angiotensin-receptor blockers and other anti-hypertensives [119,120]. When possible, these variables should be matched between patient populations to disambiguate their effect.

So, how can this information transfer from bench to bedside? Looking towards the future, linking population-based *ex vivo* mechanics (like those given in **Table 3.S.1**) to clinical imaging modalities, including MRA, transesophageal echocardiography (TEE) and CTA, might be used to distinguish between stable and unstable aortic pathologies. As we've shown, some work has been reported using non-invasive *in vivo* strain-mapping of the ascending aorta; however, additional population-based mechanical studies are invariably needed to define the criteria by which these models are assessed. Finally, there is a need to bridge the biological definitions of aortic tissue dysfunction, which characterize cellular function and the imbalance of proteases and structural proteins, with end result mechanical dysfunction. We believe that image based *in vivo* strain assessment, once well validated with histopathologic and *ex vivo* mechanical data, will help stratify patients for ascending TAA intervention.

3.9 Supplemental Material

The following appeared as supplementary material made available with the published article:

Table 3.S.1. Most common parameters in tensile testing (expanded)

	Parameter	Authors	Definition	Test	Study population				Result	Significance
					N (TAV/ BAV)	Age (Year)	Sex (Male)	Size (cm)		
STIFFNESS	E_m(kPa)	100	Engineering strain: 40%	**	***7(7/0)^{TAV}***	***51±18^{TAV}***	***6^{TAV}***	***2.4±0.4^{TAV}***	E_m(TAA): 150±30 *vs* E_m(ascending aorta): 100±30	S
					34(12/20)^{TAA}	64±12 ^{TAA}	23 ^{TAA}	5.2±0.7 ^{TAA}	E_m(TAV) *vs* E_m(BAV)	NS
									E_m(Proportions of collagen) *vs* E_m(Proportions of elastin)	NS
		88	Maximum elastic modulus	*	15(15/0)^{TAV}	66±11 ^{TAV}		5.7±1.4 ^{TAV}	*TAV:* E_m(Circ):3351±222, E_m(Ax):2207±203	
					23(0/23)^{BAV}	54±4 ^{BAV}		5.0±0.5 ^{BAV}	*BAV:* E_m(Circ):3504±160, E_m(Ax):1916±96	
		98	Physiological Cauchy stress : 72.8kPa	**	***14***	***47±14***			E_m(Circ):988.7±489.7 *vs* E_m(Ax):952.1±479.1	NS
									Circ,Ax: E_m(Anterior) *vs* E_m(Posterior)	NS
		93	Low/high tension (60/120 Nm^{-1})	*,**	20^{TAA}	59.45±7.86 ^{TAA}	3:1 ^{TAA}	4.94±0.48 ^{TAA}	*Ax, High/Low tensions:* E_m(BAV) is stiffer than [E_m(TAA), E_m(BAA)]	S
					20(0/20)^{BAV}	55±9.65^{BAV}	3:1 ^{BAV}	5.01±0.50 ^{BAV}	*Circ, High tension:* E_m(BAV) *vs* E_m(TAA) *vs* E_m(BAA)	NS
									Circ, Low tension: E_m(BAV) is stiffer than [E_m(TAA), E_m(BAA)]	S
					15^{BAA}	58.07±14.70 ^{BAA}	11:4 ^{BAA}	4.93±0.53 ^{BAA}	*TAA, BAA*: E_m(Circ) is stiffer than E_m(Ax)	S
									BAV: E_m(Circ) *vs* E_m(Ax)	NS
		89	Maximum elastic modulus	*	13^{TAA}	13-75^{TAA}		5.42±0.732^{TAA}	*Lesser curv*: E_m (Circ) *vs* E_m (Ax)	NS
									Circ: E_m (Greater curv):8780, E_m (Lesser curv): 9190	
									Ax: E_m (Greater curv):5890, E_m (Lesser curv): 3130	
		121	Low stress modulus (E_{mL}): elastin High stress modulus (E_{mH}): elastin and collagen	**	***11(5/6)*** 97^{TAA}	58±11^{TOT}	6^{TOT}		*Circ:* E_{mL}(TAA) *vs* E_{mL}(ascending aorta)	S
									E_{mL}(TAV) is lower than E_{mL}(ascending aorta)	S
									E_{mL}(TAV) is lower than E_{mL}(BAV)	S
									E_{mL} of the different quadrants	S
		102	Engineering strain: 7.5,25%	**	***30*** 14^{TAA}	***53±15*** 62±10^{TAA}	***20*** 12^{TAA}		*7.5%:* E_m(TAA) *vs* E_m(ascending aorta)	NS
									25%: E_m(TAA) *vs* E_m(ascending aorta)	NS
		122	Maximum elastic modulus	*	***15*** 26^{TAA}	***66±3*** 69±2 ^{TAA}		***3.3±0.2*** 5.9±0.3 ^{TAA}	E_m(TAA) is higher than E_m(ascending aorta)	S
									Ascending aorta, TAA, Circ: No regional variation	
									Ascending aorta, TAA, Ax: E_m(Right Lat) is the highest	
		99	NA	*	6^{TAA}	25±2^{TAA}			E_m(loading):285±164, E_m(unloading): 542±221	
		101	Maximum elastic modulus	*	***14*** 40^{TAA}	***51±6*** 66±2 ^{TAA}		***3.3±0.2*** 5.8±0.3 ^{TAA}	*Ax*: E_m(TAA):4480±590 is higher than E_m(ascending aorta):2610±260	S
									Circ: E_m(TAA):4670±420 *vs* E_m(ascending aorta):3250±630	NS
									Ascending aorta, TAA: E_m(Circ) vs E_m(Ax)	NS
	λ	90	Physiological stress	**	20(0/20)^{BAV}	55±12^{BAV}	5.0±0.7^{BAV}		λ(≥55yr) is lower than λ(<55yr)	
					7^{DAN}	64±9^{DAN}		5.1±0.7^{DAN}		
					8^{MFS}	38±14 ^{MFS}		5.4±0.8^{MFS}		
	DIS (kPa)	90	Cylindrical model	**	20(0/20)^{BAV}	55±12^{BAV}	5.0±0.7^{BAV}		DIS(BAV):2.21±0.83 *vs* DIS(DAN):1.46±.83	S
					7^{DAN}	64±9^{DAN}		5.1±0.7^{DAN}	DIS(BAV):2.21±0.83 *vs* DIS(MFS):1.43±0.68	S
					8^{MFS}	38±14 ^{MFS}		5.4±0.8^{MFS}		
ELONGATION	TS (kPa)	88	Maximum Cauchy stress	*	15(15/0)^{TAV}	66±11 ^{TAV}		5.7±1.4 ^{TAV}	*TAV*: TS(Circ): 961±61 *vs* TS(Ax):540±37	S
					23(0/23)^{BAV}	54±4 ^{BAV}		5.0±0.5 ^{BAV}	*BAV*: TS(Circ): 1656±987 *vs* TS(Ax):698±31	S
									TS(BAV) is higher than TS(TAV)	S
		93	Maximum second Piola-Kirchhoff stress	*,**	20^{TAA}	59.45±7.86 ^{TAA}	3:1 ^{TAA}	4.94±0.48 ^{TAA}	*TAA:* TS(Circ) is higher than TS(Ax)	S
					20(0/20)^{BAV}	55±9.65^{BAV}	3:1 ^{BAV}	5.01±0.50 ^{BAV}	*BAV,BAA:* TS(Circ) *vs* TS(Ax)	NS
					15^{BAA}	58.07±14.70 ^{BAA}	11:4 ^{BAA}	4.93±0.53 ^{BAA}	*Ax:* TS(BAV) is higher than TS(TAA)	S
		86	Maximum Cauchy stress	*	***7(7/0)^{TAV}*** 24(1/16) ^{TAA}	41-79^{TOT}	24^{TOT}	4.0-6.8^{TOT}	TS is higher for the circumferential direction and the half adventitia/surface of the sample	
		122	Maximum Cauchy stress	*	***15*** 26^{TAA}	***66±3*** 69±2 ^{TAA}		***3.3±0.2*** 5.9±0.3 ^{TAA}	TS(Circ) is higher than TS(Ax)	S
		101	Maximum Cauchy stress	*	***14*** 40^{TAA}	***51±6*** 66±2 ^{TAA}		***3.3±0.2*** 5.8±0.3 ^{TAA}	*Ax*: TS(TAA):1210±90 is lower than TS(ascending aorta):1710±140	S
									Circ: TS(TAA):1180±120 is lower than TS(ascending aorta):1800±240	S
									Ascending aorta, TAA: TS(Circ) vs TS(Ax)	NS
		87	Maximum Cauchy stress	*	11(0/11)$^{BAV<50yr}$	39±10$^{BAV<50yr}$	11$^{BAV<50yr}$		*<50yr:* TS(BAV) *vs* TS (MFS)	NS
					15(0/15)$^{BAV≥50yr}$	63±8$^{BAV≥50yr}$	15$^{BAV≥50yr}$		*≥50yr:* TS (BAV) *vs* TS(TAV)	NS
					6^{MFS}	39±13^{MFS}	11^{MFS}		TS(<50yr) is greater than TS(≥50yr)	S
		87	NA	*	11(0/11)$^{BAV<50yr}$	39±10$^{BAV<50yr}$	11$^{BAV<50yr}$		λ_{max}(<50yr) is greater than λ_{max}(≥50yr)	S
					15(0/15)$^{BAV≥50yr}$	63±8$^{BAV≥50yr}$	15$^{BAV≥50yr}$		*Circ, Ax:* λ_{max}(BAV) *vs* λ_{max}(MFS)	NS
					6^{MFS}	39±13^{MFS}	11^{MFS}			
AI (%)		93	NA	*,**	20^{TAA}	59.45±7.86 ^{TAA}	3:1 ^{TAA}	4.94±0.48 ^{TAA}	BAV is more isotropic than TAA and BAA	
					20(0/20)^{BAV}	55±9.65^{BAV}	3:1 ^{BAV}	5.01±0.50 ^{BAV}		
					15^{BAA}	58.07±14.70 ^{BAA}	11:4 ^{BAA}	4.93±0.53 ^{BAA}		
		121	NA	**	***11(5/6)*** 5^{TAA}	58±11^{TOT}	6^{TOT}		AI>0 : Axial direction is stiffer than circumferential	
		102	Engineering strain: 7.5,25%	**	***30*** 14^{TAA}	***53±15*** 62±10^{TAA}	***20*** 12		AI(7.5%) *vs* AI(25%)	S

MATERIAL PARAMETERS	88	Stress model : $\sigma = [2\alpha + 4\beta(\lambda^2 + 2\lambda^{-1} - 3)][\lambda^2 - \lambda^{-1}]$	*	15(15/0)^{TAV} 23(0/23)^{BAV}	66±11 ^{TAV} 54±4 ^{BAV}	5.7±1.4 ^{TAV}	 5.0±0.5 ^{BAV}	*TAV:* α(Circ):6.8±2.3 *vs* α(Ax):6.2±0.8 β(Circ):71.0±22.2 *vs* β(Ax):120.0±31.5 *BAV:* α(Circ):4.8±0.3 vs α(Ax):4n.5±0.4 β(Circ):12.3±1.1 vs β(Ax):18.1±1.8 *Ax*: α(BAV) *vs* α(TAV) *Circ,Ax*: β(BAV) is lower than β(TAV)	NS NS NS S S S
	98	Fung energy function: $W = \frac{c}{2}(e^Q - 1)$	**	14 ^{TAA}	47±14 ^{TAA}			c: 55.17±49.10, b_1: 3.35±3.88, b_2: 3.18±3.59, b_3: 0.42±0.42	
	99	Stress model $\frac{d}{d\lambda}\begin{cases}\alpha_1(T+\beta_1), \frac{dT}{dt} > 0 \\ \alpha_2(T+\beta_2), \frac{dT}{dt} < 0\end{cases}$	*	6 ^{TAA}	25±2 ^{TAA}			α_1: 10.82±3.57, α_2: 13.57±4.21	
	101	Stress model: $\sigma = [2\alpha + 4\beta(\lambda^2 + 2\lambda^{-1} - 3)][\lambda^2 - \lambda^{-1}]$	*	***14*** 40^{TAA}	***51±6*** 66±2 ^{TAA}		***3.3±0.2*** 5.8±0.3 ^{TAA}	*Circ:* α(TAA):80±10 *vs* α(ascending aorta):150±50 *Ax:* α(TAA): 100±20 *vs* α(ascending aorta): 110±40 *Circ:* β(TAA):170±40 *vs* β(ascending aorta):40±10 *Ax:* β(TAA):530±150 *vs* β(ascending aorta): 90±30 *ATA, TAA:* α(Circ) *vs* α(Ax) *TAA:* β(Circ) *vs* β(Ax) *ATA:* β(Circ) *vs* β(Ax)	NS NS S S NS S NS
	90	Exponential constitutive relation: $\rho_0 W = \frac{c}{2}e^Q$	**	20(0/20)^{BAV} 7^{DAN} 8^{MFS}	55±12^{BAV} 64±9^{DAN} 38±14 ^{MFS}	5.0±0.7^{BAV}	 5.1±0.7^{DAN} 5.4±0.8^{MFS}	c: 5.8,b_1: 15.3, b_2: 11.9, b_3: 25.0	

AI: Anisotropic index, TAA: Ascending thoracic aortic aneurysm, BAA: Bovine aortic arch, BAV: Bicuspid aortic valve with aneurysm, Curv.: Curvature, DAN: Degenerative aneurysm, DIS: Distensibility, EH: High stress modulus, E_m: Incremental elastic modulus, E_{mH}: High stress modulus, E_{mL}: Low stress modulus MFS: Marfan syndrome, N(TAV/BAV): Number of specimen (numbers of TAV/BAV), NS: No significance, S: Significance, TA: True aneurysm, TAV: Tricuspid aortic valve with aneurysm, TOT: Total, TS: Ultimate tensile strength, λ: Stretch ratio, *: Uniaxial tensile test, **: Biaxial tensile test, *,**: Both uniaxial and biaxial tensile tests.

Chapter 4: Expanded Literature Review of Speckle-Track Echocardiography of the Ascending Aorta

4.1 Transthoracic and Transesophageal Echocardiography

Echocardiography is the application of ultrasound imaging to the heart and great vessels, including the thoracic aorta. Depending on the plane of view required by the clinician, the sonographer images through the chest (transthoracic echocardiography, TTE) or the esophagus (transesophageal echocardiography, TEE). TTE is non-invasive and is frequently used to capture a parasternal long-axis view of the heart or vessels and is often used to assess left ventricle function. TEE, in contrast, places the probe closer to the imaging plane by insertion within the esophagus and, in some cases, into the stomach. As a result, patients require sedation.

Owing to the required focal depth of each modality (TEE, *low depth*, proximal & TTE, *high depth*, distal), TTE uses low ultrasonic frequency transducers of 2-5 MHz while TEE uses high frequency transducers of 3.5-7 MHz. Physically, this is described by the attenuation ($A=af[2x]$) which is the product of the pulse frequency (f), the distance from the transducer to the image plane (x) and the attenuation coefficient (a) of the transmitting material (soft tissue, blood, bone, *etc.*)[123, 124]. As a result, the attenuation per unit depth is proportional to the transducer frequency. Since TEE is performed proximal to the thoracic

aorta (*i.e.*, ↓x) one can compromise on increased signal attenuation for superior axial* (parallel to the beam) and lateral† resolution (orthogonal to the beam) as both increase with transducer frequency.

4.2 2D Speckle-track Echocardiography

Two-dimensional (2D) speckle-track echocardiography (STE) is an imaging modality that exploits the presence of natural acoustic markers (*i.e.*, "speckles") from standard B-mode (brightness mode) ultrasound images. Speckles are both stable and evenly distributed within the area of the imaged tissue[125]. As a result, speckles can be tracked within a time series of B-Mode images allowing for the measurement of tissue velocity. Strain (ε) can be obtained from STE by measuring the deformation between adjacent speckles: $\varepsilon=\delta/L_0$, where L_0 is the original length between the two speckles and δ is the change in length (*i.e.*, $\delta=L-L_0$)[126]. This process can be scaled and applied to larger segmentations of a tissue; for instance, a quadrant of the circumference of the aortic wall.

* Axial resolution is inversely related to pulse length (L_P) which is defined as the product of the number of cycles per pulse (N_C) and the wavelength ($\lambda=v/f$, where v is the acoustic velocity in the transmitting medium): $L_P=N_C\lambda$.

† Lateral resolution is increased as the beam diameter is decreased. As the beam converges to a minimum of half the transducer diameter (D) at the *near-field length* (L_{NF}), having a larger L_{NF} ensures a greater "axial window" beyond which the beam diverges: $L_{NF}=D^2f/4v$, where v is the acoustic velocity in the transmitting medium.

Depending on the angle at which the beam intersects the tissue, different planes of view corresponding to different axes of strain can be imaged for various cardiovascular structures. For the AA, two standard TEE views are available with the probe at the level of the mid-esophagus. The first is the short-axis (SAX) view that captures a transverse cross-section of the AA (**Figure 4.1-A**). A SAX view allows for the measurement of circumferential (ε_{CIRC}) and radial strain (ε_{RAD}). The second is the long-axis (LAX) view that captures a longitudinal view of the inner and outer curvature[‡] of the AA (**Figure 4.1-B**). A LAX view allows for the measurement of longitudinal strain (ε_{LONG}) as well as radial strain and 2D diameter change, although both are limited to the intersecting plane.

[‡] The inner and outer curvature of the AA are commonly referred to as the lesser and greater curvature, respectively.

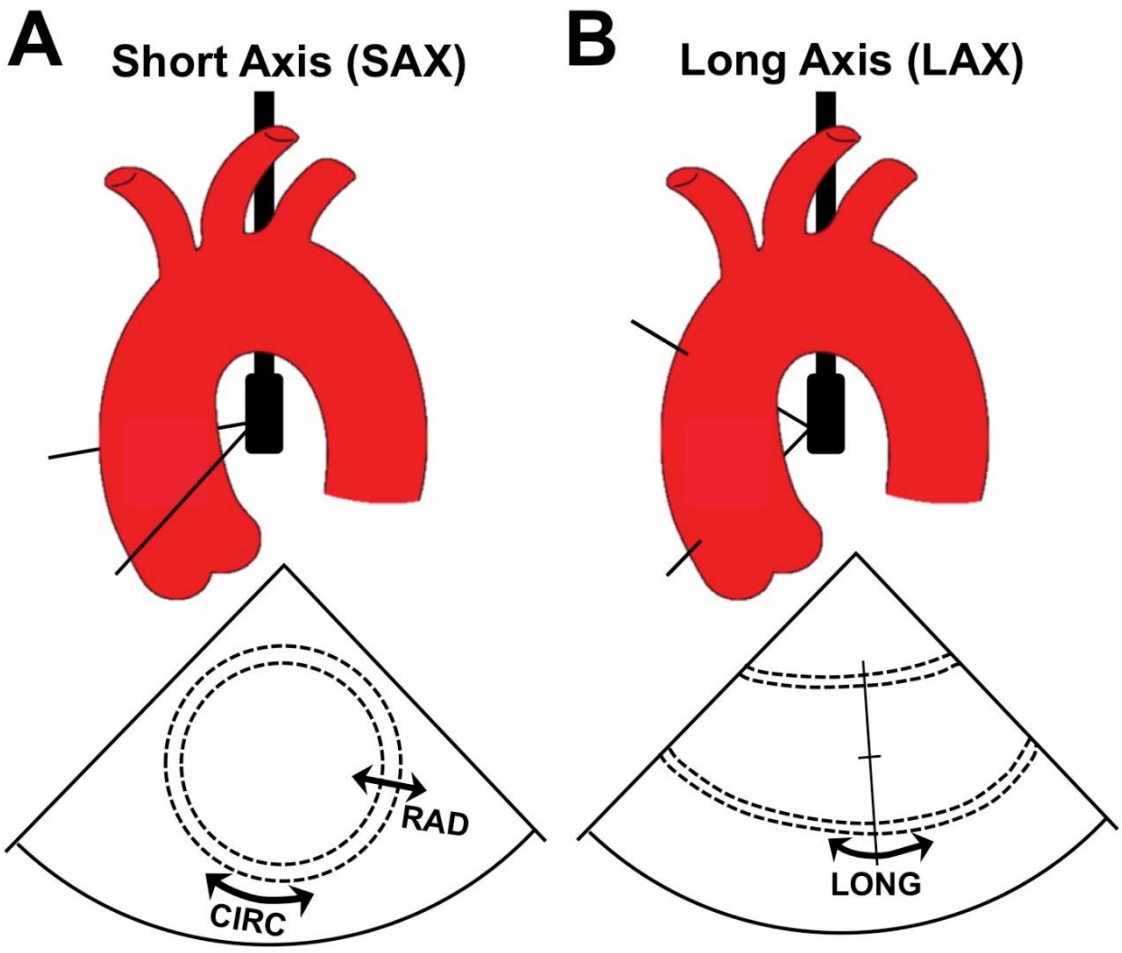

Figure 4.1. Standard planes of view used in transesophageal echocardiographic imaging of the ascending aorta. Probe height with beam intersection and schematic of the corresponding B-mode image for the A) short-axis and B) long-axis view of the ascending aorta. Axes labels: CIRC–circumferential, RAD–radial, LONG–longitudinal.

4.3 Echo-derived Mechanical Indices

The previous chapter (Chapter 3) introduced the concept of mechanical dysfunction in the thoracic aorta. In a clinical context, without access to a tissue biopsy, mechanical assessment is confined to an *in situ* analysis of the passive vessel deformation in response

to the blood pressure waveform of the cardiac cycle. Tensile strength and other yielding properties cannot be measured under these conditions and therefore stiffness, or its approximation, has been used as the surrogate measure of the mechanical properties of the vessel wall. Several stiffness parameters have been developed previously that use one or more of the blood pressure measurements, the systolic (P_S) and diastolic (P_D) pressures and the vessel geometry by echo-measured deformation:

1. *The Stiffness Index (β)*[109, 127]: $\beta=\ln(P_S/P_D)/([D_{max}-D_{min}]/D_{min})$, *unitless*

   Where D_{min} and D_{max} correspond to the minimum and maximum vessel diameters, respectively.

2. *Elastic Modulus (E)*[109, 127]: $E=(P_S-P_D)\times D_{min}/(D_{max}-D_{min})$, *units of force/area*

3. *Pulse Wave Velocity (PWV)*[109, 127, 128]: $PWV=d_{P1-P2}/\Delta t_{P1-P2}$, *units of length/time*

   Where d_{P1-P2} is the arterial distance between two measurement points along an arterial branch and Δt_{P1-P2} is the time for the pressure wave to travel between these points. According to the Moens-Korteweg equation, $PWV\propto\sqrt{E_Y}$,[§] where is E_Y is the Young's modulus of the vessel wall.

[§] The complete Moens-Korteweg equation: $PWV=\sqrt{[E_Y\tau/2r\rho]}$, where τ is the vessel wall thickness, r is the vessel radius and ρ is the blood density[126].

4. *Incremental Modulus (E_{inc})*[129]: $E_{inc}=0.75R\times d\sigma/dR$, *units of force/area*

   Where R is the mid-wall radius[**] and σ is the stress according to an expanded Laplace's Law that relates luminal pressure (P) to stress (σ). The derivation of this equation is provided in Pagani *et al*.[129] In practice, E_{inc} is proportional to the linear fit of the stress *vs.* diameter relation over a full cardiac cycle.

Each of these parameters has its advantages and limitations. The advantage of parameters 1-3 is the availability and simplicity of the measured inputs. However, their primary limitation is that there is no accounting for the tissue thickness. As a result, this simplification requires a substitution of pressure, acting normal to the vessel wall, for stresses within the wall. Conversely, parameter 4 (E_{inc}) overcomes this limitation by accounting for wall stresses by an adapted expanded Laplace equation but is limited in its application due to poor resolution in measuring aortic wall thickness with echo.

When full-cycle measurements of blood pressure and strain are obtained for the aorta (*e.g.*, for E_{inc}), they are temporally related to each other by end-diastolic gating using the patient's ECG. Due to procedural restrictions/conventions, it is not always possible to place the pressure catheter at the site of imaging. In fact, it's common to obtain the blood pressure trace from an invasive catheter in a peripheral artery (*e.g.*, radial artery). As a result of a phase shift (φ) in pressure between central and peripheral arteries, the pressure waveform needs to be corrected to temporally align with the change in aortic strain (Figure 4.2).

[**] The mid-wall radius R is defined as: R=(a+b)/2, where a and b are the inner and outer radii of the vessel wall.

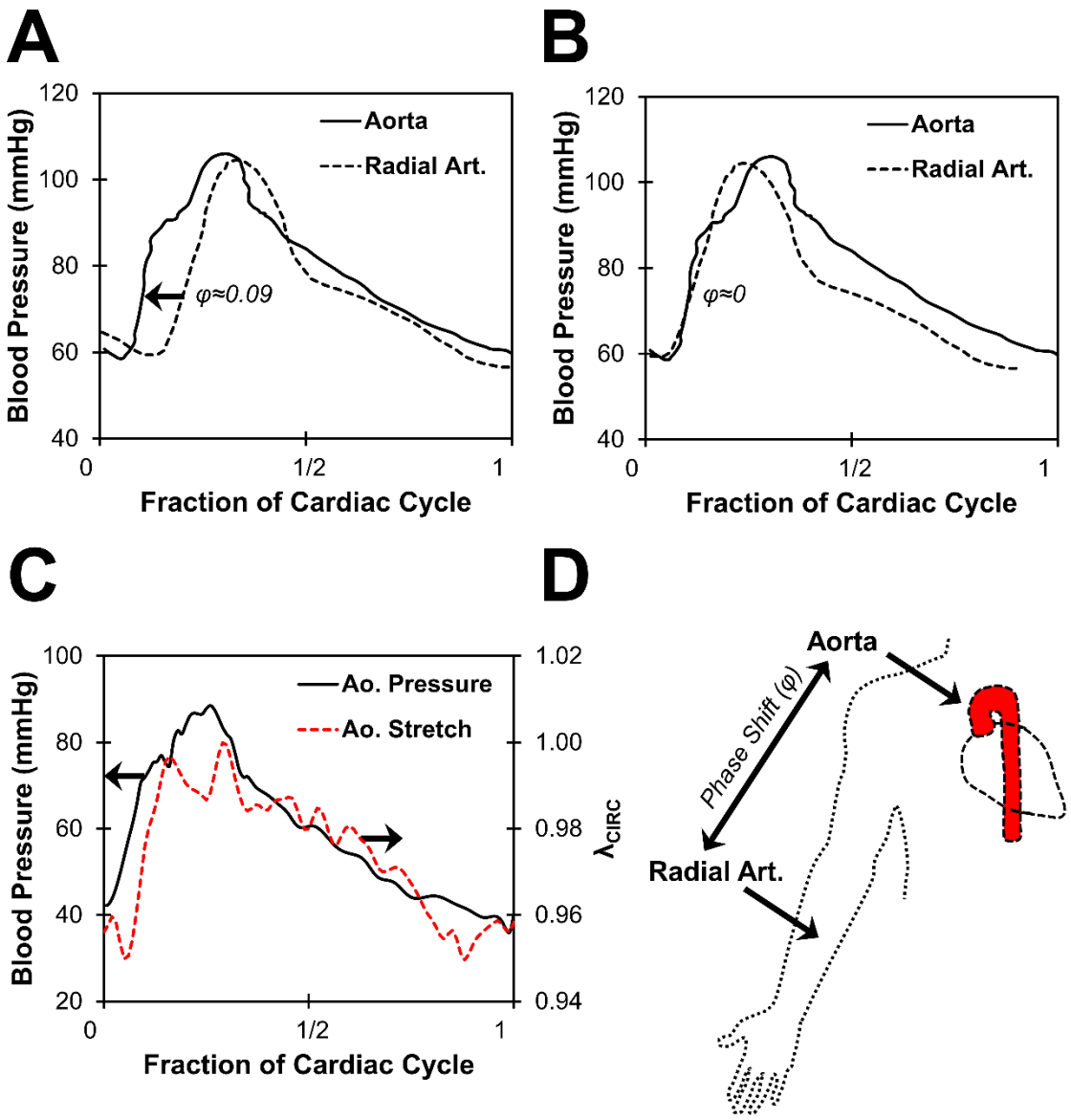

Figure 4.2. Relationship between aortic and radial artery pressure catheterization and aortic strain for biomechanical assessment. The A) normal and B) corrected radial pressure waveform overlaid with the aortic pressure waveform showing relative phase shifts (φ). C) Typical aortic pressure waveform overlaid with the circumferential aortic stretch (λ_{CIRC}) profile. D) Schematic showing the relative anatomical locations of catheterization points.

4.4 Aortic Biomechanics by Echocardiography

Several studies have investigated the mechanical behaviour of the aorta under physiological conditions by echocardiography (**Table 4.1**). A common modality has been TTE with M-mode (motion mode). M-mode is used to capture a 1D ultrasound image, for instance the aortic cross-section showing opposite walls, over a period of time with very high temporal resolution. In this way, the aortic diameter can be measured with precision over a full cardiac cycle. Baumgartner *et al.* used this technique to measure an ~2-fold increase in AA stiffness in age-matched patients with Marfan syndrome compared to clinically healthy individuals[13]. Similarly, Vitarelli *et al.* and Oishi *et al.* used this echo modality to demonstrate that aortic stiffness is increased in persons with hypertension and >50 years, respectively[16, 130].

Speckle tracking has been used to identify the peak aortic strain or the full cyclic strain profile. Karatolios *et al.* demonstrated that, in patients with abdominal aortic aneurysm, the cyclic strain profile was more regionally heterogeneous than in healthy individuals[131]. Wittek *et al.* used 3D TTE to identify the circumferential and longitudinal strain profiles in the AA and abdominal aorta[17]. They reported that circumferential and longitudinal strains are similar in magnitude in the AA but that longitudinal strain becomes negligible in the abdominal aorta[17].

Lang *et al.* used a unique approach to identify the increased aortic stiffness with age by the incremental modulus, E_{inc}, using TEE 2D SAX and M-mode imaging[132]. In that study, stress-strain curves were determined as described by Pagani *et al.*[129] using a subclavian

pressure tracing, aortic wall thickness by M-mode imaging and area strain of the aorta in the transverse plane by the relative change in the aortic radius.

Table 4.1. Studies examining the stiffness properties of the aorta, using echo

Study	Echo Modality	Stiffness Parameter	Location
Lang *et al.*, 1994 [132]	TEE SAX & M-mode	E_{inc}	DA
Sugioka *et al.*, 2002 [133]	TEE M-Mode	β	DA
Nemes *et al.*, 2004 [134]	TEE SAX	E	DA
Baumgartner *et al.*, 2005 [13]	TTE M-mode	β	AA
Drozdz *et al.*, 2005 [135]	3D TEE	β	ND
Vitarelli *et al.*, 2010 [16]	TTE M-mode	Strain, β, E, PWV	AA
Oishi *et al.*, 2011 [130]	TTE SAX & M-mode	Strain, β	Abd.A
Teixeira *et al.*, 2013 [15]	ND SAX & M-mode	Strain, β	AA
Karatolios *et al.*, 2013 [131]	3D TTE (SAX & LAX)	Strain	Abd.A
Petrini *et al.*, 2014 [136]	TEE SAX & M-mode	Strain, β	DA
Wittek *et al.*, 2016 [17]	3D TTE (SAX & LAX)	Strain	AA/Abd.A
Bieseviciene *et al.*, 2017 [14]	TTE LAX	β, E	AA
Alreshidan *et al.*, 2017 [137]	TEE SAX	β	AA

AA – ascending aorta, Abd.A – abdominal aorta, DA – descending aorta, ND – not disclosed

The common link between these *in vivo* studies is their use of echo to estimate aortic stiffness. However, this approach requires an *a priori* assumption that these metrics indeed represent tissue stiffness and are not measurement artefacts of a complex and heterogeneous physiological environment. This thesis, herein, endeavoured to validate

both global (*i.e.*, circumference-averaged) and regional echo-derived *in vivo* stiffness metrics by a rigorous comparison with *ex vivo* mechanical indices and histopathology.

Chapter 5: Transesophageal echocardiographic strain imaging predicts aortic biomechanics: Beyond diameter

5.1 Preface

This chapter is a published manuscript in The Journal of Thoracic and Cardiovascular Surgery (2018). As discussed in Chapter 3, several studies have used echo imaging to estimate the mechanical properties of the aorta in different disease states or as a function of age. However, these *in vivo* methods had not previously been validated with *ex vivo* measurements to confirm their accuracy. Second, nearly all of these studies used *in vivo* stiffness definitions (namely E and β) that substituted aortic pressure for wall stress due to a limitation in measuring tissue thickness *in vivo*. This article addressed these points by defining novel *in vivo* echo-derived stiffness moduli (see CCPM and CCSM) that estimated stiffness from both the pressure-strain and stress-strain relations. These moduli were measured in a cohort of 21 patients receiving elective aortic resection surgery and subsequently correlated with *ex vivo* mechanical indices (energy loss and stiffness). Furthermore, this study found a correlative link between the echo-derived moduli and the relative vessel wall composition of collagen and elastin.

Ultimately, this article proposed a novel methodology to address a clinical limitation in identifying patients for surgery that may be miscategorised by aortic size criteria. Results demonstrated that patients could be identified by abnormal moduli that, in turn, related the

degree of histopathological remodelling of the aortic wall thereby providing information that was independent of aortic size.

5.2 Article

Transesophageal echocardiographic strain imaging predicts aortic biomechanics: Beyond diameter

Alexander Emmott,[a,b] Haitham Alzahrani,[c] Mohammed Alreshidan,[c] Judith Therrien,[d] Richard L. Leask,[a,b] Kevin Lachapelle[c,*]

a-Department of Chemical Engineering, McGill University, Montreal, QC, Canada

b-Research Centre, Montreal Heart Institute, Montreal, QC, Canada

c-Department of Surgery, Royal Victoria Hospital, McGill University, Montreal, QC, Canada

d-Division of Cardiology, Royal Victoria Hospital, McGill University, Montreal, QC, Canada

Address of corresponding author:

Kevin Lachapelle, MD, FACS, FRCSC, Cardiac Surgery Department, McGill University Health Centre – Glen Site, 101 Boul. Decarie, C07-1284, H3A 3J1, Montreal, QC, Canada (email: kevin.lachapelle@mcgill.ca). Phone: 1-514-934-1934; Fax: 1-514-843-1602

5.3 Abstract

Background: Clinical guidelines recommend resection of ascending aortic (AA) aneurysms at diameters ≥5.5cm to prevent rupture or dissection. However, ~40% of all AA dissections occur below this threshold. We propose new TEE strain-imaging moduli coupled with blood pressure measurements to predict aortic dysfunction below surgical threshold.

Methods: 21 patients undergoing aortic resection were recruited to participate in this study. TEE imaging of the aortic short axis and invasive radial blood pressure traces were taken for 3 cardiac cycles. Using EchoPac™ and post-processing in Matlab™, circumferential stretch profiles were generated and combined with the blood pressure traces. From this data, two *in vivo* stiffness moduli were calculated: the CCPM and CCSM. From the resected aortic ring, testing squares were isolated for *ex vivo* mechanical analysis and histopathology. Each square underwent equibiaxial tensile testing to generate stress-stretch profiles for each patient. Two *ex vivo* indices were calculated from these profiles (energy loss and incremental stiffness) for comparison with the CCPM and CCSM.

Results: The echo-derived stiffness moduli demonstrate positive significant covariance with *ex vivo* tensile biomechanical indices: energy loss (*vs.* CCPM: R^2=0.5873, P<0.0001; *vs.* CCSM: R^2=0.6401, P<0.0001) and apparent stiffness (*vs.* CCPM: R^2=0.2079, P=0.0378; *vs.* CCSM: R^2=0.3575, P=0.0042). Similarly, these TEE-derived moduli are highly predictive of the histopathological composition of collagen and elastin (collagen/elastin ratio *vs.* CCPM: R^2=0.6165, P<0.0001; *vs.* CCSM: R^2=0.6037, P<0.0001).

Conclusion: TEE-derived stiffness moduli correlate strongly with aortic wall biomechanics and histopathology, which demonstrates the added benefit of using simple echo-derived biomechanics to stratify patient populations.

5.4 Introduction

Acute dissection and rupture are usually fatal complications of aortic aneurysms and prevention is only possible with surgical intervention before these acute complications. Presently all guidelines use the maximum aortic diameter as the decisional criterion for surgical intervention[138, 139]. Unfortunately, nearly 40% of patients who present with dissection have aortic diameters below surgical criteria[140]. Accordingly, novel criteria are needed to identify those who are at risk of dissection or rupture.

Ascending aortic (AA) aneurysms result from pathological remodeling of the vessel wall[141]. Thinning and fragmentation of elastic lamellae, deposition of collagens and accumulation of extracellular glycosaminoglycans are the most common characteristics of non-syndromic and non-traumatic aneurysm formation[42, 49, 52]. This extensive tissue remodeling alters the biomechanical properties of the aorta[32, 33]. Aortic rupture and dissection occur due to a loss of mechanical integrity of the vessel wall. Notably, *ex vivo* mechanical measures of AA tissue, such as stiffness, energy loss and ultimate strength have been shown to vary with tissue remodeling. Stiffness[53, 85] and energy loss[94, 142] both increase with pathological remodeling while strength of the aorta decreases[85]. These changes in biomechanics were demonstrated using the *ex vivo* stress-strain relationship based on testing of resected tissue. Reliably estimating these metrics *in vivo* would provide more information for surgical decision-making.

Dynamic echocardiography is routinely used to assess cardiovascular function due to its high temporal resolution without the need to expose patients to contrast agents or ionizing

radiation. Dynamic speckle-track strain imaging of the aorta is an attractive approach to translate the measurement of tissue mechanics from a postoperative *ex vivo* analysis to a preoperative *in vivo* assessment.

Previous studies have suggested that aortic stiffness can be deduced from echo strain-imaging[14, 15, 130, 136, 137]. Indeed, TEE studies have revealed that the aortic wall of a subset of patients with bicuspid aortic valve (BAV)[136] and patients <50 years-old[130] are less stiff than those with tricuspid aortic valve (TAV) or >50 years-old. However, no direct comparison between intrinsic risk factors, including *ex vivo* mechanics and the underlying wall pathology has been made.

In this study, we demonstrate that speckle tracking echocardiography can reliably estimate the biomechanics of aortic tissue obtained *ex vivo*. Specifically, we used pre-operative TEE strain imaging of the aorta with concurrent blood pressure tracing to calculate two new stiffness moduli of the aortic wall, which were then compared with *ex vivo* mechanical analysis and tissue histopathology in patients undergoing aortic resection.

5.5 Methods

Study Cohort

In compliance with the Canadian tri-council policy statement on ethical conduct for research involving humans, informed consent was obtained from 21 patients undergoing elective aortic valve and or aortic resection surgery. AA diameters ranged from 3.6–6.1 cm- that is from mild to severe dilation.

Ex vivo Tensile Analysis

A specimen of the aortic ring was obtained for each patient immediately following resection, clipped for anatomical orientation and stored in physiological saline at 4°C until further processing and testing. The maximum aortic diameter was measured for each ring before sectioning four $1.5\times1.5cm^2$ testing squares, equally distributed around the circumference of the aorta representing the 1-anterolateral wall, 2-posterolateral wall and the 3-inner and 4-outer curvature. Five unique thickness measurements were taken for each testing square using a Mitutoyo Litematic VL-50A constant force digital micrometer (Mitutoyo Corp., Japan). The testing squares were then connected to an EnduraTEC ELF 3200 planar biaxial tensile tester (Bose, Eden Prairie, MN) using hooked 4-0 silk sutures in a 37°C bath of Ringers-Lactate solution. The testing squares were oriented for equibiaxial stretching along their circumferential and longitudinal axes. Each sample was pre-conditioned for seven cycles (*i.e.*, stretch and relaxation) followed by three cycles of data acquisition at a constant displacement rate of 0.1mm/s in the range of 0-60% strain. The resultant stress-strain relations were analyzed using Matlab™ (vR2014a, Natick, MA). More detailed tensile methodology using this setup has been described previously[40, 53, 94, 97].

Circumferential *ex vivo* energy loss and stiffness were calculated from the circumferential engineering stress-strain relation. Energy loss is the percentage of elastic energy needed to stretch the testing square that is dissipated when the tissue is relaxed. The physiological interpretation of energy loss is the percent loss of elastic recoil energy in the tissue that is

not returned to blood flow (*i.e.*, maintaining normal Windkessel function). Its physical definition is the ratio of the area between the loading and unloading curve over the area under the loading curve (**Figure 5.1-A)**. Since aortic tissue has a nonlinear stress-strain curve (**Figure 5.1-A**), stiffness is defined as the slope of a line tangent to the stress-strain loading curve; formally, this parameter is the apparent elastic modulus (defined at 50% strain) and has been reported previously to describe aortic stiffness in humans[94, 142].

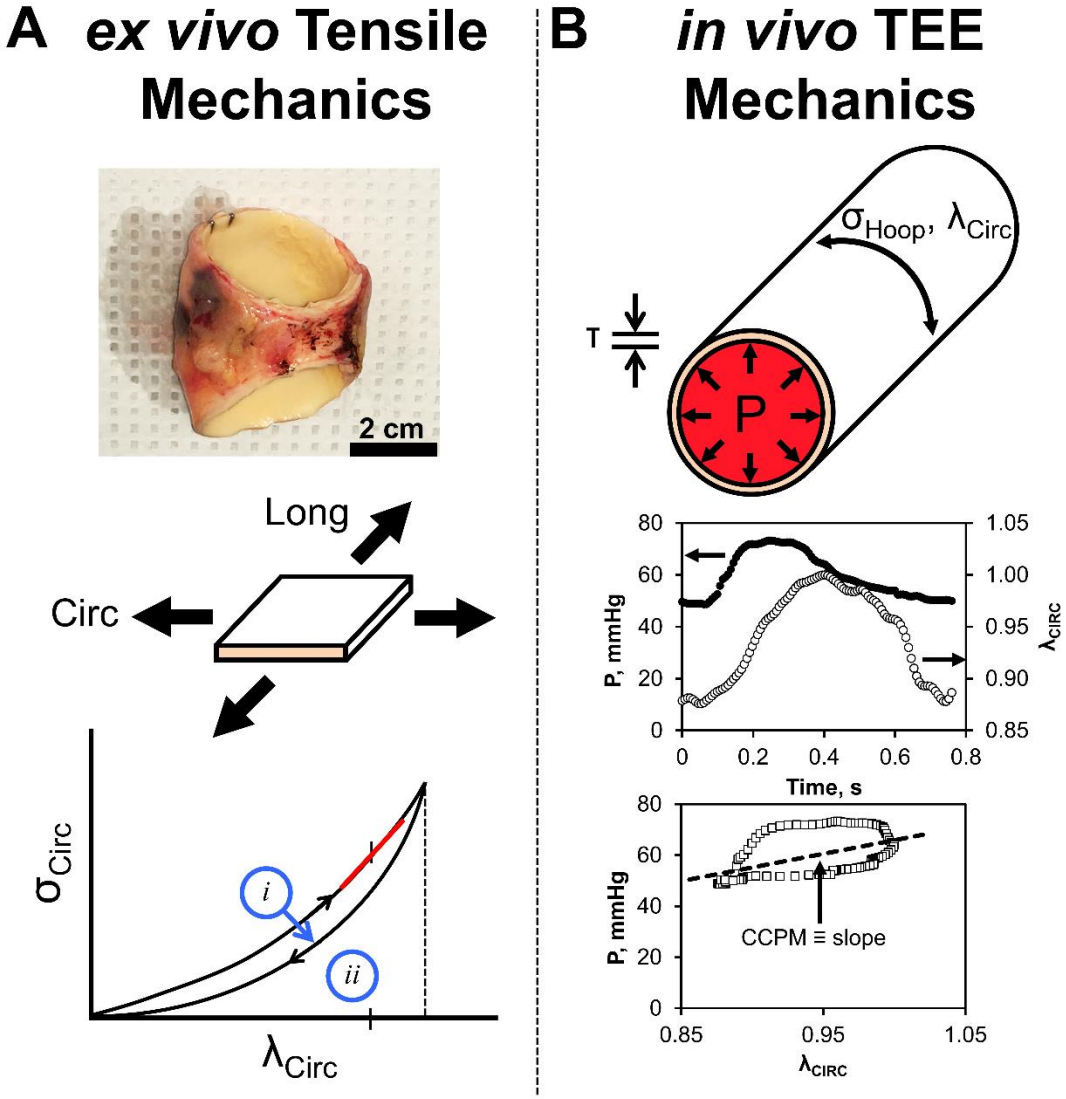

Figure 5.1. Ascending aortic mechanics using *ex vivo* tensile analysis and TEE-derived *in vivo* metrics. A) 1.5x1.5cm^2 testing squares were isolated from an aortic specimen and stretched biaxially along the circumferential (Circ) and longitudinal (Long) axes to obtain the stress-stretch profile of the aortic wall segment. Energy Loss is defined as the area between the loading curve and the unloading curve divided by the area under the loading curve: Energy Loss = Area(i)/[Area(i)+Area(ii)]x100%. Stiffness (*i.e.*, apparent modulus at 50% strain) is defined as the slope of a tangent to a defined point on the stress-strain

curve. B) *In vivo*, the aorta expands and recoils with changes in blood pressure leading to increased stresses in the vessel wall. A global (region-averaged) TEE speckle-track strain imaging profile (○) and blood pressure profile (●) were plotted for a full cardiac cycle. Blood pressure-stretch curves (□) were subsequently determined with the slope of the linear fit being defined as a novel TEE modulus, the CCPM.

Transesophageal Echocardiographic Strain Imaging

All TEE imaging was performed at the time of surgery, after administered anesthetic but before the sternotomy, using a GE Vivid 7 echocardiographic unit (GE Healthcare, Madison, WI). The TEE probe was inserted into the esophagus to the level of the great vessels to capture the point of maximum aortic dilatation. A 2-dimensional short-axis (2D-SAX) view of the AA was captured for three cardiac cycles, ensuring one non-truncated cycle. In tandem, an invasive arterial pressure trace was taken from the patient's radial artery for the same measurement interval.

TEE speckle-tracking strain analysis was performed using GE's EchoPAC™ software (GE Healthcare). Using the Q-Analysis function for the aortic short-axis, markers were manually placed around the aortic circumference and the region of interest (maximal aortic diameter) was adjusted to fit the thickness of the aortic wall. 2D ECG-gated radial strain profiles were obtained for six segments around the circumference of the aorta (**Figure 5.S.1**). Post-processing of the radial strain ($\varepsilon_{Rad}=[\lambda_{Rad}-1]\times100\%$) profile was done in Matlab™ to generate a global circumferential stretch profile of the aorta for each patient by making the assumptions *i)* of tissue incompressibility in the physiological range[143] and

ii) that physiological aortic stretch is approximately equal in the circumferential and longitudinal axes[17, 144], and therefore related by the following equation:

$$\lambda_{Circ} = \sqrt{(1/\lambda_{Rad})} \quad (5.1)$$

where λ_{Circ} and λ_{Rad} are the circumferential and radial stretches, respectively.

TEE-derived Stiffness Moduli

ECG-gating of both the radial blood pressure and the aortic stretch allowed each profile to be defined on the same cardiac cycle time domain (**Figure 5.1-B**). Then, plotting each value of stretch and the phase shifted pressure at each time step generated a unique pressure-stretch curve for each patient (**Figure 5.1-B**). The generated curve creates a hysteresis loop similar to the *ex vivo* stress-strain curve. However, the shapes of the curves are distinctly different because of the assumption of translating blood pressure to a tissue stress and the limitations in the scale and rate of strain produced *in vivo*. Therefore, we use the average slope of the pressure stretch-loop as a metric for comparison. This novel mechanical parameter, termed the Cardiac Cycle Pressure Modulus (CCPM), is in effect a simple measure of the average aortic stiffness which does not account for variations in tissue thickness between patients. This measure captures the dynamics of both the loading (increasing tissue stresses) and unloading (decreasing tissue stresses) states of the cycle but is notably different from the *ex vivo* analysis where, by convention, stiffness is evaluated only on the loading curve.

The circumferential stress in the aortic wall was then estimated by applying Laplace's Law, which states that, for thin-walled, isotropic, cylindrical vessels, the circumferential wall stress (formally "*Hoop Stress*", σ_{Hoop}) is related to the luminal blood pressure (P) by the following:

$$\sigma_{Hoop} = PD/(2\tau) \tag{5.2}$$

where D is the aortic diameter (*i.e.*, maximum echo-measured aortic diameter) and τ is the aortic wall thickness. Using this relation, converting the pressure-stretch profile to a hoop stress-stretch profile, we generated a second stiffness modulus, termed the Cardiac Cycle Stress Modulus (CCSM) that has the following definition:

$$CCSM \equiv CCPM \times D/(2\tau) \tag{5.3}$$

This measure requires *a priori* knowledge of the aortic thickness that, for this study, was the *ex vivo* tissue thickness.

Histology

A small piece of aortic tissue adjacent to each testing square was preserved in 10%(v/v) buffered formalin. The tissue was paraffin-embedded and 7μm sections were prepared and stained with Movat's pentachrome. Two 10x-magnified images were obtained for each section: one representing the intima-media and the other representing the media-adventitia. Percent micrograph field coverage of medial elastin and collagens were quantified for each

image using ImageJ™. A single data point per patient represents an average histological quantification of all regions of inquiry around the aortic circumference.

Statistical Analysis

Statistical analysis was performed using GraphPad Prism 5.01 (GraphPad, San Diego, CA). Linear regression analysis was used to determine covariance. Covariance plots are presented with a linear regression line (solid, black) and a 95% confidence interval (dotted, black) and were considered significant with a P value ≤ 0.05.

5.6 Results

A total of 21 patients were recruited for this study. **Table 1** summarizes our study group by aortic valve phenotype, age, sex, maximum aortic diameter, pre-existing comorbidities and chronic medication. A total of 7 tricuspid aortic valve patients (TAV) and 14 bicuspid aortic valve patients (BAV) were included with mean ages of 72±12 years and 57±17 years, respectively. For 6 patients, fewer than 4 quadrants were available for *ex vivo* testing due to specimen size.

Table 5.1. Study cohort demographics—patients are distributed by aortic valve phenotype, sex and age. Pre-existing comorbidities and chronic medication use are presented.

Patient No.	Age	Sex	Ao. Valve	Max Ao. Diameter (mm)	Comorbidities	Medication
1	44	F	BAV	36	AS	BB
2	50	F	BAV	42	AS	
3	52	F	BAV	42	AS, HT	ACEI, BB
4	56	F	BAV	42	HT, AS	BB
5	81	F	BAV	68	AS	
6	22	M	BAV	75	FH, latent tuberculosis	BB
7	38	M	BAV	58	AI	ARB, Statin
8	46	M	BAV	36	AS, MI	ACEI, BB, CCB, Statin
9	57	M	MECH (BAV)	55	AVR at 22years	ACEI
10	61	M	BAV	45	AI, Hypothyroidism	Levothyroxine
11	69	M	BAV	47	AS	Statin
12	72	M	BAV	49	AS, MI	
13	76	M	BAV	57	AS, AFib, Asthma	ARB, CCB, Digoxin
14	79	M	BAV	53	AS, HTN, DM	ACEI, Amiodarone
15	71	F	TAV	61	AI, COPD, MI	BB
16	86	F	TAV	60	AI, HT	ACEI, BB
17	88	F	TAV	55	AI	ACI, CCB
18	57	M	TAV	40	AI, OI	BB
19	58	M	TAV	53	AI	ARB
20	66	M	TAV	50	AS, HTN	ARB, CCB
21	77	M	TAV	50	AI, DM, HT	ACEI, CCB, Statin

Comorbidities: AFib=atrial fibrillation, AI=aortic insufficiency, AS=aortic stenosis, AVR=aortic valve replacement, COPD=chronic obstructive pulmonary disease, DM=diabetes mellitus, FH=family history, HT=hypertension, MI=myocardial infarction, OI=osteogenesis imperfecta

Medication: ACEI=ACE inhibitor, ARB=angiotensin receptor blocker, BB=beta blocker, CCB=calcium channel blocker

TEE strain imaging-derived measures of impaired aortic biomechanics

The CCPM (**Figure 5.2-A**) as well as the CCSM (**Figure 5.2-C**) demonstrated a strongly significant co-variance with *ex vivo* circumferential energy loss, (R^2=0.5873, P<0.0001) and (R^2=0.6401, P<0.0001) respectively, with larger moduli being measured in aortas with increased energy loss.

The two TEE-derived moduli were compared with *ex vivo* aortic wall stiffness, with *ex vivo* stiffness being defined as the apparent modulus at 50% strain. Our findings demonstrate that CCPM demonstrates a positive, significant covariance with the *ex vivo* apparent elastic modulus (R^2=0.2079, P=0.0378), **Figure 5.2-B**. Similarly, we observed a significant positive covariance when comparing CCSM to the *ex vivo* apparent modulus (R^2=0.3575, P=0.0042), **Figure 5.2-D**.

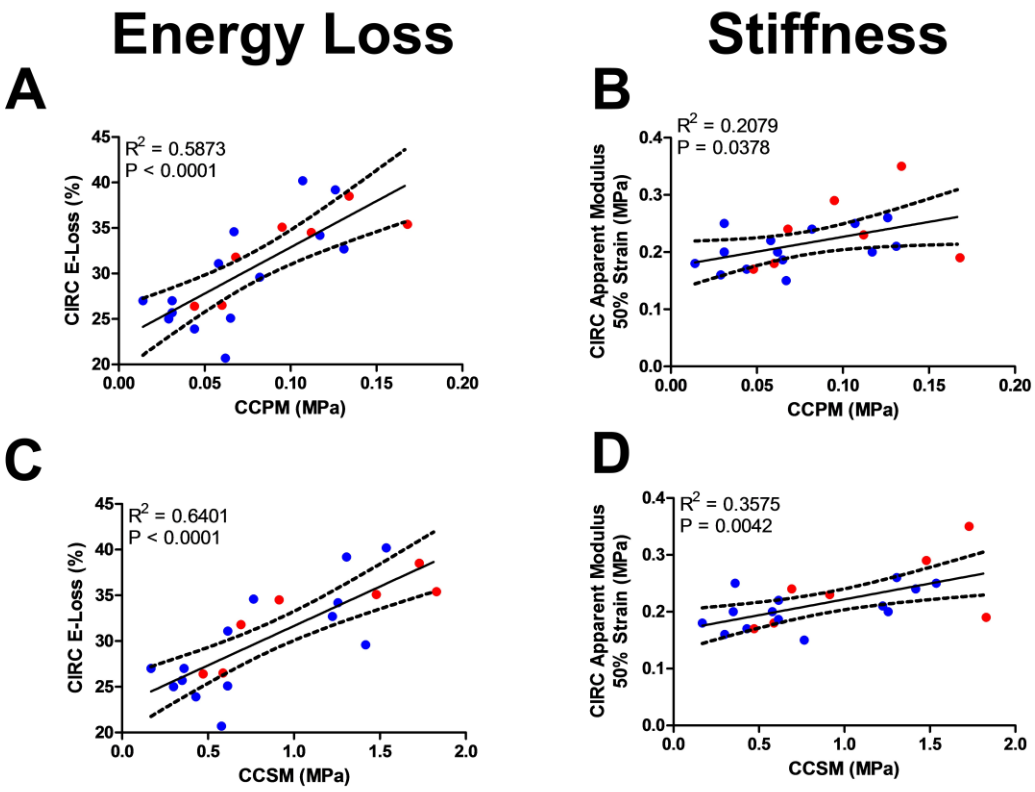

Figure 5.2. Comparison of TEE-derived moduli with *ex vivo* measures of energy loss and stiffness by regression analysis. A) *Ex vivo* circumferential energy loss and B) circumferential stiffness *vs.* CCPM. C) *Ex vivo* circumferential energy loss and D) circumferential stiffness *vs.* CCSM. Data points are distinguished by aortic valve phenotype: tricuspid aortic valve (●) and bicuspid aortic valve (●).

TEE strain imaging-derived measures as a predictor of aortic histopathology

The collagen/elastin ratio, which is a unitless fraction of the two species, co-varied significantly with the CCPM (**Figure 5.3-A**) and CCSM (**Figure 5.3-B**), (R^2=0.6165, P<0.0001) and (R^2=0.6037, P<0.0001) respectively, revealing that patients with higher proportions of medial collagens relative to elastin had greater TEE-measured moduli.

Representative histological images are presented in **Figure 5.3** to highlight the range of tissue remodeling observed in this patient cohort. This range includes little to no loss of the *de novo* aortic wall composition (bottom panel) to severe medial degeneration with nearly-complete loss of the elastic structure with sizeable deposition of collagens (top panel).

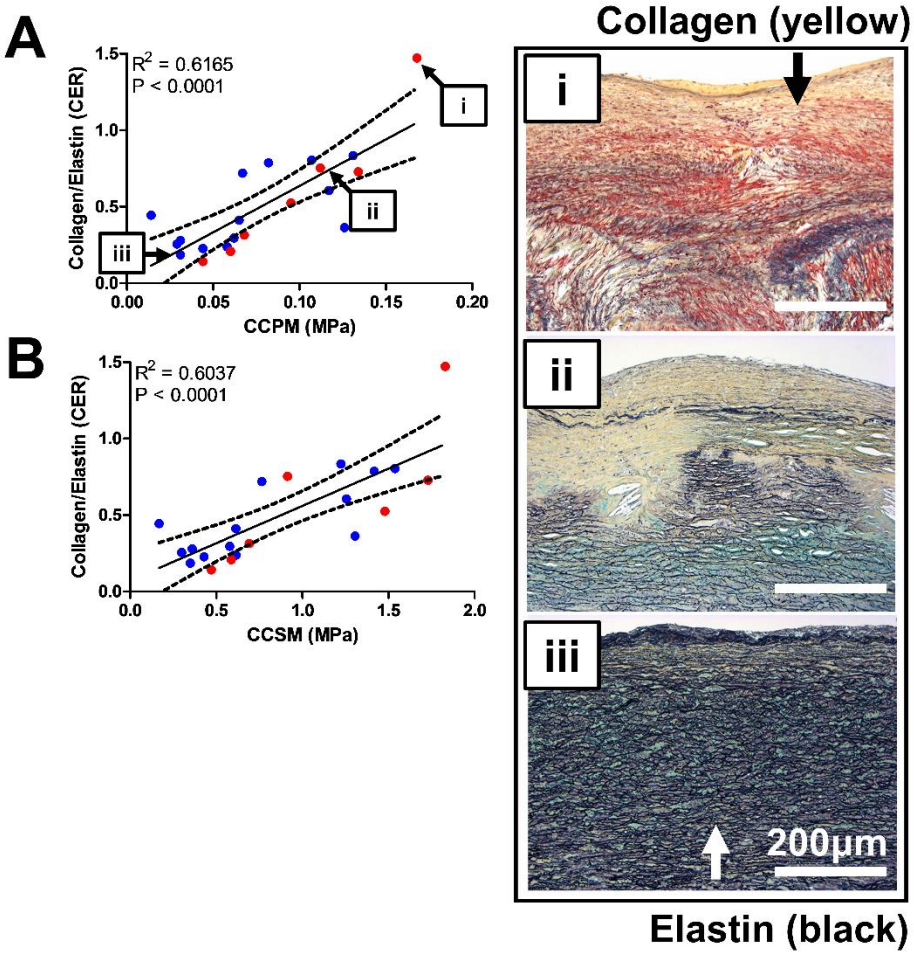

Figure 5.3. Comparison of TEE-derived moduli with aortic wall histopathology by regression analysis. A) Aortic wall collagen/elastin *vs.* CCPM. B) Aortic wall collagen/elastin *vs.* CCSM. Representative Movat-stained histological images of 3 patients reveal varied levels of collagen deposition (stained yellow) and intact or disrupted elastic

sheets (stained black). Data points are distinguished by aortic valve phenotype: tricuspid aortic valve (●) and bicuspid aortic valve (●).

Aortic Diameter as a Predictor of Impaired Aortic Biomechanics

In vivo aortic diameter was significantly correlated with *ex vivo* circumferential energy loss (R^2=0.3800, P=0.0029), **Figure 5.4-A,** but not with *ex vivo* measured circumferential stiffness (R^2=0.1486, P=0.0855), **Figure 5.4-B**. Aortic diameter was modestly correlated with aortic wall histopathology, with larger diameter aortas containing a greater proportion of collagen/elastin (R^2=0.2155, P=0.0340), **Figure 5.4-C**.

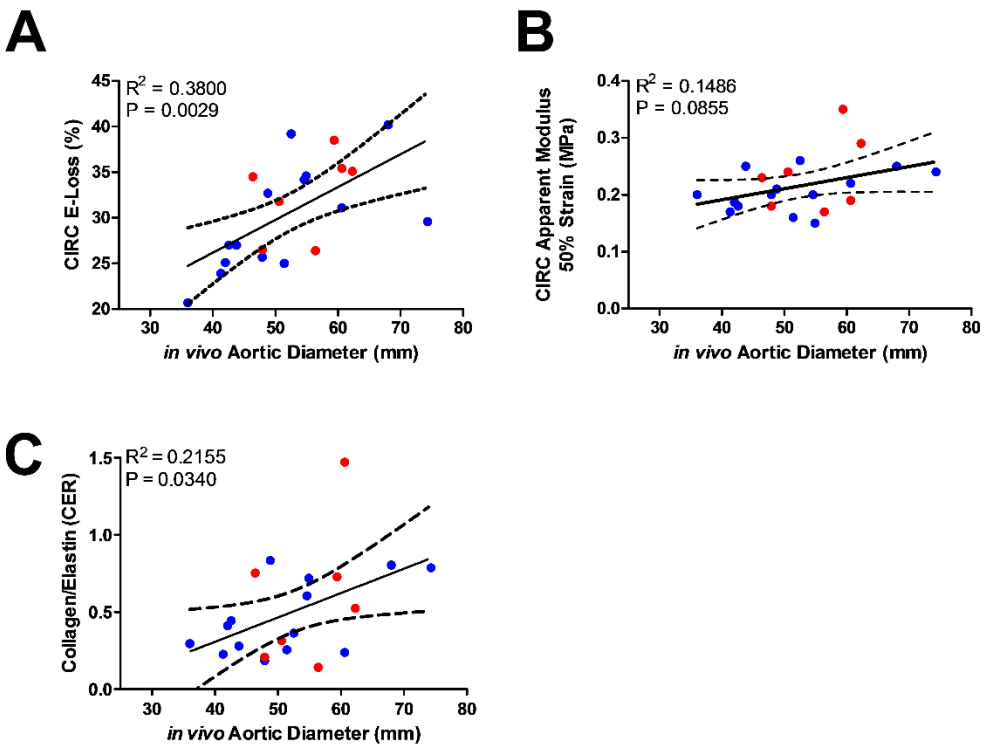

Figure 5.4. Comparison of aortic size with *ex vivo* biomechanics and histopathology. A) *Ex vivo* circumferential energy loss *vs. in vivo* aortic diameter. B) *Ex vivo* circumferential stiffness *vs. in vivo* aortic diameter. C) Aortic wall collagen/elastin *vs. in vivo* aortic diameter. Data points are distinguished by aortic valve phenotype: tricuspid aortic valve (●) and bicuspid aortic valve (●).

Finally, to illustrate how the CCPM and CCSM can be applied to improving patient outcome, these values were plotted as a function of aortic diameter to establish a 2-dimensional risk assessment (**Figure 5.5-A&B, respectively**). The CCPM or CCSM as the vertical axis describes the risk associated with impaired mechanical function and pathological remodeling that can occur irrespective of aortic diameter. The correlations are low. This indicates that both indices identify features that are not identical with aortic

diameter and therefore, potentially, could contribute independent information as to risk. Indeed, 3 patients below the surgical threshold with large echo moduli were identified. Histological assessment of these patients confirmed a pathological disruption of the elastic structure with accumulated collagen deposition (**Figure 5.5-panels:*,†,‡**). Furthermore, 2 patients above the surgical threshold with low echo moduli were identified as having a less pathological aortic wall with intact elastic lamellae and little collagen (**Figure 5.5-panels:§,‖**).

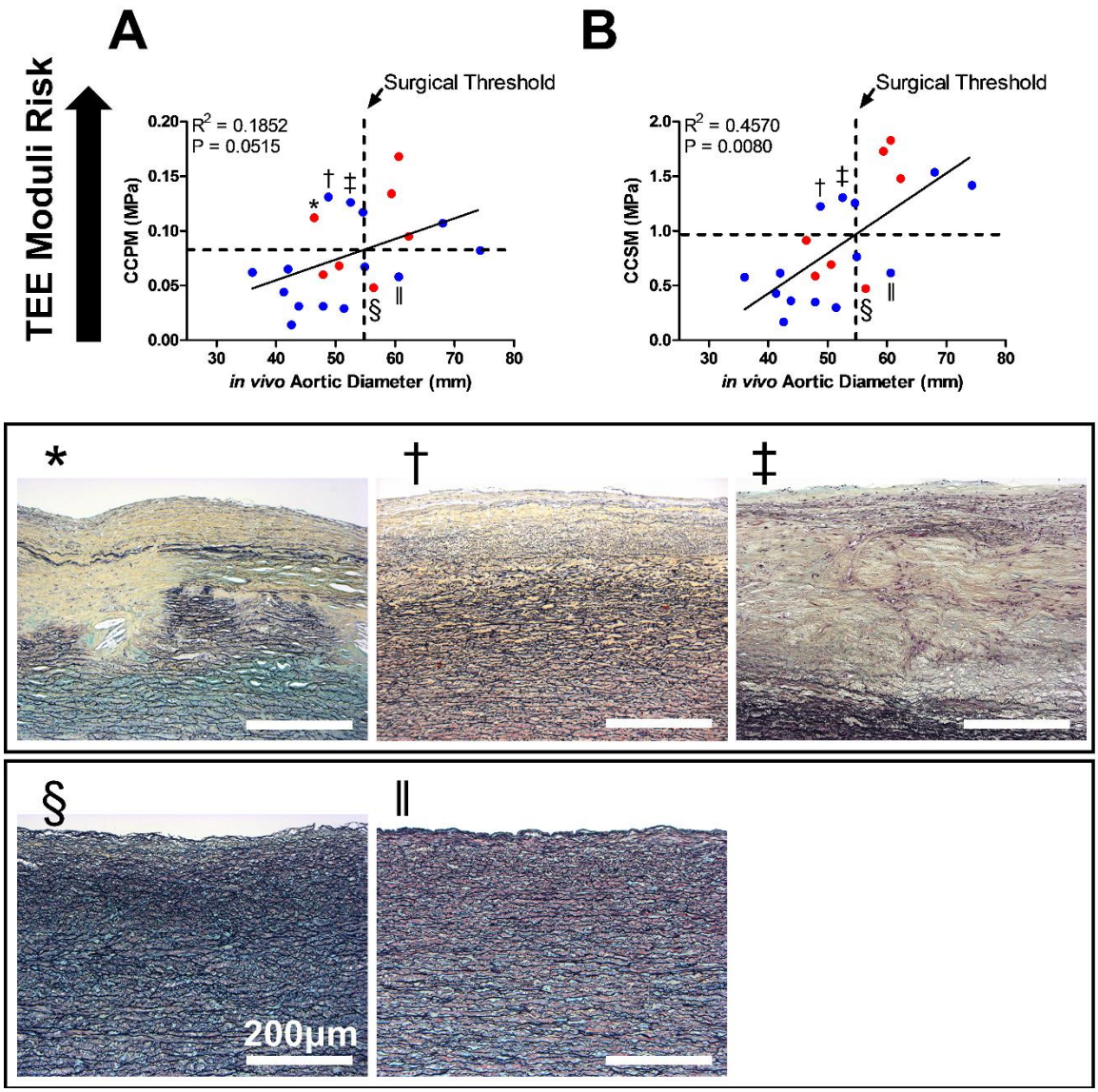

Figure 5.5. Comparison of TEE-derived moduli with aortic size as a method to identify at-risk patients. A) CCPM *vs. in vivo* aortic diameter. B) CCSM *vs. in vivo* aortic diameter. The vertical dotted line is the current surgical threshold of ≥5.5 cm while the horizontal dotted line is defined at the intercept of the linear regression and the surgical threshold. Histopathology panels of Movat-stained sections of the AA wall: high echo moduli, low AA diameter (patients:*,†,‡); low echo moduli, large AA diameter (patients:§,‖). Data

points are distinguished by aortic valve phenotype: tricuspid aortic valve (●) and bicuspid aortic valve (●).

A summary of the comparisons between the TEE-derived aortic measurements and moduli and *ex vivo* measures, including the tensile mechanics and wall histopathology, are presented in **Table 5.2**.

Table 5.2. Aortic size, mechanical and histopathological comparisons and the corresponding regression coefficients and P-values.

		***Ex vivo* tensile mechanics**		**Histopathology**
		Energy Loss	Stiffness (Apparent Modulus)	Collagen/Elastin
In vivo **Aortic Diameter**		** R^2=0.3800, P=0.0029	n.s. R^2=0.1486, P=0.0855	* R^2=0.2155, P=0.0340
***In vivo* TEE mechanics**	CCPM	*** R^2=0.5873, P<0.0001	* R^2=0.2079, P=0.0378	*** R^2=0.6165, P<0.0001
	CCSM	*** R^2=0.6401, P<0.0001	** R^2=0.3575, P=0.0042	*** R^2=0.6037, P<0.0001

5.7 Discussion

Current clinical guidelines assume that there is a critical aortic diameter at which the risk of catastrophic tissue failure increases dramatically[22, 145]. Aortic dilation is, unquestionably, a hallmark of the disease but does not represent an intrinsic tissue material property. Aortic dilatation also fails to relay the magnitude of stress or concentration of stress in the aortic

wall. Accordingly, our aim was to use TEE speckle tracking with blood pressure to devise novel *in vivo* stiffness moduli based on tissue biomechanics, which might help stratify at-risk patients beyond aortic diameter alone.

Using 2D-SAX AA strain imaging with concurrent blood pressure tracing, we developed moduli of the pressure-stretch (CCPM) and stress-stretch (CCSM) cardiac cycle average loop. Both the CCPM and CCSM significantly predicted the variance of *ex vivo* energy loss. Similarly, the CCPM and CCSM significantly predict *ex vivo* stiffness. Both indices performed better than aortic diameter.

Both echo moduli and aortic diameter were much more closely related to energy loss than to *ex vivo* stiffness. These observations are of interest since other studies have shown that energy loss is representative of aortic wall histopathology[94, 142, 146] and has been found to increase in regions of chronic aortic dissection[147] while aortic stiffness did not significantly correlate with tissue histopathology[94]. Moreover, *ex vivo* stiffness (50% apparent modulus) is defined at a single strain value. Accordingly, small variations in *ex vivo* measurements, such as the suture placement during tensile testing, can have a considerable impact on the calculated stiffness because of its highly nonlinear relationship with strain. By contrast, *ex vivo* energy loss is much less susceptible to these pitfalls since it is, by definition, a self-normalizing value, averaged over a full stress-stretch cycle.

CCSM was more highly correlated with *ex vivo* aortic energy loss and stiffness than the CCPM. This may be due to including actual aortic anatomical dimension in the calculation

of CCSM rather than simple blood pressure in calculation of CCPM. On the other hand, CCPM has the practical advantage that it requires only standard blood pressure tracing and TEE strain imaging whereas CCSM requires measurement of the aortic wall thickness that, for this study, was taken *ex vivo*. For the CCSM to become a fully *in vivo* measure, an accurate methodology to measure aortic tissue thickness must be established. MRI has sufficient resolution[45] while axial high-frequency echo resolution is ~0.25 mm[148] and therefore cannot precisely measure regional and inter-patient differences in aortic thickness[53, 93].

Histopathological change in the AA wall is a central marker of the disease process in degenerative AA aneurysm[141]. In particular, the content of the structural proteins, collagen and elastin, is altered significantly in the pathological remodeling process of the AA wall[141]. Both the CCSM and CCPM correlated strongly with the collagen/elastin ratio in the AA. Aortic diameter also significantly correlated with collagen/elastin but the strength of the correlation was much less.

Other TEE measures have been used to describe stiffness in the ascending aorta[14, 15, 130, 136, 137]. The most common is the β stiffness index ($\beta=\ln[P_S/P_D]/[(D_{max}-D_{min})/D_{min}]$), a two-point measure that relates the systolic/diastolic pressure ratio to the change in AA diameter (D)[109]. Unlike the moduli presented in this study, β does not account for the temporal component of strain or pressure. In a study of 17 patients, Alreshidan *et al.* have shown that the β stiffness index is not predictive of regional *ex vivo* stiffness in the AA[137]. In this cohort, we observed that β did not significantly correlate with *ex vivo* stiffness and only

moderately correlated with energy loss and histopathology, performing worse than both the CCPM and CCSM (**Figure 5.S.2**).

Aortic diameter is, unquestionably, an important maker of the risk of rupture or dissection. However, equally clearly, it is not sufficient, since at least 40% of these catastrophic events occur at an aortic diameter below the threshold for surgical intervention. To be of clinical value, any additional marker must contribute new information as to risk. That is why the relatively low correlation between CCSM and CCPM with aortic diameter is encouraging because it suggests that if CCSM and CCPM are shown in prospective studies to be significant markers of risk that they may well contribute prognostic information that is independent of, and therefore additive to, aortic diameter.

5.8 Study Limitations

Our cohort is similar in size to others that have been designed to compare *in vivo* parameters with *ex vivo* measures of risk [53, 85, 137]. It was designed to validate two novel non-invasive measures against *ex vivo* measures of aortic wall function and structure. It was not designed to determine whether these novel measures contribute significant prognostic information as to the risk of a catastrophic aortic event in patients with aneurysms of the ascending aorta. Second, assigning one modulus value per patient relies on the average strain profile around the circumference of the aorta which was rarely uniform regionally. This potentially limits our understanding of the regional differences in AA wall behavior and its connection to patient risk. Finally, this method relies on a non-truncated short-axis view of the aorta.

Owing to a known blind spot at the level of the tracheal carina, the distal ascending aorta and aortic arch are obscured from TEE view.

Although energy loss has been reported as a robust mechanical measure that corresponds to the pathological state of the aortic wall, no prospective study has been conducted that links energy loss with clinical occurrence of acute dissection or rupture. Furthermore, the limited range of strain during the cardiac cycle makes estimating *in vivo* energy loss difficult.

5.9 Conclusion

This study involved a cohort of patients with a broad range of AA dilation above and below surgical criteria of ≥5.5cm. We have demonstrated that two novel TEE-derived strain imaging moduli can be obtained non-invasively and correlate highly with *ex vivo* mechanics and histopathology. AA diameter, which is used as surgical criteria, is considerably less predictive of these properties. The present findings support prospective testing of CCPM and CCSM as novel non-invasive markers of the risk of aortic rupture or dissection.

5.10 Supplementary Material

The following appeared as supplementary material made available with the published article:

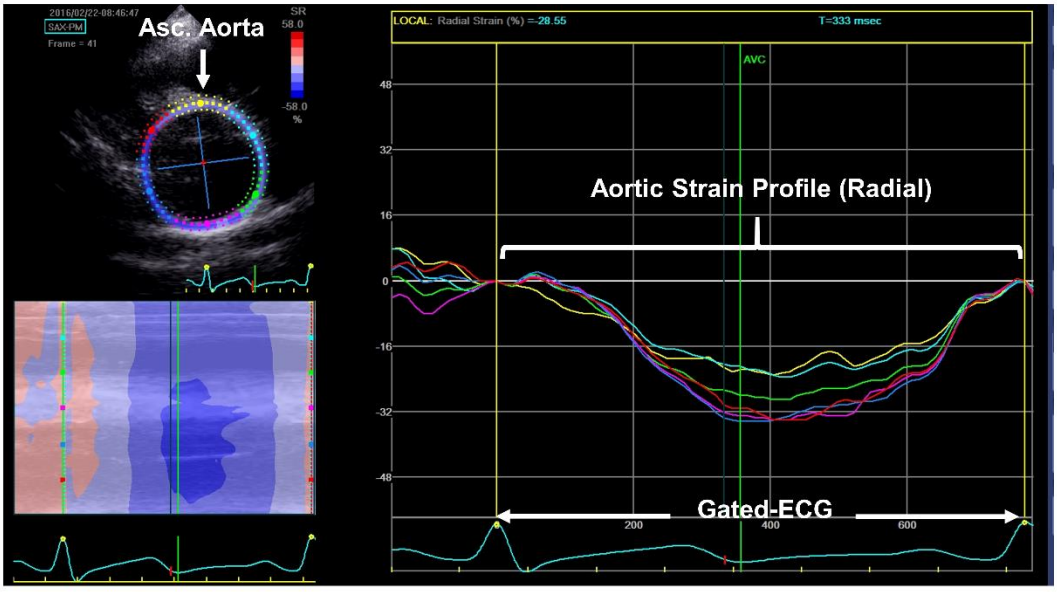

Figure 5.S.1. Representative ECG-gated radial strain profile of the ascending aorta using EchoPac™.

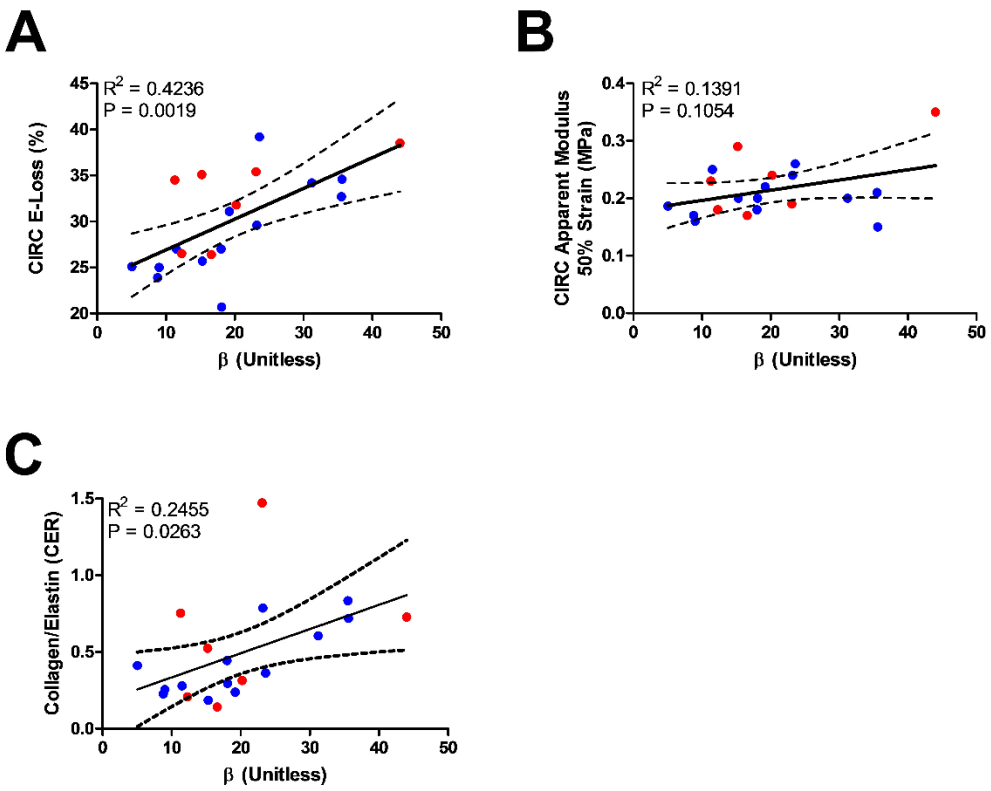

Figure 5.S.2. Comparison of β stiffness index with *ex vivo* biomechanics and histopathology**.** A) *Ex vivo* circumferential energy loss *vs.* β stiffness index. B) *Ex vivo* circumferential stiffness *vs.* β stiffness index. C) Aortic wall collagen/elastin *vs.* β stiffness index. Data points are distinguished by aortic valve phenotype: tricuspid aortic valve (●) and bicuspid aortic valve (●).

Chapter 6: Measuring Non-uniform Wall Motion and Regional Biomechanics of the Ascending Aorta Using Transesophageal Echocardiography

6.1 Preface

This chapter is a submitted manuscript in The Journal of Thoracic and Cardiovascular Surgery (April 2018). As discussed in the previous chapter, global (*i.e.*, circumference-averaged) CCPM and CCSM were predictive tensile indices (energy loss and stiffness) as well as collagen/elastin content. Although global values appear to accurately represent the mechanical state of the aortic wall, they do not provide any information about local differences in tissue motion or stiffness. Since dissection of the aortic wall is a localized phenomenon, global parameters limit the interpretation of our moduli in this context. This chapter addresses this limitation by identifying the values of CCPM and CCSM at four distinct regions around the aortic circumference. Similarly, *ex vivo* energy loss, stiffness, aortic thickness and histology were measured from resected tissue samples at the identical loci. It was found that considerable heterogeneity in regional strain occurred and occasionally resulted in compression of one or more of the regional segments. From this data, regional heterogeneity in CCPM and CCSM was discovered to increase as the vessel wall exhibited increase energy loss and stiffness.

6.2 Article

Measuring Non-uniform Wall Motion and Regional Biomechanics of the Ascending Aorta Using Transesophageal Echocardiography

Emmott, Alexander[a,b]; Alzahrani, Haitham[c]; Therrien, Judith[d]; Lachapelle, Kevin[c]; Leask, Richard L.[a,b,*]

a-Department of Chemical Engineering, McGill University, Montreal, QC, Canada

b-Research Centre, Montreal Heart Institute, University of Montreal, Montreal, QC, Canada

c-Department of Cardiac Surgery, Royal Victoria Hospital – Glen Campus, MUHC, Montreal, QC, Canada

d-Department of Adult Cardiology, Royal Victoria Hospital – Glen Campus, MUHC, Montreal, QC, Canada

*Corresponding Author: Leask, Richard L. Room 3060, 3610 University Street Montreal, QC, Canada, H3A 0C5. Phone: 1-514-398-4494; Fax: 1-514-398-6678 (email: **richard.leask@mcgill.ca)**

6.3 Abstract

Background: *In vivo* ascending aortic (AA) stiffness measurements using speckle track echocardiography (STE) have been shown to adequately describe the average mechanical dysfunction of the vessel wall. Dissection and rupture of the AA are localized failure of the tissue. This study identifies regional heterogeneity in the STE-derived *in vivo* strain and calculated stiffness and compares the results with *ex vivo* biomechanics and histopathology.

Methods: Twenty-one patients undergoing aortic resection were recruited for this study. TEE imaging of the aortic short-axis and invasive radial blood pressure traces were taken to calculate the cardiac cycle pressure modulus (CCPM) and cardiac cycle stress modulus (CCSM) for 4 regions around the aortic circumference: inner (IC) and outer (OC) curvature and the anterolateral (AL) and posterolateral wall (PL). From the resected aortic ring, testing squares were isolated from the identical regions for *ex vivo* mechanical analysis and histopathology. *Ex vivo* energy loss and apparent stiffness were calculated for comparison with the CCPM and CCSM.

Results: Twelve patients showed at least one region of compression over the cardiac cycle. Regional CCPM and CCSM were correlated with the regional *ex vivo* energy loss (*vs.* regional CCPM: R^2=0.2226, P<0.0001; *vs.* regional CCSM: R^2=0.3447, P<0.0001) and regional apparent stiffness (*vs.* regional CCSM: R^2=0.2022, P<0.001). Furthermore, an increase in Max ΔCCPM and Max ΔCCPM, measures of regional heterogeneity, coincides with an increase in average *ex vivo* stiffness and energy loss.

Conclusion: Compression of one or more regions was seen in half the patients. CCPM and CCSM showed increased regional heterogeneity in degenerative AA tissue. The AL and OC

regions were found to be under tensile strain more frequently and the thinnest regions on average (14 of 21 patients).

6.4 Introduction

Aneurysm of the ascending aorta (AA) is an insidious disease that carries significant risk of mortality that can be corrected with elective surgery. The predominant criterion for surgical intervention is aortic size, which is known to be an insufficient predictor of the localized phenomenon of acute dissection or rupture[149]. Based on data from the International Registry of Acute Aortic Dissection (IRAD), Pape *et al.* reported that approximately 59% of all AA aneurysms will dissect below the threshold of intervention[140]. A biomechanics-based approach to aortic stability could add a much-needed dimension to surgical management by identifying patient-specific mechanical dysfunction in the aortic wall. So far, *ex vivo* mechanical studies on the resected AA wall have identified metrics that scale with the histopathology of the disease (*i.e.*, stiffness[53, 85], energy loss[94, 142] and ultimate strength[85]). Advances in medical strain imaging from CT, MRI and echo have made it possible to apply these metrics pre-operatively[15, 130, 132, 136, 150].

TEE-derived stiffness has identified differences in aortic compliance in patients categorized by age[130] or aortic valve phenotype[136]. Our group has recently shown that global circumferential ascending aortic echo-derived stiffness correlates with *ex vivo* mechanical measures and aortic wall histopathology, providing information that is independent of aortic size[137, 151]. These global cardiac cycle pressure and stress moduli (abbreviated as CCPM and CCSM) provide a good indication of the mechanical function of the vessel wall,[151] however a large prospective trial is needed to determine if these measures improve patient selection for intervention.

Although global parameters may accurately describe the mechanical dysfunction corresponding to aortopathy, there is evidence that AA dissections or rupturing originate from local phenomena, occurring most frequently as transverse tears[52] along the outer curvature (OC) of the vessel[152]. *Ex vivo* studies have shown that the tensile properties of the AA are only moderately heterogeneous around the aortic circumference in both healthy[153] and dilated pathologies[53, 95]. However, testing aortic tissue *ex vivo* is dependent on applying uniform strain or stress to the tissue. This testing does not take into consideration the biomechanical effects of surrounding structures and the composite physiologic behavior of the aorta as a whole unit through the cardiac cycle.

This present study sought to determine the *in vivo* regional tissue deformations and regional stiffness in the ascending aortic aorta using transesophageal 2D strain echocardiography (2DSE) combined with radial blood pressure tracing. Region-adjacent differences in echo stiffness parameters were subsequently calculated to identify the level of heterogeneity in vessel wall deformation within the transverse axis of the AA. These values computed from the echo strain-imaging data and subsequently compared with *ex vivo* mechanical indices and histopathology.

6.5 Methods

Study Cohort

Informed consent was obtained from 21 patients undergoing elective aortic resection surgery with or without aortic valve correction. Mild to severe aortic dilatation was represented in this study with AA diameters ranging from 3.6–6.1 cm. This study was conducted in

compliance with the Canadian tri-council policy statement on ethical conduct for research involving humans.

Regional Biomechanics by Transesophageal Echocardiographic Strain Imaging

TEE imaging was performed using GE Vivid 7 echocardiographic units (GE Healthcare, Madison, WI) on anesthetized patients before receiving sternotomy. The TEE probe was inserted into the esophagus to the level of the aortic root or proximal AA to capture a 2-dimensional short-axis (2D-SAX) view at the point of maximum dilatation. Three ECG-gated strain cycles were captured and, in tandem, an ECG-gated invasive radial artery pressure trace was taken for the same three heartbeats.

TEE speckle-tracking strain analysis was performed using the quantitative analysis toolkit in GE's EchoPAC™ software (GE Healthcare, Norway) and described previously[151]. In brief, user-selected markers were placed around the aortic circumference and adjusted to fit the inner and outer wall aortic radii. 2D radial strain profiles were obtained for six default segments around the circumference of the aorta and subsequently combined to generate regional circumferential stretch profiles for the inner (IC) and outer curvature (OC) and the anterolateral (AL) and posterolateral (PL) walls, **Figure 6.1-A**. Strain-gating was performed with the reference position at end-diastole (QRS).

Using the strain definition provided by Voigt *et al.*[126] for 2D speckle-track echo ($\varepsilon=[\lambda-1]$; $\lambda=L/L_0$), radial strain (ε_{Rad}) was converted to radial stretch (λ_{Rad}). Second, the circumferential stretch (λ_{Circ}) profile was calculated from the λ_{Rad} profile by $\lambda_{Circ}=\sqrt{(1/\lambda_{Rad})}$, which describes

the conservation of tissue volume assuming stretching is both incompressible[143] and that circumferential and longitudinal stretching is equibiaxial[17, 144] in the physiological range. Using these values, pressure-stretch loops for each quadrant were generated from the time-shifted radial pressure trace and the λ_{Circ}, **Figure 6.1-B,** similar to those described by Lang *et al.*[132] and Pagani *et al.*[129]

Two echo-derived moduli were calculated. The Cardiac Cycle Pressure Modulus (CCPM), is defined as the slope of the linear fit through the pressure-stretch data, **Figure 6.1-B**. The Cardiac Cycle Stress Modulus (CCSM), is a correction of the pressure-derived CCPM by calculating the circumferential stress using Laplace's Law: $CCSM \equiv CCPM \times D/(2\tau)$, **Figure 6.1-C**. In this definition, which assumes a thin-walled cylindrical vessel, τ is *ex vivo* the tissue thickness and D is the maximum echo-measured AA diameter.

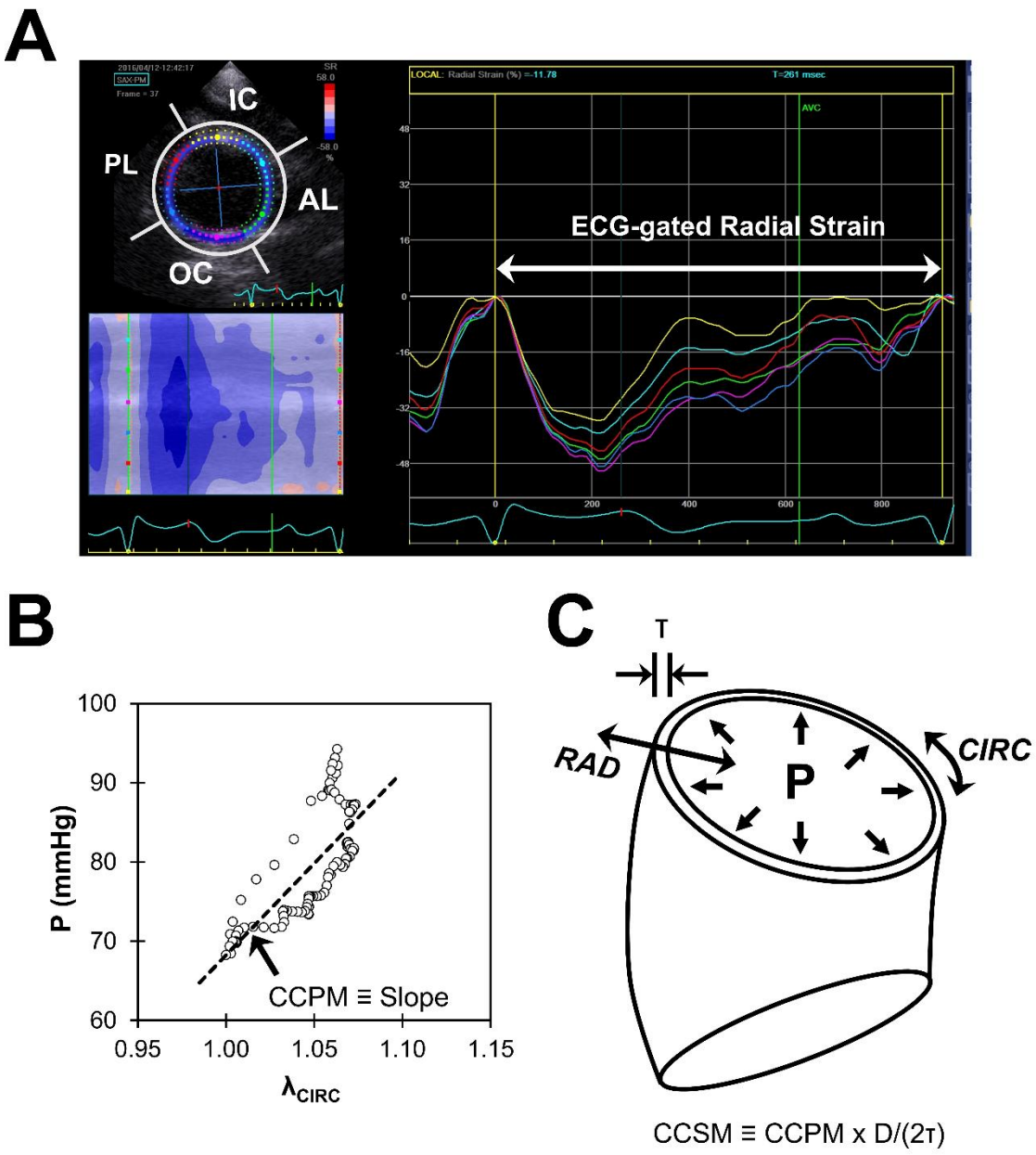

Figure 6.1. *In vivo* ascending aortic biomechanics by transesophageal echocardiography. A) Regional ECG-gated strain imaging of the aortic short axis using GE EchoPac™. B) Gated regional circumferential stretch (λ_{CIRC}) and gated blood pressure (P) data were used to generate the CCPM, defined as the slope of a linear fit through the pressure-stretch curve. C) A second regional modulus (CCSM) was derived by using Laplace's law to convert blood

pressure to circumferential stress. IC-inner curvature, AL-anterolateral wall, OC-outer curvature, PL-posterolateral wall.

The regional variabilities corresponding to each of the moduli were calculated (**Max ΔCCPM** and **Max ΔCCSM**). They are defined as the maximum absolute value per patient of the moduli difference between nearest-neighbor regions, *e.g.*, Max ΔCCPM≡abs[$CCPM_i$-$CCPM_{i\pm1}$]. For instance, if *i* represents the IC quadrant then $i_{\pm1}$ represents either the AL or PL quadrant; this was repeated for all possible nearest-neighbor combinations, and the maximum value for each patient was reported.

Ex vivo Tensile Analysis

During the surgical procedure, the resected aortic ring was obtained, clipped for anatomical orientation by the surgeon and stored in physiological saline at 4°C (**Figure 6.2-A**). Within 24 hours of resection, four 1.5×1.5cm^2 testing squares were prepared from the specimen for each of the defined regions around the aortic circumference: the inner curvature (IC), the anterolateral (AL) wall, the outer curvature (OC) and the posterolateral (PL) wall (**Figure 6.2-B**). Five unique thickness measurements were taken for each testing square using a Mitutoyo Litematic VL-50A constant force digital micrometer (Mitutoyo Corp., Japan). The testing squares were then placed in a 37°C bath of Ringers-Lactate solution and fastened to the displacement arms of an Electroforce ELF 3200 planar biaxial tensile tester (TA Instruments, New Castle, DE) using hooked 4-0 silk sutures. The testing squares were oriented for equibiaxial stretching along their circumferential (CIRC) and longitudinal (LONG) axes (**Figure 6.2-C**). Each sample was pre-conditioned for seven testing cycles of

stretch and relaxation followed by three cycles of data acquisition at a constant displacement rate of 0.1mm/s from 0-60% strain. The subsequent regional stress-strain relations were analyzed using Matlab™ (vR2014a, Natick, MA) following a methodology that has been previously described [40, 53, 94, 97].

Two *ex vivo* parameters were calculated from the circumferential engineering stress-strain relation for each regional testing square: 1) energy loss and 2) stiffness. The first, energy loss, is a viscoelastic measure that is defined as the ratio of the area between the loading and unloading curves to the area under the loading curve (**Figure 6.2-D**). Energy loss represents the percentage of elastic energy needed to stretch the testing square that is not recovered when the tissue is relaxed. The second *ex vivo* parameter, stiffness, is presented as the apparent elastic modulus at 50% strain. The apparent elastic modulus is defined as the slope of a line tangent to the hyperelastic stress-strain loading curve at a 50% strain value (**Figure 6.2-D**) and has been used previously to describe AA stiffness[94, 142, 151].

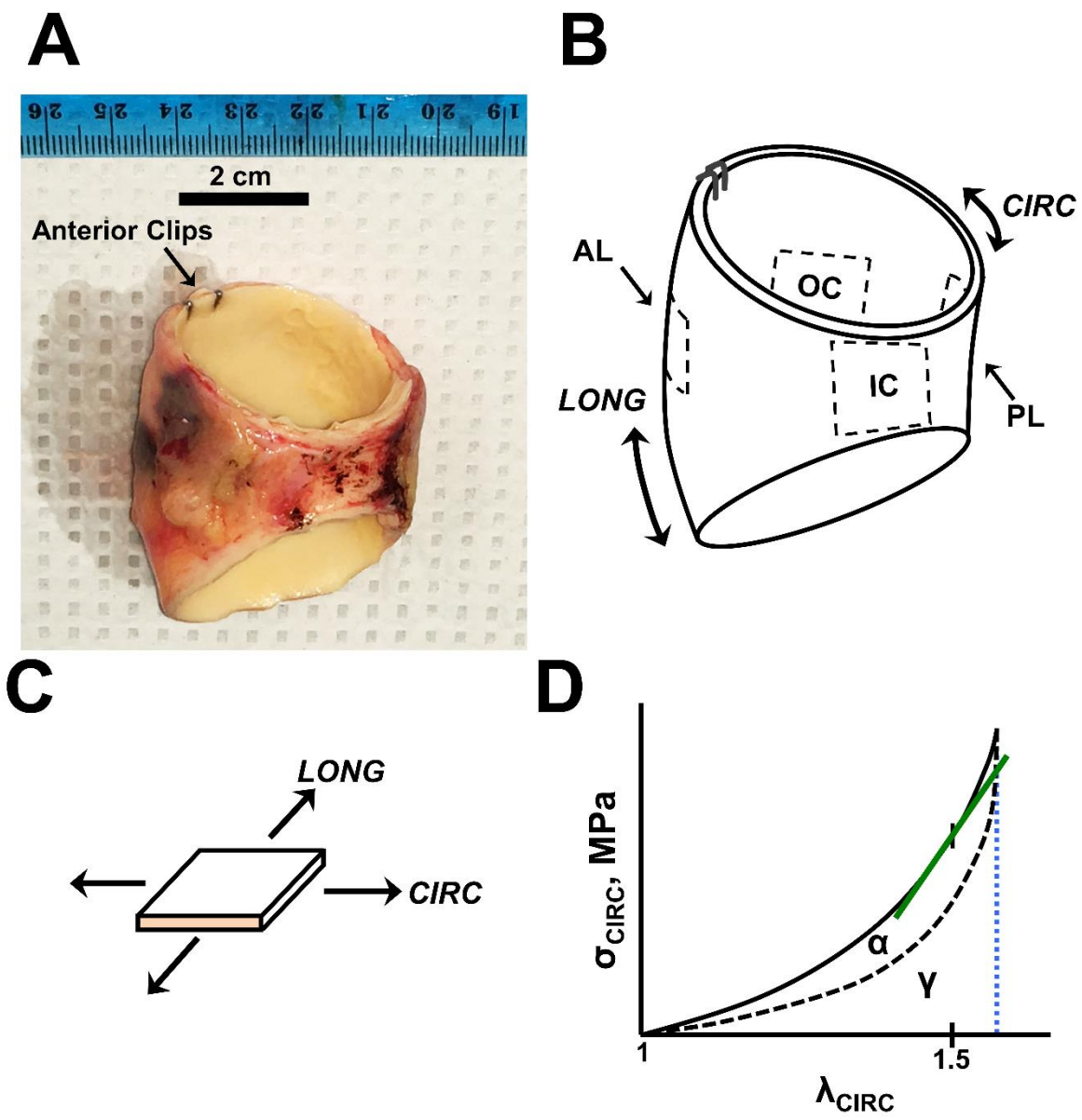

Figure 6.2. *Ex vivo* ascending aortic biomechanics by biaxial tensile testing. A) Surgical specimens were clipped for orientation and B) 1.5x1.5cm^2 testing squares were isolated for each of the four aortic regions. C) Each square underwent biaxial tensile testing to 60% strain with stretching along the circumferential (CIRC) and longitudinal (LONG) axes. D) Two *ex vivo* parameters were calculated from the circumferential stress-strain data for each testing square: 1) energy loss (≡100%×Area[α]/Area[α+γ]) and 2) the apparent elastic modulus at

50% engineering strain (slope of the green line). IC-inner curvature, AL-anterolateral wall, OC-outer curvature, PL-posterolateral wall.

Statistical Analysis

Statistical analysis was performed using GraphPad Prism 5.01 (GraphPad, San Diego, CA). Box-whisker diagrams use a two-way ANOVA and Bonferroni post-hoc test to determine regional differences in our study group. Each box represents the position of the 1st and 3rd quartile with a horizontal line representing the group median and whiskers representing the maximum and minimum values in each respective group. Linear regression analysis was used to determine covariance. Covariance plots are presented with a linear regression line (solid, black) and a 95% confidence interval (dotted, black) and were considered significant with a P-value ≤ 0.05.

6.6 Results

Twenty-one patients receiving aortic resection with or without concomitant aortic valve repair were recruited for this study. **Table 6.1** characterizes this patient cohort by age, sex, aortic valve phenotype, existing comorbidities and medication use. A total of 7 tricuspid aortic valve (TAV) and 14 bicuspid aortic valve (BAV) patients were included with mean ages of 72±12 years and 57±17 years, respectively. For 6 patients, fewer than 4 quadrants were available for *ex vivo* testing due to specimen size.

Table 6.1. Study cohort demographics—patients are distributed by aortic valve phenotype, sex and age. Pre-existing comorbidities and chronic medication use are presented.

Patient No.	Age	Sex	Ao. Valve	Max Ao. Diameter (mm)	Comorbidities	Medication
1	44	F	BAV	36	AS	BB
2	50	F	BAV	42	AS	
3	52	F	BAV	42	AS, HT	ACEI, BB
4	56	F	BAV	42	HT, AS	BB
5	81	F	BAV	68	AS	
6	22	M	BAV	75	FH, latent tuberculosis	BB
7	38	M	BAV	58	AI	ARB, Statin
8	46	M	BAV	36	AS, MI	ACEI, BB, CCB, Statin
9	57	M	MECH (BAV)	55	AVR at 22years	ACEI
10	61	M	BAV	45	AI, Hypothyroidism	Levothyroxine
11	69	M	BAV	47	AS	Statin
12	72	M	BAV	49	AS, MI	
13	76	M	BAV	57	AS, AFib, Asthma	ARB, CCB, Digoxin
14	79	M	BAV	53	AS, HTN, DM	ACEI, Amiodarone
15	71	F	TAV	61	AI, COPD, MI	BB
16	86	F	TAV	60	AI, HT	ACEI, BB
17	88	F	TAV	55	AI	ACI, CCB
18	57	M	TAV	40	AI, OI	BB
19	58	M	TAV	53	AI	ARB
20	66	M	TAV	50	AS, HTN	ARB, CCB
21	77	M	TAV	50	AI, DM, HT	ACEI, CCB, Statin

Comorbidities: AFib=atrial fibrillation, AI=aortic insufficiency, AS=aortic stenosis, AVR=aortic valve replacement, COPD=chronic obstructive pulmonary disease, DM=diabetes mellitus, FH=family history, HT=hypertension, MI=myocardial infarction, OI=osteogenesis imperfecta

Medication: ACEI=ACE inhibitor, ARB=angiotensin receptor blocker, BB=beta blocker, CCB=calcium channel blocker

Regional Ascending Aortic Strain

Regional TEE strain profiles for each respective patient revealed that strain was not uniform around the AA circumference with two different patterns of strain. One pattern consisted of tensile strain in all regions. For example, in **Patient 18**, all regions experienced a temporal increase in strain with an increase in blood pressure (*i.e.*, all regions under tension), **Figure 6.3-A**. The second pattern consisted of tensile strain in some regions with compressive strain in others. In **Patient 16**, one region (IC) experienced a temporal decrease in strain with an increase in blood pressure (*i.e.*, IC is under compression), **Figure 6.3-B**. Within the 21 patient cohort, N=10 (48%) patients exhibited compression of one-or-more regions (N_{TAV}=3/7 & N_{BAV}=7/14). **Table 2** presents the regional frequency in which compression was observed out of a total of 12 observations.

Table 2. Frequency of compression observations categorized by aortic quadrant

Total	IC	AL	OC	PL
N=12 (100%)	N=4 (33.3%)	N=3 (25.0%)	N=1 (8.33%)	N=4 (33.3%)

Regional Ascending Aortic Echo Moduli

The regional echo moduli reflected the variation in strain around the aortic circumference. A 2D map of the regional modulus identifies both the tissue behavior (tension=blue, compression=red) and the magnitude of stiffness and is presented for the two representative patients (**Figure 6.3-C&D**, respectively).

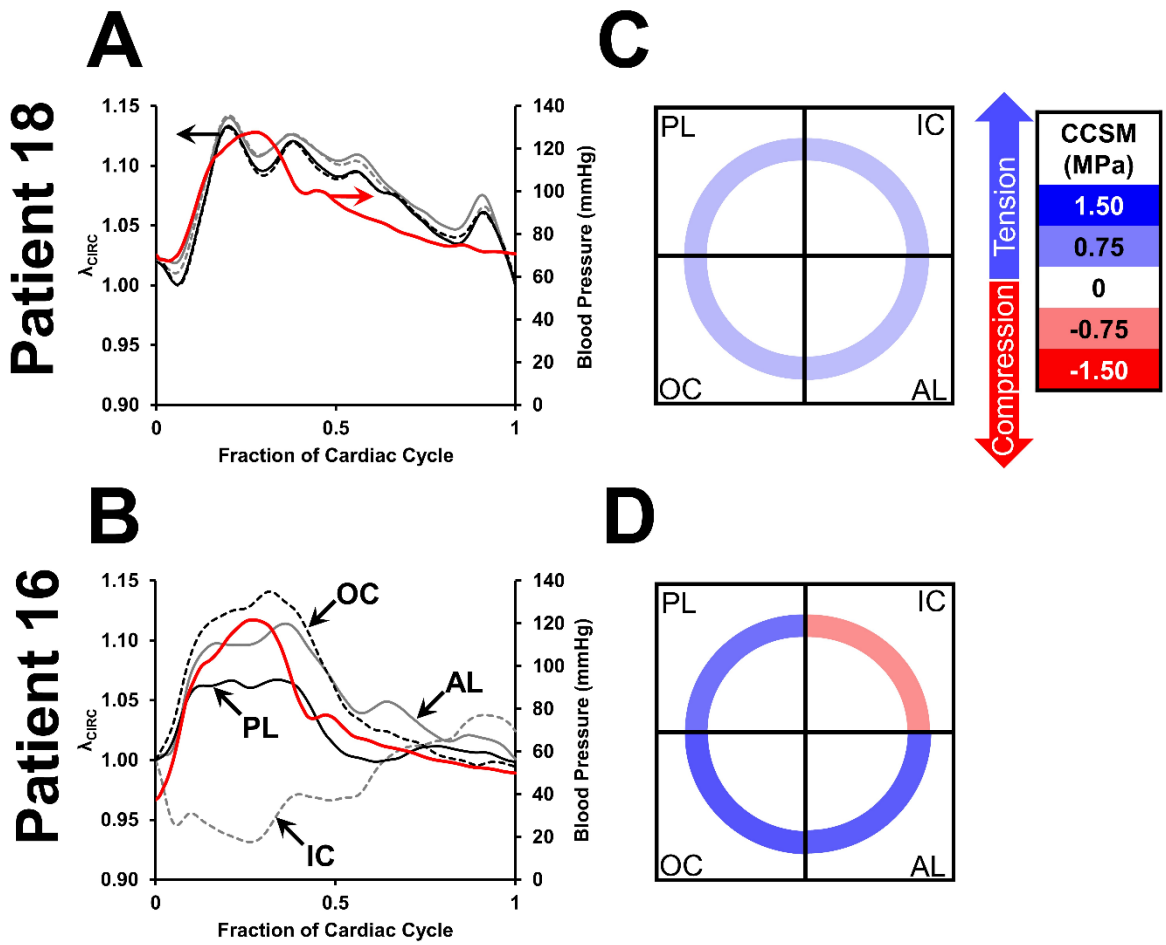

Figure 6.3. TEE-derived *in vivo* biomechanical profile of two representative patients. A) Regional stretch (λ_{CIRC}) and blood pressure profile of **Patient 18** with uniform tensile wall behavior and B) corresponding 2D map of the regional echo modulus (CCSM). C) Regional stretch and blood pressure profile of **Patient 16** with tissue compression in the IC quadrant and D) corresponding 2D map of the regional echo modulus (CCSM). IC-inner curvature, AL-anterolateral wall, OC-outer curvature, PL-posterolateral wall.

The echo moduli for each quadrant were subsequently compared with the *ex vivo* tensile energy loss and apparent elastic modulus at 50% strain (stiffness) for the corresponding

location. Since the *ex vivo* data was only captured under tension, those echo-derived moduli under compression were excluded from the correlations. The regional CCPM significantly correlated with regional *ex vivo* energy loss (R^2=0.2226, P<0.0001) but not *ex vivo* stiffness (R^2=0.0420, P=0.1042), **Figure 6.4-A&B** respectively, for *in vivo* regions of tension. The regional CCSM significantly correlated with both *ex vivo* energy loss (R^2=0.3447, P<0.0001) and *ex vivo* stiffness (R^2=0.2022, P=0.0002), **Figure 6.4-C&D** respectively in regions of *in vivo* tension. Similarly, these comparisons were completed for each of the quadrants and presented in **Table 6.3**.

Table 6.3. Regional correlations of the CCPM and CCSM with *ex vivo* energy loss and stiffness excluding compressive echo moduli. IC-inner curvature, AL-anterolateral wall, OC-outer curvature, PL-posterolateral wall. Note, P>0.05 (n.s,), P<0.05 (*), P<0.01 (**).

	IC (*N=14*)		**AL (*N=17*)**		**OC (*N=20*)**		**PL (*N=12*)**	
	P-Value	***R^2***	***P-Value***	***R^2***	***P-Value***	***R^2***	***P-Value***	***R^2***
CCPM								
vs. Energy Loss	n.s.	0.249	*	0.234	*	0.298	n.s.	0.617
vs. Stiffness	n.s.	0.009	n.s.	0.051	n.s.	0.117	n.s.	0.026
CCSM								
vs. Energy Loss	*	0.437	*	0.292	**	0.388	*	0.416
vs. Stiffness	*	0.350	n.s.	0.139	**	0.322	n.s.	0.155

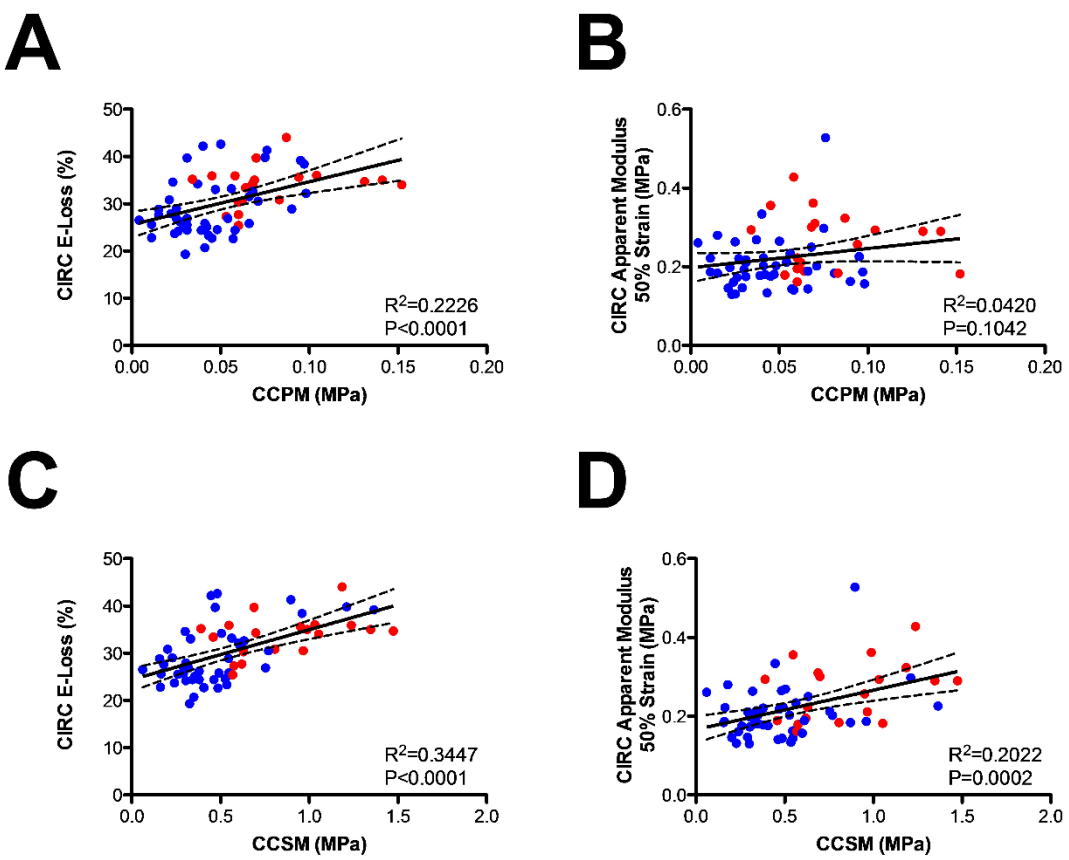

Figure 6.4. Comparison of TEE-derived regional moduli with regional *ex vivo* measures of energy loss and stiffness by regression analysis. A) Regional *ex vivo* circumferential energy loss and B) regional circumferential stiffness *vs.* CCPM. C) *Ex vivo* circumferential energy loss and D) circumferential stiffness *vs.* CCSM. Data points are distinguished by aortic valve phenotype: tricuspid aortic valve (●) and bicuspid aortic valve (●).

The maximum difference in region-adjacent moduli (*i.e.*, Max ΔCCPM & Max ΔCCPM) were calculated for each patient and compared to the global *ex vivo* energy loss and stiffness. The Max ΔCCPM had a significant, positive correlation with both energy loss (R^2=0.3465, P=0.0050) and stiffness (R^2=0.2862, P=0.0125), **Figure 6.5-A&B** respectively. Using the

circumferential stress-derived echo modulus strengthened the correlations with the Max ΔCCSM having a very significant, positive correlation with both energy loss (R^2=0.4364, P=0.0011) and stiffness (R^2=0.4101, P=0.0018), **Figure 6.5-C&D** respectively.

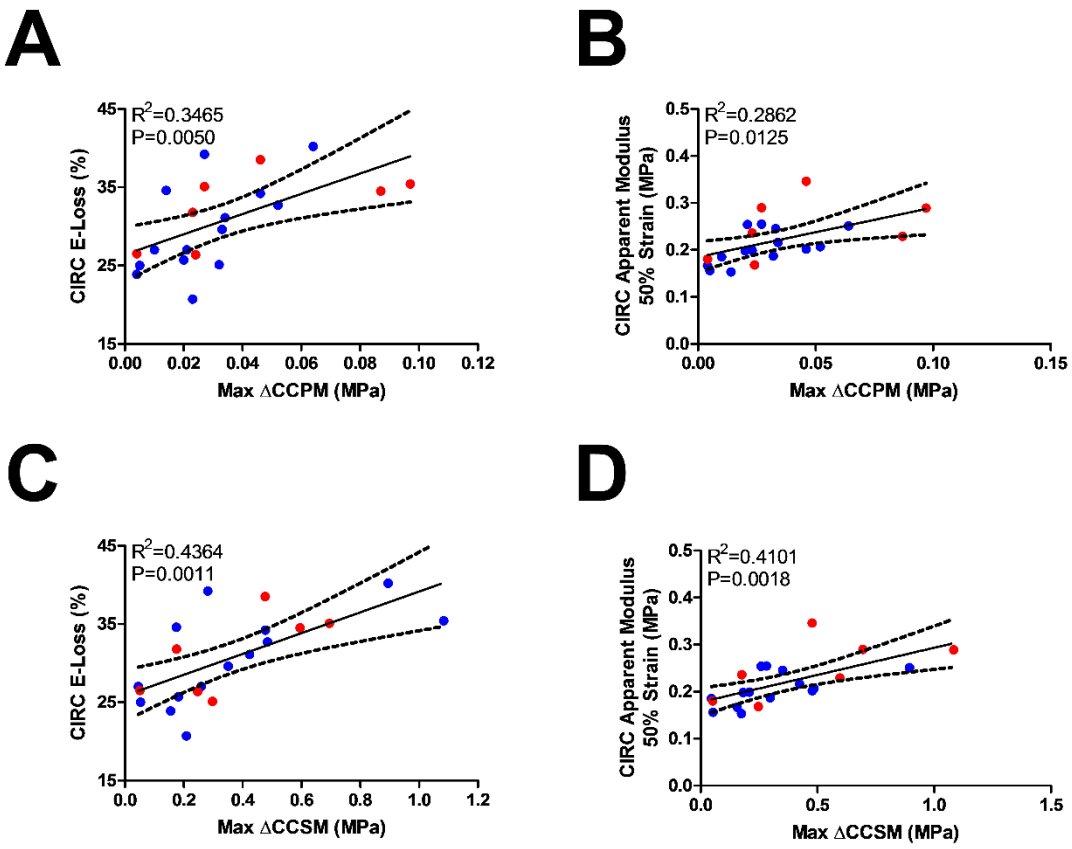

Figure 6.5. Maximum nearest-neighbor regional variability in *in vivo* modulus as predictors of *ex vivo* mechanical behavior. A) *Ex vivo* circumferential energy loss and B) stiffness *vs.* Max ΔCCPM. C) *Ex vivo* circumferential energy loss and D) stiffness *vs.* Max ΔCCSM. Data points are distinguished by aortic valve phenotype: tricuspid aortic valve (●) and bicuspid aortic valve (●).

Regional Ascending Aortic Thickness and Composition

Aortic wall thickness was measured for each tissue sample that was analyzed *ex vivo*. Regional wall thickness from each of the 4 quadrants was analyzed for the full study cohort and for groups that binned patients according to the surgical criterion of <5.5cm and ≥5.5cm maximum AA diameter (**Figure 6.6-A**). A two-way ANOVA revealed that aortic region accounted for ~8.1% of the variance ($P<0.01$) but patient binning by diameter had no statistical significance. A Bonferroni post-hoc test revealed significant differences ($P<0.05$) between the relatively thick IC and PL quadrants in comparison to the ~15% thinner AL and OC quadrants for the full patient cohort.

The aortic wall composition was measured by the relative ratio of collagens to elastin (*i.e.*, "collagen/elastin") for each quadrant of the aorta. As with aortic thickness measurements, patients from the full cohort were subsequently binned by AA diameter about the surgical criteria of 5.5cm (**Figure 6.6-B**). A two-way ANOVA revealed that aortic diameter accounted for ~4.8% of the variance ($P<0.05$) while the effect of aortic region was statistically insignificant. Although a trend of increased collagen/elastin was observed in the larger diameter group, a Bonferroni post-hoc test did not demonstrate any significant differences within the data. The aortic wall histopathology taken adjacent to the *ex vivo* mechanical testing squares revealed approximate regional uniformity in composition for **Patients 18** and **16** (**Figure 6.6-C&D**, respectively).

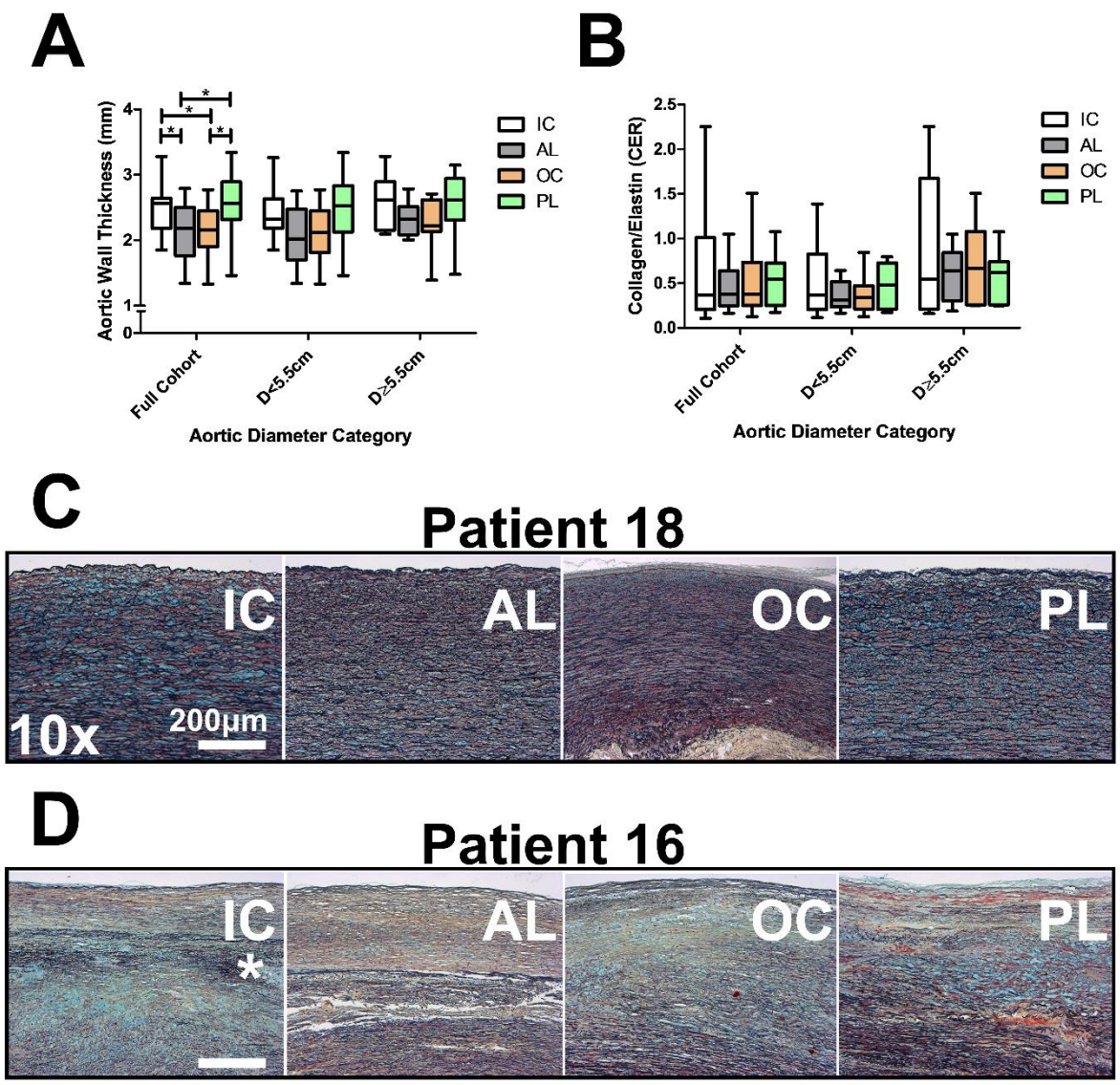

Figure 6.6. A) Two-way ANOVA of regional aortic wall thickness categorized by maximum aortic diameter: effect of aortic region (**, P<0.01), effect of diameter categorization (n.s., P>0.05). B) Two-way ANOVA of regional collagen/elastin categorized by maximum aortic diameter: effect of aortic region (n.s., P>0.05), effect of diameter categorization (*, P<0.05). Regional aortic wall histology (Movat's pentachrome) for C) **Patient 18** and D) **Patient 16**. Statistical differences within the datasets were assessed using a Bonferroni post-hoc test (*,

P<0.05). IC-inner curvature, AL-anterolateral wall, OC-outer curvature, PL-posterolateral wall.

6.7 Discussion

We have recently shown that global (*i.e.*, circumference-averaged) cycle average moduli can be assessed by TEE 2DSE and blood pressure tracing[151]. Global echo moduli predicted global *ex vivo* stiffness, viscous energy loss and aortic wall histopathology[151]. Data from this present study demonstrates that these trends are conserved when comparing regional echo moduli measured at the time of surgery to the regional *ex vivo* stiffness and energy loss obtained from mechanical testing of the resected aorta (**Figure 6.4** & **Table 6.3**). These observations are promising since stiffness in the physiological range has been shown to correlate with the rupture potential of AA tissue[154,150] which helps substantiate the use of mechanical indices derived from 2DSE to contribute to patient management.

It is understood that the process that leads to tearing of the aortic wall is a local mechanical failure of the tissue. According to Moon *et al.*, roughly two-thirds of the sites of primary intimal tearing of the AA or aortic arch occurred along the OC[152]. Here, we used transesophageal 2DSE and blood pressure tracing to determine the observed echo derived moduli of four quadrants around the aortic circumference. We subsequently compared these values with *ex vivo* mechanical indices, obtained from biaxial tensile testing of the resected aorta, as well as aortic wall composition of collagens and elastin and its thickness.

We observed wall deformation by each region's cyclic stretch profile and found that in certain patients we could observe either tensile stretching (**Figure 6.3-A**) or compressive stretching where one-or-more walls exhibited a temporal decrease in strain while the blood pressure was increasing (**Figure 6.3-B**). With or without compression, regional variation in echo-derived moduli was observed (**Figure 6.3-C&D**, visualized in two representative patients using the CCSM). Krishnan *et al.* have used finite element stress mapping of aneurysmal AAs from 4D-MRI to reveal considerable heterogeneity of localized stresses,[111] suggesting that the stress is not shared evenly around the aorta. Furthermore, Karatolios *et al.* have identified significant regional heterogeneity in strain distribution around the abdominal aortic circumference using 3D echo[131].

Ex vivo mechanical studies have not revealed stark differences in the AA's mechanical properties around the aortic circumference. In an *ex vivo* study of 12 patients with AA aneurysm, Iliopoulos *et al.* showed that regional variation in ultimate strength and peak stiffness was not significant among the four quadrants tested[95]. Similarly, in a study on non-dilated donor tissues, Azadani *et al.* found no difference in AA stiffness between the anterior and posterior walls[153].

Based on the two echo-derived moduli, two predictive parameters were developed that describe the maximum difference between observed echo stiffness in adjacent regions per patient: Max ΔCCPM & Max ΔCCSM, respectively. Both the Max ΔCCPM and Max ΔCCSM significantly correlated with global *ex vivo* energy loss and stiffness (**Figure 6.5**). This suggests that as the aorta becomes more mechanically dysfunctional, characterized by

higher viscous energy loss and stiffness, the magnitude of nearest-neighbor regional differences between *in vivo* moduli are exacerbated.

The CCPM and CCSM from the OC region had the strongest regional correlation with *ex vivo* energy loss and stiffness (**Table 6.3**) and a trend of increased echo moduli (both CCPM and CCSM) in the OC region was observed in patients above surgical criteria (≥5.5cm) (**Figure 6.S.1-A&B**, respectively). Furthermore, compression in the OC region was the least frequent, occurring once out of 12 observations (**Table 6.2**). This suggests that the OC region may be the quadrant that is the most mechanically engaged in tension. This may be due in part to the hemodynamic profile in the AA. For instance, in patients with bicuspid aortic valve, eccentric systolic jet flow has been observed for patients with or without aortic stenosis[69, 117] with prevalence towards the OC of the aorta[118].

Regardless of its origin, a difference in region-adjacent compliance and tissue deformation is known to be mechanically unstable. Although data in the aorta is limited, compliance mismatch between the parent artery and the coronary bypass graft is known to cause high stress at the graft-artery junction leading to hyperplasia[155]. Similarly, coronary lesion instability by intimal tearing occurs as a result of stress concentration at the plaque cap-intima junction due to local differences in stiffness[156]. With respect to this present study, these data suggest that a greater regional difference in strain or in turn, echo modulus, would be indicative of concentrated stress.

We found that the AA wall was thinner along the OC and AL quadrants than on the IC or PL wall and that average wall thickness is not different at large AA diameters (**Figure 6.6-A**), which agrees with previously published data[53, 55]. Due to diminished tensile strength at sites of decreased aortic thickness[157], the reduced thickness of the wall of the OC may contribute to the propensity for dissection at this location. However, we did not observe significant changes in regional collagen or elastin content (**Figure 6.6-B**). This point is highlighted using the representative patients from **Figure 6.3**, with their regional wall histology presented in **Figure 6.6-C&D**. For both patients the histology was uniformly pathological in all quadrants, despite Patient 16 (**Figure 6.6-D**) exhibiting compression of the wall in the IC quadrant (*****). Notably, studies have shown that there is reduced radial elastic fiber orientation[158] and moderate extracellular matrix disruption as a result of heightened wall shear stress[159] in the OC region of the aortic wall is patients with BAV aortopathy. Combined with tensile fatigue, these features may weaken the wall, increasing the risk of an acute tear.

2DSE is an emerging modality for identifying the mechanical properties of the aorta, providing additive information for surgical decision-making beyond simple size criteria. Global echo moduli provide a reliable estimation of the mechanical state of the AA wall, but regional wall deformation can identify areas of abnormal stress concertation and focal tissue weakness. Using *in vivo* mechanical criteria as an added dimension to aortic stability may prove advantageous as regional differences in *in vivo* moduli appears to increase as the wall becomes more mechanically-impaired.

6.8 Limitations

This work was completed using data from a heterogeneous cohort of patients receiving aortic correction surgery. Although this cohort size is comparable to other *in vivo* studies[17, 132, 159] , the limited patient numbers restrict group analysis by aortic valve phenotype, which would be of value in a larger follow-up study. Second, the measurement of mechanical heterogeneity around the aortic circumference was of central importance in this study since circumferential strain is largely driven by the aortic blood pressure waveform. However, as primary transverse tearing is a predominant characteristic of aortic dissection, mechanical heterogeneity in the longitudinal axis may relay pertinent information in the mechanism of acute aortic syndrome.

6.9 Conclusion

We have previously shown that global stiffness moduli accurately describe the mechanical properties of the vessel wall as they are measured *ex vivo*. This study, however, demonstrates that considerable heterogeneity in *in vivo* strain can be seen in certain patients and appears to be a feature of a mechanically dysfunctional state. The implication of heterogeneous moduli or strain is an uneven stress distribution within the aortic wall. The OC region, in particular, is a region of interest due to its relatively thin wall and the fact that it is consistently engaged in tensile strain when other walls may not be. We believe that regional differences in mechanical behavior and tissue strain could play an important role in acute aortic syndrome. However, how this is linked to the aortic hemodynamic environment, the surrounding tissue structure or disease of the aortic valve is yet to be determined but may provide useful

prognostic information–in additional to global moduli and aortic size–if presented in a larger study.

6.10 Supplementary Material

The following is submitted as supplementary material made available with the article:

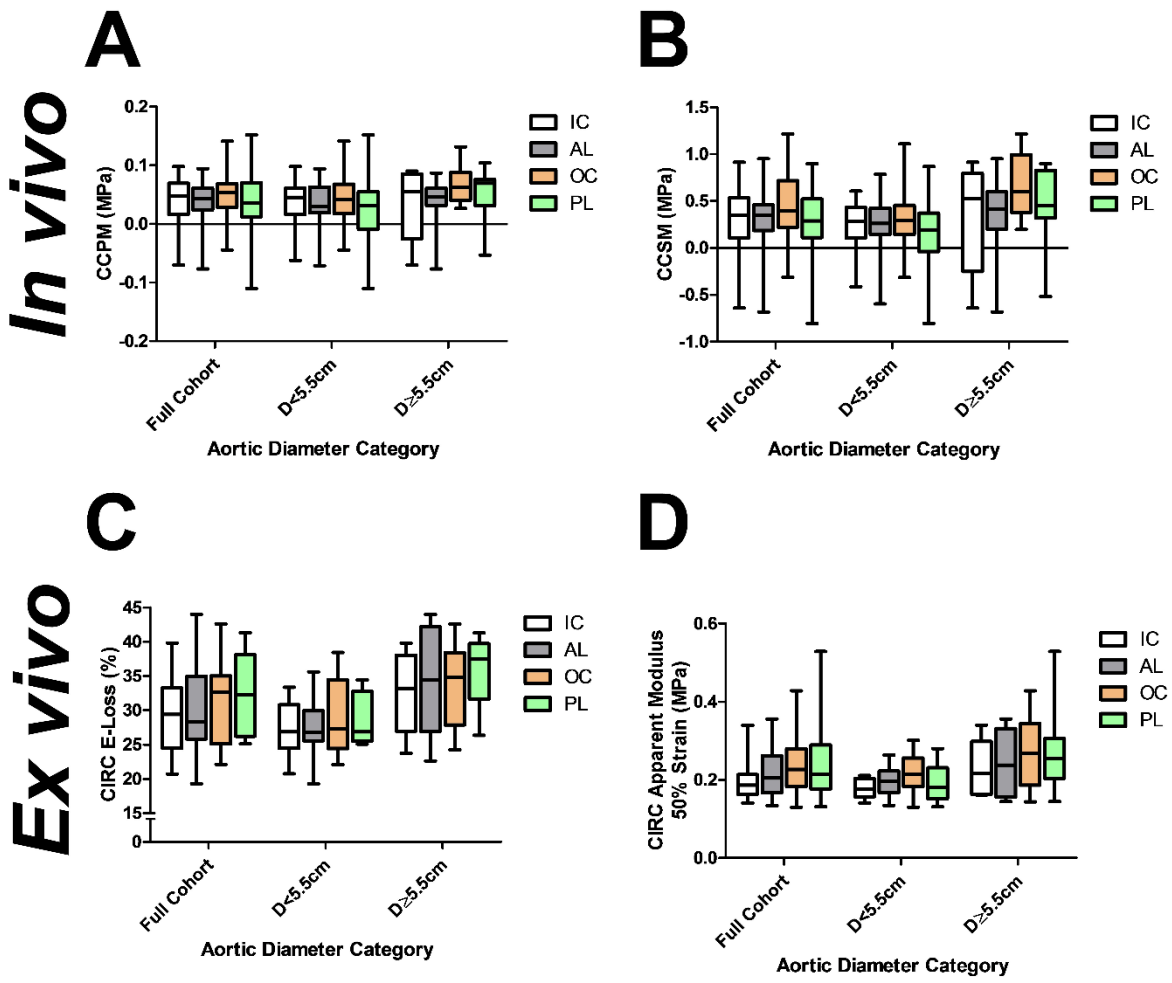

Figure 6.S.1. Comparison of regional mechanical properties in *in vivo* and *ex vivo* methods. Two-way ANOVA of regional differences in 2DSE-measured A) CCPM and B) CCSM categorized by maximum aortic diameter: effect of aortic region (n.s., P>0.05), effect of

diameter categorization (n.s., P>0.05). Two-way ANOVA of regional differences in *ex vivo* measured C) circumferential energy loss and D) circumferential stiffness categorized by maximum aortic diameter: effect of aortic region (n.s., P>0.05), effect of diameter categorization (E-Loss: ***, P<0.0001; Stiffness: **, P<0.01). Statistical differences within the datasets were assessed using a Bonferroni post-hoc test (all comparisons n.s., P>0.05). IC-inner curvature, AL-anterolateral wall, OC-outer curvature, PL-posterolateral wall.

Chapter 7. Discussion

The culmination of work in this thesis was presented as two primary manuscripts (Chapters 5 & 6) with a third short published manuscript presented in Appendix A. The latter is a two-patient case study on the mechanical properties of aortic tissue in patients with chronic aortic dissection. Such cases are clinically rare yet they are invaluable specimens to study pathological aortic wall remodelling and the corresponding mechanical changes that arise as a result. In the analysis presented in Appendix A, the chronically dissected wall was isolated from the intact ascending aorta and each region underwent mechanical testing, histological analysis and MMP-2 and MMP-9 expression by gelatin zymography. For each patient, we found that the aortic wall was both mechanically and functionally altered in the region of chronic dissection, thus highlighting the focal effect disease has on the properties of the aorta.

The central focus of Chapter 5 was to present global *in vivo* echo-derived stiffness moduli, CCPM and CCSM that were calculated from 2D speckle-track strain imaging of the transverse ascending aorta and invasive blood pressure tracing from the patient's radial artery. Both moduli were subsequently correlated with *ex vivo* stiffness and energy loss that were measured directly from tensile analysis on resected aorta, and were found to co-vary significantly (**Figure 5.2**). Using CCPM and CCSM, patients with aortic diameters below the surgical criteria of ≥5.5cm could be distinguished by abnormal *in vivo* moduli that were indicative of pathological wall remodelling. Notably, this thesis did not investigate whether CCPM or CCSM directly related prognostic information on the likelihood of rupture or dissection. However, a study by Duprey *et al.* used *ex vivo* bulge inflation testing of the

ascending aortic wall to reveal that apparent stiffness in the physiological range positively correlates with the rupture potential of aortic tissue,[154] which further suggests following patients with biomechanics-based metrics.

Previous studies have used echo-derived mechanical indices to identify aortic stiffness in various disease states (reviewed in Chapter 4); however, to date, no other study has validated an echo-based methodology by comparisons to *ex vivo* mechanical properties. Notably, Trabelsi *et al.* measured *in vivo* stiffness that was calculated through the pressure-volume relation obtained through CT scan and found that it compared to *ex vivo* stiffness obtained through bulge inflation testing[150]. This provides further incentive to adopt an *in vivo* biomechanics methodology, obtained through medical imaging, to identify aortic disease.

In analyzing the global CCPM and CCSM, it was apparent that considerable regional heterogeneity existed in the strain profile around the aortic circumference. Indeed others have reported that a feature of aortic aneurysms was an *in vivo* "dyssynchronous" strain profile around the aortic circumference in both the ascending[15] and abdominal aorta[131]. Owing to our observations and these reported trends, the manuscript presented in Chapter 6 identified the regional *in vivo* CCPM and CCSM of patients to compare with regional *ex vivo* mechanics, tissue thickness and histology. As they were not submitted with the manuscript, the CCSM heat diagrams for the full 21-patient cohort are presented in **Figure B.1** (Appendix B). A notable finding was the presence of compressive strain that occurred in approximately equal frequency in all regions except for the OC region where it was noted in just 1 of 12 observations. Furthermore, it was found that the OC region had the strongest correlations

between *in vivo* CCPM or CCSM and *ex vivo* mechanics. For the full study cohort, mean tissue thickness was significantly thinner in both the OC and AL regions compared to the IC and PL regions but the mean collagen/elastin content was not significantly different at any location around the aortic circumference. The combined risk in the OC region associated with a relatively thin aortic wall (decreased thickness significantly predicts decreased tissue strength[157]) and consistent tension supports the clinical observation that proximal aortic dissections occur most frequently (~67%) in the OC[152].

Notably, aortic valve phenotype (*i.e.*, TAV and BAV) was distinguished in the data presented in Chapters 5 & 6. Although not reported in the published manuscript, comparisons (student t-tests) of global CCPM and CCSM by aortic valve phenotype were made and no significant differences were found, **Figure B.2**. However a trend of increased *in vivo* moduli (~30% increase of the mean) were found in the TAV group compared with the BAV group. Previous studies have explored aortopathy and aneurysm as it relates to aortic valve phenotype and found that the ascending aortic wall in patients with BAV is exposed to eccentric systolic flow as opposed to patients with TAV where the flow is more concentric[69, 118]. Higher focal wall shear stress in the OC region of BAV aortopathy has been found to alter the medial ECM which has been characterized by fragmented elastin and increased MMP expression[159]. Furthermore, the aortic wall in patients with BAV has reduced (or genetically impaired[66]) expression of Fibrillin-1, a component of microfibrils that link elastic fibrils with VSMCs[8], and fewer radially-oriented elastic fibrils in the OC region of the AA[158].

Similarly aortic CCPM and CCSM were evaluated as a function of aortic valve pathology and compared between patients with aortic stenosis (AS) and aortic insufficiency (AI), **Figure B.1**. No significant difference between the means was observed, although, as with our analysis by aortic valve phenotype, limited numbers in each group makes a reliable comparison difficult. This analysis, however, is worth exploring further in a larger study, as aortic valve pathology is known to affect aortic hemodynamics as well as contribute to left ventricle remodelling. Untreated AS leads to concentric left ventricle hypertrophy and decreased pulse pressure, while AI leads to eccentric left ventricle remodelling and often results from dilation of the aortic annulus[160]. Indeed, there may be an underlying disease mechanism that links vessel dilation and AI, as patients with pre-operative AI who receive pulmonary valve autograft transplantation into the aortic position (*i.e.*, Ross Procedure) are subsequently more likely to develop autograft dilation[161]. This suggests that both the pulmonary and aortic wall in these patients may exhibit an underlying pathology.

In summary, we have developed novel echo-derived markers of *in vivo* stiffness in the AA (CCPM and CCSM) and validated these metrics with *ex vivo* energy loss, stiffness and histopathology. Global CCPM and CCSM accurately predict the overall mechanical properties and the degree of pathological remodelling of the aortic wall. Ultimately, this methodology was able to identify patients with abnormally large *in vivo* moduli whose aortic diameters were below the surgical threshold. Correspondingly, regional CCSM and CCPM relayed the magnitude of circumferential mechanical heterogeneity in the vessel wall that was found to increase in those patients where mechanical dysfunction was more pronounced. The OC region of the AA was found to be consistently under tension within the patient cohort

while being a relative site of decreased wall thickness. A larger prospective study using *in vivo* echo-derived moduli would provide useful information in identifying group differences in the mechanical properties of aortic aneurysm (*e.g.*, TAV vs. BAV) while also assessing its utility in contributing important prognostic information for patient care.

Chapter 8. Original Contributions

The work presented in this thesis, written as independent manuscripts (**Chapters 3, 5, 6 & Appendix A**), is my contribution to the body of literature of aortic biomechanics. The following highlights the original contributions of this thesis:

1. Development of two novel echo-derived moduli (CCPM and CCSM) for the assessment of physiological levels of ascending aortic stiffness. Both the CCPM and CCSM were calculated from the dynamic, global aortic stain and blood pressure cycles. The comparison between the CCPM and CCSM related the effect of using either blood pressure or wall stress respectively, when defining an *in vivo* stiffness modulus.

2. Validation of both the global CCPM and CCSM by their significant correlation with *ex vivo* mechanical properties (energy loss and stiffness) and aortic wall histology (collagen and elastin content). Comparisons were made with a common *in vivo* metric, the stiffness index (β), which was less predictive of the *ex vivo* mechanical properties and histology.

3. Demonstration of the potential to identify at-risk patients who do not meet surgical criteria by aortic size by identification of large global echo-derived moduli. Several patients were identified by their abnormally high CCPM or CCSM with aortic diameters below surgical criteria (≥5.5cm diameter); medial degeneration was confirmed in these patients by histology.

4. Development of a second set of metrics that relayed the maximum region-adjacent heterogeneity per patient, termed the Max ΔCCPM and Max ΔCCSM. These values co-varied positively with *ex vivo* energy loss and stiffness, suggesting that these values could have implications in identifying dissection-prone dynamic behaviour based on regional wall motion.

5. Identification of the mechanical and histopathological properties of the ascending aortic wall in regions of chronic type A aortic dissection. This was the first report to present the mechanical properties of the region of chronic dissection.

Chapter 9. Conclusions

Aneurysms of the ascending aorta carry a serious risk of death and disability in the event of an acute aortic tear. Although treatable with prophylactic surgery, patient qualification for a procedural aortic resection uses thresholds based on the aortic diameter that have been shown to exclude at-risk patients who could benefit from a life-saving intervention. Ultimately, the measurement of the mechanical properties of the aorta can accurately reveal the degeneration of mechanical integrity and pathological remodelling of the vessel wall in patients with aneurysm. For this thesis we used 2D echocardiography and blood pressure tracing to predict tissue stiffness *in vivo*, thereby contributing to the development of this methodology as a pre-operative assessment for patient management.

Chapters 5 and 6 presented a novel method by which to calculate *in vivo* stiffness moduli from transesophageal echocardiography (*i.e.*, CCPM and CCSM) by accounting for the full dynamic range of the pressure waveform and strain profile. These moduli were measured peri-operatively within a cohort of patients receiving elective aortic resection surgery and subsequently correlated with the *ex vivo* mechanical properties (energy loss and stiffness) and histopathology (collagen/elastin) of the aortic wall which validated their measurement. Furthermore, this work demonstrated the potential for identifying patients who might be miscategorised based on an aortic size criterion by identification of abnormal moduli.

Chapter 6 presented an analysis of the regional echo-derived stiffness moduli about the aortic circumference. This work identified that regional *in vivo* echo moduli correlate to the regional *ex vivo* mechanical properties of the aortic wall. However, in the context of commenting on

the propensity for the aortic wall to dissect (*i.e.*, an acute tear), we identified that the echo moduli heterogeneity correlates with the overall mechanical properties of the vessel wall and that, occasionally, compression of the vessel wall within an aortic quadrant was observed. This suggested that stresses might become more regionally concentrated as the mechanical integrity of the vessel deteriorates, thereby suggesting focal sites of potential tissue failure. Aortic wall thickness was highly variable around the aortic circumference but did not change significantly between patients with pre-clinical (<5.5cm diameter) and clinical (≥5.5cm diameter) aortic dilation. However, the aortic wall histopathology (collagen/elastin) did not significantly vary around the circumference but did become more pathological (*i.e.*, increased collagen/elastin) in the clinical (≥5.5cm diameter) group.

Appendix A presented an analysis of the mechanical and remodelling properties of the ascending aortic wall in two patients with chronic type A aortic dissection. It was found that significant histological remodelling occurred in the dissected medial wall characterized by an increase in MMP expression and a considerable degradation of the elastic tissue structure. Measurements of energy loss showed an increase in the dissected region compared to the non-dissected region and aortic stiffness appeared to coincide with the level of medial collagen deposition.

The findings in this thesis support our hypothesis that biomechanical measures of the AA can be reliably obtained through echo-based techniques. The speckle tracking derived metrics correlate with *ex vivo* tissue mechanical properties and histopathology. These results indicate

that a large scale multi-institutional prospective trial of the global and regional CCPM and CCSM should be conducted to determine if they can improve patient outcomes.

Chapter 10. Future Work

The following are recommendations for the continuation of this study based on personal experience from the project as well as through feedback from clinicians on the topic of practical implementation of these measures:

1. Testing of TTE of the aortic long axis to identify if the CCPM and CCSM can be measured accurately using this modality and correlate with *ex vivo* tensile mechanics. Although TEE has advantages in image quality and access to additional planes of view (*i.e.*, short axis of AA), it requires patient sedation and is therefore unlikely to be used for high-throughput patient screening. TTE is measured externally and therefore requires no medications or convalescence from the procedure.

2. In this thesis, blood pressure tracing had been measured through an invasive catheter in the radial artery. To make the measurement completely non-invasive, a method should be developed that infers the blood pressure from a benign measurement. Several ideas exist, for instance, *i*) using an oxygen saturation monitor worn on the patient's index finger or, *ii*) back-calculating the aortic pressure waveform from spectral Doppler flow imaging through the aorta using TTE. We believe that the latter could be done using a Fourier Transform and Womersely-type analysis that relates pressure and flow in a closed pulsatile flow system. Furthermore, this would have a secondary benefit of measuring the pressure waveform directly at the site of the strain measurements.

3. A large-scale prospective study is needed to identify if mechanical markers, including the CCPM and CCSM, predict clinical outcomes. To achieve adequate patient numbers (~200), this would require a multi-centre collaboration that includes pre-surgical patient monitoring using echo and, for those receiving corrective surgery, pre-operative echo followed by *ex vivo* mechanical testing and histopathology on resected specimens.

References

1. Clouse WD, Hallett JW, Jr., Schaff HV, Gayari MM, Ilstrup DM, Melton LJ, 3rd. Improved prognosis of thoracic aortic aneurysms: a population-based study. *JAMA : the journal of the American Medical Association.* 1998;280:1926-1929.

2. Isselbacher EM. Thoracic and abdominal aortic aneurysms. *Circulation.* 2005;111:816-828.

3. Kouchoukos NT, Dougenis D. Surgery of the thoracic aorta. *The New England journal of medicine.* 1997;336:1876-1888.

4. Bonow RO. Bicuspid Aortic Valves and Dilated Aortas: A Critical Review of the Critical Review of the ACC/AHA Practice Guidelines Recommendations. *The American Journal of Cardiology.* 2008;102:111-114.

5. Hiratzka LF, Bakris GL, Beckman JA, Bersin RM, Carr VF, Casey DE, Jr., et al. 2010 ACCF/AHA/AATS/ACR/ASA/SCA/SCAI/SIR/STS/SVM guidelines for the diagnosis and management of patients with Thoracic Aortic Disease: a report of the American College of Cardiology Foundation/American Heart Association Task Force on Practice Guidelines, American Association for Thoracic Surgery, American College of Radiology, American Stroke Association, Society of Cardiovascular Anesthesiologists, Society for Cardiovascular Angiography and Interventions, Society of Interventional Radiology, Society of Thoracic Surgeons, and Society for Vascular Medicine. *Circulation.* 2010;121:e266-369.

6. Kuzmik GA, Sang AX, Elefteriades JA. Natural history of thoracic aortic aneurysms. *Journal of vascular surgery.* 2012;56:565-571.

7. Erbel R, Eggebrecht H. Aortic dimensions and the risk of dissection. *Heart.* 2006;92:137-142.

8. Fedak PW, de Sa MP, Verma S, Nili N, Kazemian P, Butany J, et al. Vascular matrix remodeling in patients with bicuspid aortic valve malformations: implications for aortic dilatation. *The Journal of thoracic and cardiovascular surgery.* 2003;126:797-806.

9. Loeys BL, Schwarze U, Holm T, Callewaert BL, Thomas GH, Pannu H, et al. Aneurysm syndromes caused by mutations in the TGF-beta receptor. *The New England journal of medicine.* 2006;355:788-798.

10. Booher AM, Eagle KA. Diagnosis and management issues in thoracic aortic aneurysm. *American heart journal.* 2011;162:38-46.e31.

11. Pape LA, Tsai TT, Isselbacher EM, Oh JK, O'Gara P T, Evangelista A, et al. Aortic diameter >or = 5.5 cm is not a good predictor of type A aortic dissection: observations

from the International Registry of Acute Aortic Dissection (IRAD). *Circulation.* 2007;116:1120-1127.

12. Parish LM, Gorman JH, 3rd, Kahn S, Plappert T, St John-Sutton MG, Bavaria JE, et al. Aortic size in acute type A dissection: implications for preventive ascending aortic replacement. *European journal of cardio-thoracic surgery : official journal of the European Association for Cardio-thoracic Surgery.* 2009;35:941-945; discussion 945-946.

13. Baumgartner D, Baumgartner C, Matyas G, Steinmann B, Loffler-Ragg J, Schermer E, et al. Diagnostic power of aortic elastic properties in young patients with Marfan syndrome. *The Journal of thoracic and cardiovascular surgery.* 2005;129:730-739.

14. Bieseviciene M, Vaskelyte JJ, Mizariene V, Karaliute R, Lesauskaite V, Verseckaite R. Two-dimensional speckle-tracking echocardiography for evaluation of dilative ascending aorta biomechanics. *BMC cardiovascular disorders.* 2017;17:27.

15. Teixeira R, Moreira N, Baptista R, Barbosa A, Martins R, Castro G, et al. Circumferential ascending aortic strain and aortic stenosis. *European heart journal cardiovascular Imaging.* 2013;14:631-641.

16. Vitarelli A, Giordano M, Germano G, Pergolini M, Cicconetti P, Tomei F, et al. Assessment of ascending aorta wall stiffness in hypertensive patients by tissue Doppler imaging and strain Doppler echocardiography. *Heart.* 2010;96:1469-1474.

17. Wittek A, Karatolios K, Fritzen CP, Bereiter-Hahn J, Schieffer B, Moosdorf R, et al. Cyclic three-dimensional wall motion of the human ascending and abdominal aorta characterized by time-resolved three-dimensional ultrasound speckle tracking. 2016;15:1375-1388.

18. Johansson G, Markstrom U, Swedenborg J. Ruptured thoracic aortic aneurysms: a study of incidence and mortality rates. *Journal of vascular surgery.* 1995;21:985-988.

19. Rampoldi V, Trimarchi S, Eagle KA, Nienaber CA, Oh JK, Bossone E, et al. Simple risk models to predict surgical mortality in acute type A aortic dissection: the International Registry of Acute Aortic Dissection score. *The Annals of thoracic surgery.* 2007;83:55-61.

20. Williams JB, Peterson ED, Zhao Y, O'Brien SM, Andersen ND, Miller DC, et al. Contemporary results for proximal aortic replacement in North America. *Journal of the American College of Cardiology.* 2012;60:1156-1162.

21. Elefteriades JA, Farkas EA. Thoracic aortic aneurysm clinically pertinent controversies and uncertainties. *Journal of the American College of Cardiology.* 2010;55:841-857.

22. Coady MA, Rizzo JA, Hammond GL, Mandapati D, Darr U, Kopf GS, et al. What is the appropriate size criterion for resection of thoracic aortic aneurysms? *The Journal of thoracic and cardiovascular surgery.* 1997;113:476-491; discussion 489-491.

23. Nishimura RA, Otto CM, Bonow RO, Carabello BA, Erwin JP, 3rd, Guyton RA, et al. 2014 AHA/ACC Guideline for the Management of Patients With Valvular Heart Disease: executive summary: a report of the American College of Cardiology/American Heart Association Task Force on Practice Guidelines. *Circulation.* 2014;129:2440-2492.

24. Etz CD, Misfeld M, Borger MA, Luehr M, Strotdrees E, Mohr FW. Current indications for surgical repair in patients with bicuspid aortic valve and ascending aortic ectasia. *Cardiology research and practice.* 2012;2012:313879.

25. Verma S, Yanagawa B, Kalra S, Ruel M, Peterson MD, Yamashita MH, et al. Knowledge, attitudes, and practice patterns in surgical management of bicuspid aortopathy: a survey of 100 cardiac surgeons. *The Journal of thoracic and cardiovascular surgery.* 2013;146:1033-1040.e1034.

26. Humphrey JD, Schwartz MA, Tellides G, Milewicz DM. Role of Mechanotransduction in Vascular Biology: Focus on Thoracic Aortic Aneurysms and Dissections. *Circulation research.* 2015;116:1448-1461.

27. Schlatmann TJ, Becker AE. Histologic changes in the normal aging aorta: implications for dissecting aortic aneurysm. *Am J Cardiol.* 1977;39:13-20.

28. Morton LF, Barnes MJ. Collagen polymorphism in the normal and diseased blood vessel wall. Investigation of collagens types I, III and V. *Atherosclerosis.* 1982;42:41-51.

29. Tsamis A, Krawiec JT, Vorp DA. Elastin and collagen fibre microstructure of the human aorta in ageing and disease: a review. *Journal of the Royal Society, Interface / the Royal Society.* 2013;10:20121004.

30. Belz GG. Elastic properties and Windkessel function of the human aorta. *Cardiovascular drugs and therapy / sponsored by the International Society of Cardiovascular Pharmacotherapy.* 1995;9:73-83.

31. Gosline J, Lillie M, Carrington E, Guerette P, Ortlepp C, Savage K. Elastic proteins: biological roles and mechanical properties. *Philosophical Transactions of the Royal Society B: Biological Sciences.* 2002;357:121-132.

32. Weisbecker H, Viertler C, Pierce DM, Holzapfel GA. The role of elastin and collagen in the softening behavior of the human thoracic aortic media. *Journal of biomechanics.* 2013;46:1859-1865.

33. Gasser TC, Ogden RW, Holzapfel GA. Hyperelastic modelling of arterial layers with distributed collagen fibre orientations. *Journal of the Royal Society Interface.* 2006;3:15-35.

34. Grote K, Flach I, Luchtefeld M, Akin E, Holland SM, Drexler H, et al. Mechanical stretch enhances mRNA expression and proenzyme release of matrix metalloproteinase-2 (MMP-2) via NAD(P)H oxidase-derived reactive oxygen species. *Circulation research.* 2003;92:e80-86.

35. Kim BS, Nikolovski J, Bonadio J, Mooney DJ. Cyclic mechanical strain regulates the development of engineered smooth muscle tissue. *Nature biotechnology.* 1999;17:979-983.

36. Leung DY, Glagov S, Mathews MB. Cyclic stretching stimulates synthesis of matrix components by arterial smooth muscle cells in vitro. *Science (New York, N.Y.).* 1976;191:475-477.

37. El-Hamamsy I, Yacoub MH. Cellular and molecular mechanisms of thoracic aortic aneurysms. *Nature reviews. Cardiology.* 2009;6:771-786.

38. Ruiz-Ortega M, Rodriguez-Vita J, Sanchez-Lopez E, Carvajal G, Egido J. TGF-beta signaling in vascular fibrosis. *Cardiovascular research.* 2007;74:196-206.

39. Clark JM, Glagov S. Transmural organization of the arterial media. The lamellar unit revisited. *Arteriosclerosis (Dallas, Tex.).* 1985;5:19-34.

40. Tremblay D, Cartier R, Mongrain R, Leask RL. Regional dependency of the vascular smooth muscle cell contribution to the mechanical properties of the pig ascending aortic tissue. *Journal of biomechanics.* 2010;43:2448-2451.

41. Milewicz DM, Guo DC, Tran-Fadulu V, Lafont AL, Papke CL, Inamoto S, et al. Genetic basis of thoracic aortic aneurysms and dissections: focus on smooth muscle cell contractile dysfunction. *Annual review of genomics and human genetics.* 2008;9:283-302.

42. Humphrey JD. Possible mechanical roles of glycosaminoglycans in thoracic aortic dissection and associations with dysregulated transforming growth factor-beta. *Journal of vascular research.* 2013;50:1-10.

43. Hager A, Kaemmerer H, Rapp-Bernhardt U, Blucher S, Rapp K, Bernhardt TM, et al. Diameters of the thoracic aorta throughout life as measured with helical computed tomography. *The Journal of thoracic and cardiovascular surgery.* 2002;123:1060-1066.

44. Turkbey EB, Jain A, Johnson C, Redheuil A, Arai AE, Gomes AS, et al. Determinants and normal values of ascending aortic diameter by age, gender, and race/ethnicity in the Multi-Ethnic Study of Atherosclerosis (MESA). *Journal of magnetic resonance imaging : JMRI.* 2014;39:360-368.

45. Li AE, Kamel I, Rando F, Anderson M, Kumbasar B, Lima JA, et al. Using MRI to assess aortic wall thickness in the multiethnic study of atherosclerosis: distribution by race, sex, and age. *AJR. American journal of roentgenology.* 2004;182:593-597.

46. Hosoda Y, Kawano K, Yamasawa F, Ishii T, Shibata T, Inayama S. Age-dependent changes of collagen and elastin content in human aorta and pulmonary artery. *Angiology.* 1984;35:615-621.

47. Hosoda Y, Minoshima I. ELASTIN CONTENT OF THE AORTA AND THE PULMONARY ARTERY IN THE JAPANESE. *Angiology.* 1965;16:325-332.

48. Andreotti L, Bussotti A, Cammelli D, di Giovine F, Sampognaro S, Sterrantino G, et al. Aortic connective tissue in ageing--a biochemical study. *Angiology.* 1985;36:872-879.

49. Carlson RG, Lillehei CW, Edwards JE. Cystic medial necrosis of the ascending aorta in relation to age and hypertension. *Am J Cardiol.* 1970;25:411-415.

50. Sans M, Moragas A. Mathematical morphologic analysis of the aortic medial structure. Biomechanical implications. *Analytical and quantitative cytology and histology / the International Academy of Cytology [and] American Society of Cytology.* 1993;15:93-100.

51. Collins MJ, Dev V, Strauss BH, Fedak PW, Butany J. Variation in the histopathological features of patients with ascending aortic aneurysms: a study of 111 surgically excised cases. *Journal of clinical pathology.* 2008;61:519-523.

52. Hirst AE, Jr., Johns VJ, Jr., Kime SW, Jr. Dissecting aneurysm of the aorta: a review of 505 cases. *Medicine.* 1958;37:217-279.

53. Choudhury N, Bouchot O, Rouleau L, Tremblay D, Cartier R, Butany J, et al. Local mechanical and structural properties of healthy and diseased human ascending aorta tissue. *Cardiovascular pathology : the official journal of the Society for Cardiovascular Pathology.* 2009;18:83-91.

54. Tang PC, Coady MA, Lovoulos C, Dardik A, Aslan M, Elefteriades JA, et al. Hyperplastic cellular remodeling of the media in ascending thoracic aortic aneurysms. *Circulation.* 2005;112:1098-1105.

55. Tremblay D, Zigras T, Cartier R, Leduc L, Butany J, Mongrain R, et al. A comparison of mechanical properties of materials used in aortic arch reconstruction. *The Annals of thoracic surgery.* 2009;88:1484-1491.

56. Della Corte A, Quarto C, Bancone C, Castaldo C, Di Meglio F, Nurzynska D, et al. Spatiotemporal patterns of smooth muscle cell changes in ascending aortic dilatation with bicuspid and tricuspid aortic valve stenosis: focus on cell-matrix signaling. *The Journal of thoracic and cardiovascular surgery.* 2008;135:8-18, 18.e11-12.

57. Agozzino L, Ferraraccio F, Esposito S, Trocciola A, Parente A, Della Corte A, et al. Medial degeneration does not involve uniformly the whole ascending aorta: morphological, biochemical and clinical correlations. *European journal of cardio-*

thoracic surgery : official journal of the European Association for Cardio-thoracic Surgery. 2002;21:675-682.

58. Rabkin SW. Differential expression of MMP-2, MMP-9 and TIMP proteins in thoracic aortic aneurysm - comparison with and without bicuspid aortic valve: a meta-analysis. *VASA. Zeitschrift fur Gefasskrankheiten.* 2014;43:433-442.

59. Visse R, Nagase H. Matrix metalloproteinases and tissue inhibitors of metalloproteinases: structure, function, and biochemistry. *Circulation research.* 2003;92:827-839.

60. Dietz HC, Cutting GR, Pyeritz RE, Maslen CL, Sakai LY, Corson GM, et al. Marfan syndrome caused by a recurrent de novo missense mutation in the fibrillin gene. *Nature.* 1991;352:337-339.

61. Wu D, Shen YH, Russell L, Coselli JS, LeMaire SA. Molecular mechanisms of thoracic aortic dissection. *The Journal of surgical research.* 2013;184:907-924.

62. Hoffman JI, Kaplan S. The incidence of congenital heart disease. *Journal of the American College of Cardiology.* 2002;39:1890-1900.

63. Tutar E, Ekici F, Atalay S, Nacar N. The prevalence of bicuspid aortic valve in newborns by echocardiographic screening. *American heart journal.* 2005;150:513-515.

64. El-Hamamsy I, Yacoub MH. A measured approach to managing the aortic root in patients with bicuspid aortic valve disease. *Current cardiology reports.* 2009;11:94-100.

65. Loscalzo ML, Goh DL, Loeys B, Kent KC, Spevak PJ, Dietz HC. Familial thoracic aortic dilation and bicommissural aortic valve: a prospective analysis of natural history and inheritance. *American journal of medical genetics. Part A.* 2007;143a:1960-1967.

66. Pepe G, Nistri S, Giusti B, Sticchi E, Attanasio M, Porciani C, et al. Identification of fibrillin 1 gene mutations in patients with bicuspid aortic valve (BAV) without Marfan syndrome. *BMC medical genetics.* 2014;15:23.

67. Pasta S, Rinaudo A, Luca A, Pilato M, Scardulla C, Gleason TG, et al. Difference in hemodynamic and wall stress of ascending thoracic aortic aneurysms with bicuspid and tricuspid aortic valve. *Journal of biomechanics.* 2013;46:1729-1738.

68. Bauer M, Siniawski H, Pasic M, Schaumann B, Hetzer R. Different hemodynamic stress of the ascending aorta wall in patients with bicuspid and tricuspid aortic valve. *Journal of cardiac surgery.* 2006;21:218-220.

69. Hope MD, Hope TA, Meadows AK, Ordovas KG, Urbania TH, Alley MT, et al. Bicuspid aortic valve: four-dimensional MR evaluation of ascending aortic systolic flow patterns. *Radiology.* 2010;255:53-61.

70. Phillippi JA, Green BR, Eskay MA, Kotlarczyk MP, Hill MR, Robertson AM, et al. Mechanism of aortic medial matrix remodeling is distinct in patients with bicuspid aortic valve. *The Journal of thoracic and cardiovascular surgery.* 2014;147:1056-1064.

71. Boyum J, Fellinger EK, Schmoker JD, Trombley L, McPartland K, Ittleman FP, et al. Matrix metalloproteinase activity in thoracic aortic aneurysms associated with bicuspid and tricuspid aortic valves. *The Journal of thoracic and cardiovascular surgery.* 2004;127:686-691.

72. Ikonomidis JS, Jones JA, Barbour JR, Stroud RE, Clark LL, Kaplan BS, et al. Expression of matrix metalloproteinases and endogenous inhibitors within ascending aortic aneurysms of patients with bicuspid or tricuspid aortic valves. *The Journal of thoracic and cardiovascular surgery.* 2007;133:1028-1036.

73. LeMaire SA, Wang X, Wilks JA, Carter SA, Wen S, Won T, et al. Matrix metalloproteinases in ascending aortic aneurysms: bicuspid versus trileaflet aortic valves. *The Journal of surgical research.* 2005;123:40-48.

74. Wagsater D, Paloschi V, Hanemaaijer R, Hultenby K, Bank RA, Franco-Cereceda A, et al. Impaired collagen biosynthesis and cross-linking in aorta of patients with bicuspid aortic valve. *Journal of the American Heart Association.* 2013;2:e000034.

75. Dietz HC, Pyeritz RE. Mutations in the human gene for fibrillin-1 (FBN1) in the Marfan syndrome and related disorders. *Human molecular genetics.* 1995;4 Spec No:1799-1809.

76. Trask TM, Trask BC, Ritty TM, Abrams WR, Rosenbloom J, Mecham RP. Interaction of tropoelastin with the amino-terminal domains of fibrillin-1 and fibrillin-2 suggests a role for the fibrillins in elastic fiber assembly. *The Journal of biological chemistry.* 2000;275:24400-24406.

77. Vrhovski B, Weiss AS. Biochemistry of tropoelastin. *European journal of biochemistry / FEBS.* 1998;258:1-18.

78. Francke U, Berg MA, Tynan K, Brenn T, Liu W, Aoyama T, et al. A Gly1127Ser mutation in an EGF-like domain of the fibrillin-1 gene is a risk factor for ascending aortic aneurysm and dissection. *American journal of human genetics.* 1995;56:1287-1296.

79. Milewicz DM, Michael K, Fisher N, Coselli JS, Markello T, Biddinger A. Fibrillin-1 (FBN1) mutations in patients with thoracic aortic aneurysms. *Circulation.* 1996;94:2708-2711.

80. Germain DP. Clinical and genetic features of vascular Ehlers-Danlos syndrome. *Annals of vascular surgery.* 2002;16:391-397.

81. Cotrufo M, Della Corte A, De Santo LS, De Feo M, Covino FE, Dialetto G. Asymmetric medial degeneration of the ascending aorta in aortic valve disease: a pilot

study of surgical management. *The Journal of heart valve disease.* 2003;12:127-133; discussion 134-125.

82. Barker AJ, Markl M, Burk J, Lorenz R, Bock J, Bauer S, et al. Bicuspid aortic valve is associated with altered wall shear stress in the ascending aorta. *Circulation. Cardiovascular imaging.* 2012;5:457-466.

83. Okamoto RJ, Wagenseil JE, DeLong WR, Peterson SJ, Kouchoukos NT, Sundt TM, 3rd. Mechanical properties of dilated human ascending aorta. *Annals of biomedical engineering.* 2002;30:624-635.

84. Okamoto RJ, Xu H, Kouchoukos NT, Moon MR, Sundt TM, 3rd. The influence of mechanical properties on wall stress and distensibility of the dilated ascending aorta. *The Journal of thoracic and cardiovascular surgery.* 2003;126:842-850.

85. Vorp DA, Schiro BJ, Ehrlich MP, Juvonen TS, Ergin MA, Griffith BP. Effect of aneurysm on the tensile strength and biomechanical behavior of the ascending thoracic aorta. *The Annals of thoracic surgery.* 2003;75:1210-1214.

86. Pasta S, Phillippi JA, Gleason TG, Vorp DA. Effect of aneurysm on the mechanical dissection properties of the human ascending thoracic aorta. *The Journal of thoracic and cardiovascular surgery.* 2012;143:460-467.

87. Okamoto RJ, Wagenseil JE, DeLong WR, Peterson SJ, Kouchoukos NT, Sundt III TM. Mechanical properties of dilated human ascending aorta. *Annals of biomedical engineering.* 2002;30:624-635.

88. Pichamuthu JE, Phillippi JA, Cleary DA, Chew DW, Hempel J, Vorp DA, et al. Differential tensile strength and collagen composition in ascending aortic aneurysms by aortic valve phenotype. *The Annals of thoracic surgery.* 2013;96:2147-2154.

89. Khanafer K, Duprey A, Zainal M, Schlicht M, Williams D, Berguer R. Determination of the elastic modulus of ascending thoracic aortic aneurysm at different ranges of pressure using uniaxial tensile testing. *The Journal of thoracic and cardiovascular surgery.* 2011;142:682-686.

90. Okamoto RJ, Xu H, Kouchoukos NT, Moon MR, Sundt TM. The influence of mechanical properties on wall stress and distensibility of the dilated ascending aorta. *The Journal of thoracic and cardiovascular surgery.* 2003;126:842-850.

91. Iliopoulos DC, Kritharis EP, Giagini AT, Papadodima SA, Sokolis DP. Ascending thoracic aortic aneurysms are associated with compositional remodeling and vessel stiffening but not weakening in age-matched subjects. *The Journal of thoracic and cardiovascular surgery.* 2009;137:101-109.

92. Matsumoto T, Fukui T, Tanaka T, Ikuta N, Ohashi T, Kumagai K, et al. Biaxial Tensile Properties of Thoracic Aortic Aneurysm Tissues. *Journal of Biomechanical Science and Engineering.* 2009;4:518-529.

93. Pham T, Martin C, Elefteriades J, Sun W. Biomechanical characterization of ascending aortic aneurysm with concomitant bicuspid aortic valve and bovine aortic arch. *Acta biomaterialia.* 2013;9:7927-7936.

94. Chung J, Lachapelle K, Wener E, Cartier R, De Varennes B, Fraser R, et al. Energy loss, a novel biomechanical parameter, correlates with aortic aneurysm size and histopathologic findings. *The Journal of thoracic and cardiovascular surgery.* 2014;148:1082-1088; discussion 1088-1089.

95. Iliopoulos DC, Deveja RP, Kritharis EP, Perrea D, Sionis GD, Toutouzas K, et al. Regional and directional variations in the mechanical properties of ascending thoracic aortic aneurysms. *Medical engineering & physics.* 2009;31:1-9.

96. Della Corte A, De Santo LS, Montagnani S, Quarto C, Romano G, Amarelli C, et al. Spatial patterns of matrix protein expression in dilated ascending aorta with aortic regurgitation: congenital bicuspid valve versus Marfan's syndrome. *The Journal of heart valve disease.* 2006;15:20-27; discussion 27.

97. Tremblay D, Leask RL. Remodelling and pathology development associated with aneurysmal ascending aortic tissues. *The Canadian Journal of Chemical Engineering.* 2011;89:13-22.

98. Azadani AN, Chitsaz S, Matthews PB, Jaussaud N, Leung J, Tsinman T, et al. Comparison of mechanical properties of human ascending aorta and aortic sinuses. *The Annals of thoracic surgery.* 2012;93:87-94.

99. Li WC, Yu MH, Zhang HM, Wang HQ, Xi GM, Yao BC, et al. Biomechanical properties of ascending aorta and pulmonary trunk in pigs and humans. *Xenotransplantation.* 2008;15:384-389.

100. Chung J, Lachapelle K, Wener E, Cartier R, De Varennes B, Fraser R, et al. Energy loss, a novel biomechanical parameter, correlates with aortic aneurysm size and histopathologic findings. *The Journal of thoracic and cardiovascular surgery.* 2014;148:1082-1089.

101. Vorp DA, Schiro BJ, Ehrlich MP, Juvonen TS, Ergin MA, Griffith BP. Effect of aneurysm on the tensile strength and biomechanical behavior of the ascending thoracic aorta. *The Annals of thoracic surgery.* 2003;75:1210-1214.

102. Tremblay D, Zigras T, Cartier R, Leduc L, Butany J, Mongrain R, et al. A comparison of mechanical properties of materials used in aortic arch reconstruction. *The Annals of thoracic surgery.* 2009;88:1484-1491.

103. Pichamuthu JE, Phillippi JA, Cleary DA, Chew DW, Hempel J, Vorp DA, et al. Differential tensile strength and collagen composition in ascending aortic aneurysms by aortic valve phenotype. *The Annals of thoracic surgery.* 2013;96:2147-2154.

104. Pasta S, Phillippi JA, Gleason TG, Vorp DA. Effect of aneurysm on the mechanical dissection properties of the human ascending thoracic aorta. *The Journal of thoracic and cardiovascular surgery.* 2012;143:460-467.

105. Edwards WD, Leaf DS, Edwards JE. Dissecting aortic aneurysm associated with congenital bicuspid aortic valve. *Circulation.* 1978;57:1022-1025.

106. Edwards JE. Manifestations of acquired and congenital diseases of the aorta. *Current problems in cardiology.* 1979;3:1-62.

107. Beller CJ, Labrosse MR, Thubrikar MJ, Robicsek F. Role of aortic root motion in the pathogenesis of aortic dissection. *Circulation.* 2004;109:763-769.

108. Thubrikar MJ, Agali P, Robicsek F. Wall stress as a possible mechanism for the development of transverse intimal tears in aortic dissections. *Journal of medical engineering & technology.* 1999;23:127-134.

109. O'Rourke MF, Staessen JA, Vlachopoulos C, Duprez D, Plante GE. Clinical applications of arterial stiffness; definitions and reference values. *American journal of hypertension.* 2002;15:426-444.

110. Hoit BD. Strain and strain rate echocardiography and coronary artery disease. *Circulation. Cardiovascular imaging.* 2011;4:179-190.

111. Krishnan K, Ge L, Haraldsson H, Hope MD, Saloner DA, Guccione JM, et al. Ascending thoracic aortic aneurysm wall stress analysis using patient-specific finite element modeling of in vivo magnetic resonance imagingdagger. *Interactive cardiovascular and thoracic surgery.* 2015.

112. Schaefer BM, Lewin MB, Stout KK, Gill E, Prueitt A, Byers PH, et al. The bicuspid aortic valve: an integrated phenotypic classification of leaflet morphology and aortic root shape. *Heart.* 2008;94:1634-1638.

113. Thanassoulis G, Yip JW, Filion K, Jamorski M, Webb G, Siu SC, et al. Retrospective study to identify predictors of the presence and rapid progression of aortic dilatation in patients with bicuspid aortic valves. *Nature clinical practice. Cardiovascular medicine.* 2008;5:821-828.

114. den Reijer PM, Sallee D, 3rd, van der Velden P, Zaaijer ER, Parks WJ, Ramamurthy S, et al. Hemodynamic predictors of aortic dilatation in bicuspid aortic valve by velocity-encoded cardiovascular magnetic resonance. *Journal of cardiovascular magnetic resonance : official journal of the Society for Cardiovascular Magnetic Resonance.* 2010;12:4.

115. Bissell MM, Hess AT, Biasiolli L, Glaze SJ, Loudon M, Pitcher A, et al. Aortic dilation in bicuspid aortic valve disease: flow pattern is a major contributor and differs with valve fusion type. *Circulation. Cardiovascular imaging.* 2013;6:499-507.

116. Della Corte A, Bancone C, Conti CA, Votta E, Redaelli A, Del Viscovo L, et al. Restricted cusp motion in right-left type of bicuspid aortic valves: a new risk marker for aortopathy. *The Journal of thoracic and cardiovascular surgery.* 2012;144:360-369, 369.e361.

117. Hope MD, Hope TA, Crook SE, Ordovas KG, Urbania TH, Alley MT, et al. 4D flow CMR in assessment of valve-related ascending aortic disease. *JACC. Cardiovascular imaging.* 2011;4:781-787.

118. Mahadevia R, Barker AJ, Schnell S, Entezari P, Kansal P, Fedak PW, et al. Bicuspid aortic cusp fusion morphology alters aortic three-dimensional outflow patterns, wall shear stress, and expression of aortopathy. *Circulation.* 2014;129:673-682.

119. Dick M, Jonak P, Leask RL. Statin therapy influences endothelial cell morphology and F-actin cytoskeleton structure when exposed to static and laminar shear stress conditions. *Life sciences.* 2013;92:859-865.

120. Habashi JP, Doyle JJ, Holm TM, Aziz H, Schoenhoff F, Bedja D, et al. Angiotensin II type 2 receptor signaling attenuates aortic aneurysm in mice through ERK antagonism. *Science (New York, N.Y.).* 2011;332:361-365.

121. Choudhury N, Bouchot O, Rouleau L, Tremblay D, Cartier R, Butany J, et al. Local mechanical and structural properties of healthy and diseased human ascending aorta tissue. *Cardiovascular Pathology.* 2009;18:83-91.

122. Iliopoulos DC, Kritharis EP, Giagini AT, Papadodima SA, Sokolis DP. Ascending thoracic aortic aneurysms are associated with compositional remodeling and vessel stiffening but not weakening in age-matched subjects. *The Journal of thoracic and cardiovascular surgery.* 2009;137:101-109.

123. Ng A, Swanevelder J. Resolution in ultrasound imaging. *Continuing Education in Anaesthesia Critical Care & Pain.* 2011;11:186-192.

124. Aldrich JE. Basic physics of ultrasound imaging. *Critical Care Medicine.* 2007;35:S131-S137.

125. Leitman M, Lysyansky P, Sidenko S, Shir V, Peleg E, Binenbaum M, et al. Two-dimensional strain-a novel software for real-time quantitative echocardiographic assessment of myocardial function. *Journal of the American Society of Echocardiography : official publication of the American Society of Echocardiography.* 2004;17:1021-1029.

126. Voigt JU, Pedrizzetti G, Lysyansky P, Marwick TH, Houle H, Baumann R, et al. Definitions for a common standard for 2D speckle tracking echocardiography: consensus document of the EACVI/ASE/Industry Task Force to standardize deformation imaging. *Journal of the American Society of Echocardiography : official publication of the American Society of Echocardiography.* 2015;28:183-193.

127. Mackenzie IS, Wilkinson IB, Cockcroft JR. Assessment of arterial stiffness in clinical practice. *QJM : monthly journal of the Association of Physicians.* 2002;95:67-74.

128. Laurent S, Cockcroft J, Van Bortel L, Boutouyrie P, Giannattasio C, Hayoz D, et al. Expert consensus document on arterial stiffness: methodological issues and clinical applications. *European heart journal.* 2006;27:2588-2605.

129. Pagani M, Mirsky I, Baig H, Manders WT, Kerkhof P, Vatner SF. Effects of age on aortic pressure-diameter and elastic stiffness-stress relationships in unanesthetized sheep. *Circulation research.* 1979;44:420-429.

130. Oishi Y, Miyoshi H, Mizuguchi Y, Iuchi A, Nagase N, Oki T. Aortic stiffness is strikingly increased with age >/= 50 years in clinically normal individuals and preclinical patients with cardiovascular risk factors: assessment by the new technique of 2D strain echocardiography. *Journal of cardiology.* 2011;57:354-359.

131. Karatolios K, Wittek A, Nwe TH, Bihari P, Shelke A, Josef D, et al. Method for aortic wall strain measurement with three-dimensional ultrasound speckle tracking and fitted finite element analysis. *The Annals of thoracic surgery.* 2013;96:1664-1671.

132. Lang RM, Cholley BP, Korcarz C, Marcus RH, Shroff SG. Measurement of regional elastic properties of the human aorta. A new application of transesophageal echocardiography with automated border detection and calibrated subclavian pulse tracings. *Circulation.* 1994;90:1875-1882.

133. Sugioka K, Hozumi T, Sciacca RR, Miyake Y, Titova I, Gaspard G, et al. Impact of Aortic Stiffness on Ischemic Stroke in Elderly Patients. *Stroke.* 2002;33:2077-2081.

134. Nemes A, Forster T, Csanady M, Gruber N. Indices of aortic distensibility and coronary flow velocity reserve in patients with different grades of aortic atherosclerosis. *The international journal of cardiovascular imaging.* 2004;20:271-277.

135. Drozdz J, Krzeminska-Pakuola M, Lipiec P, Orczykowski M, Chrzanowski O, Plewka M, et al. Regional aortic function is correlated with intima-media thickness-insights from three-dimensional echocardiography. *Journal of the American Society of Echocardiography : official publication of the American Society of Echocardiography.* 2005;18:789-794.

136. Petrini J, Jenner J, Rickenlund A, Eriksson P, Franco-Cereceda A, Caidahl K, et al. Elastic properties of the descending aorta in patients with a bicuspid or tricuspid aortic valve and aortic valvular disease. *Journal of the American Society of Echocardiography : official publication of the American Society of Echocardiography.* 2014;27:393-404.

137. Alreshidan M, Shahmansouri N, Chung J, Lash V, Emmott A, Leask RL, et al. Obtaining the biomechanical behavior of ascending aortic aneurysm via the use of novel speckle tracking echocardiography. *The Journal of thoracic and cardiovascular surgery.* 2016:781-788.

138. Hiratzka LF, Bakris GL, Beckman JA, Bersin RM, Carr VF, Casey DE, Jr., et al. 2010 ACCF/AHA/AATS/ACR/ASA/SCA/SCAI/SIR/STS/SVM guidelines for the diagnosis and management of patients with Thoracic Aortic Disease: a report of the American College of Cardiology Foundation/American Heart Association Task Force on Practice Guidelines, American Association for Thoracic Surgery, American College of Radiology, American Stroke Association, Society of Cardiovascular Anesthesiologists, Society for Cardiovascular Angiography and Interventions, Society of Interventional Radiology, Society of Thoracic Surgeons, and Society for Vascular Medicine. *Circulation.* 2010;121:e266-369.

139. Boodhwani M, Andelfinger G, Leipsic J, Lindsay T, McMurtry MS, Therrien J, et al. Canadian Cardiovascular Society position statement on the management of thoracic aortic disease. *The Canadian journal of cardiology.* 2014;30:577-589.

140. Pape LA, Tsai TT, Isselbacher EM, Oh JK, O'Gara P T, Evangelista A, et al. Aortic diameter >or = 5.5 cm is not a good predictor of type A aortic dissection: observations from the International Registry of Acute Aortic Dissection (IRAD). *Circulation.* 2007;116:1120-1127.

141. Emmott A, Garcia J, Chung J, Lachapelle K, El-Hamamsy I, Mongrain R, et al. Biomechanics of the Ascending Thoracic Aorta: A Clinical Perspective on Engineering Data. *The Canadian journal of cardiology.* 2016;32:35-47.

142. Chung J, Lachapelle K, Cartier R, Mongrain R, Leask RL. Loss of mechanical directional dependency of the ascending aorta with severe medial degeneration. *Cardiovascular pathology : the official journal of the Society for Cardiovascular Pathology.* 2017;26:45-50.

143. Carew TE, Vaishnav RN, Patel DJ. Compressibility of the arterial wall. *Circulation research.* 1968;23:61-68.

144. Bell V, Mitchell WA, Sigurethsson S, Westenberg JJ, Gotal JD, Torjesen AA, et al. Longitudinal and circumferential strain of the proximal aorta. *Journal of the American Heart Association.* 2014;3:e001536.

145. Elefteriades JA. Natural history of thoracic aortic aneurysms: indications for surgery, and surgical versus nonsurgical risks. *The Annals of thoracic surgery.* 2002;74:S1877-1880; discussion S1892-1878.

146. Shahmansouri N, Alreshidan M, Emmott A, Lachapelle K, Cartier R, Leask RL, et al. Evaluating ascending aortic aneurysm tissue toughness: Dependence on collagen and elastin contents. *Journal of the mechanical behavior of biomedical materials.* 2016;64:262-271.

147. Emmott A, El-Hamamsy I, Leask RL. Histopathological and biomechanical properties of the aortic wall in 2 patients with chronic type A aortic dissection. *Cardiovascular pathology : the official journal of the Society for Cardiovascular Pathology.* 2017;29:48-52.

148. Gradus-Pizlo I, Bigelow B, Mahomed Y, Sawada SG, Rieger K, Feigenbaum H. Left anterior descending coronary artery wall thickness measured by high-frequency transthoracic and epicardial echocardiography includes adventitia. *Am J Cardiol.* 2003;91:27-32.

149. Gregory AJ, Di Martino E, Fedak PWM. Aortic diameter: The beginning of the end of an era. *The Journal of thoracic and cardiovascular surgery.* 2018;In Press.

150. Trabelsi O, Gutierrez M, Farzaneh S, Duprey A, Avril S. A non-invasive methodology for ATAA rupture risk estimation. *Journal of biomechanics.* 2018;66:119-126.

151. Emmott A, Alzahrani H, Alreishidan M, Therrien J, Leask RL, Lachapelle K. Transesophageal echocardiographic strain imaging predicts aortic biomechanics: Beyond diameter. *The Journal of thoracic and cardiovascular surgery.* 2018;In Press.

152. Moon MC, Greenberg RK, Morales JP, Martin Z, Lu Q, Dowdall JF, et al. Computed tomography-based anatomic characterization of proximal aortic dissection with consideration for endovascular candidacy. *Journal of vascular surgery.* 2011;53:942-949.

153. Azadani AN, Chitsaz S, Matthews PB, Jaussaud N, Leung J, Tsinman T, et al. Comparison of mechanical properties of human ascending aorta and aortic sinuses. *The Annals of thoracic surgery.* 2012;93:87-94.

154. Duprey A, Trabelsi O, Vola M, Favre J-P, Avril S. Biaxial rupture properties of ascending thoracic aortic aneurysms. *Acta biomaterialia.* 2016;42:273-285.

155. Ballyk PD, Walsh C, Butany J, Ojha M. Compliance mismatch may promote graft-artery intimal hyperplasia by altering suture-line stresses. *Journal of biomechanics.* 1998;31:229-237.

156. Richardson PD, Davies MJ, Born GVR. INFLUENCE OF PLAQUE CONFIGURATION AND STRESS DISTRIBUTION ON FISSURING OF CORONARY ATHEROSCLEROTIC PLAQUES. *The Lancet.* 1989;334:941-944.

157. Di Martino ES, Bohra A, Vande Geest JP, Gupta N, Makaroun MS, Vorp DA. Biomechanical properties of ruptured versus electively repaired abdominal aortic aneurysm wall tissue. *Journal of vascular surgery.* 2006;43:570-576; discussion 576.

158. Tsamis A, Phillippi JA, Koch RG, Chan PG, Krawiec JT, D'Amore A, et al. Extracellular matrix fiber microarchitecture is region-specific in bicuspid aortic valve-associated ascending aortopathy. *The Journal of thoracic and cardiovascular surgery.* 2016;151:1718-1728.e1715.

159. Guzzardi DG, Barker AJ, van Ooij P, Malaisrie SC, Puthumana JJ, Belke DD, et al. Valve-Related Hemodynamics Mediate Human Bicuspid Aortopathy: Insights From Wall Shear Stress Mapping. *Journal of the American College of Cardiology.* 2015;66:892-900.

160. Maganti K, Rigolin VH, Sarano ME, Bonow RO. Valvular Heart Disease: Diagnosis and Management. *Mayo Clinic Proceedings.* 2010;85:483-500.

161. Ryan WH, Prince SL, Culica D, Herbert MA. The Ross procedure performed for aortic insufficiency is associated with increased autograft reoperation. *The Annals of thoracic surgery.* 2011;91:64-69; discussion 69-70.

162. Akiyama M, Ohtani H, Sato E, Nagura H, Tabayashi K. Up-regulation of matrix metalloproteinase-2 and membrane-type 1-matrix metalloproteinase were coupled with that of type I procollagen in granulation tissue response after the onset of aortic dissection. *Virchows Archiv : an international journal of pathology.* 2006;448:811-821.

163. Zhang X, Wu D, Choi JC-B, Minard CG, Hou X, Coselli JS, et al. Matrix metalloproteinase levels in chronic thoracic aortic dissection. *The Journal of surgical research.* 2014;189:348-358.

164. Toth M, Fridman R. Assessment of Gelatinases (MMP-2 and MMP-9) by Gelatin Zymography. *Methods in molecular medicine.* 2001;57:10.1385/1381-59259-59136-59251:59163.

165. Yu Q, Stamenkovic I. Cell surface-localized matrix metalloproteinase-9 proteolytically activates TGF-beta and promotes tumor invasion and angiogenesis. *Genes & development.* 2000;14:163-176.

166. Wang M, Zhao D, Spinetti G, Zhang J, Jiang LQ, Pintus G, et al. Matrix metalloproteinase 2 activation of transforming growth factor-beta1 (TGF-beta1) and TGF-beta1-type II receptor signaling within the aged arterial wall. *Arteriosclerosis, thrombosis, and vascular biology.* 2006;26:1503-1509.

167. Shores J, Berger KR, Murphy EA, Pyeritz RE. Progression of aortic dilatation and the benefit of long-term beta-adrenergic blockade in Marfan's syndrome. *The New England journal of medicine.* 1994;330:1335-1341.

168. Sandor GG, Alghamdi MH, Raffin LA, Potts MT, Williams LD, Potts JE, et al. A randomized, double blind pilot study to assess the effects of losartan vs. atenolol on the biophysical properties of the aorta in patients with Marfan and Loeys-Dietz syndromes. *Int J Cardiol.* 2015;179:470-475.

Appendix A: Histopathological and biomechanical properties of the aortic wall in 2 patients with chronic type A aortic dissection

A.1 Preface

This appendix is a published manuscript in Cardiovascular Pathology (2017). Although studies have identified the mechanical and structural changes in the aorta in states of disease (*e.g.*, aneurysm), there is still a paucity of data that directly links pathological vessel remodelling to impaired mechanical function. Chronic aortic dissection is a rare occurrence but serves as a fascinating model of aortic disease. Namely, dissection is a focal phenomenon; therefore, the dissected wall properties can be compared to an adjacent non-dissected region that serves as an internal control.

This article was the first report of its kind that identified the remodelling process in the region of chronic aortic dissection by histology, expression of MMPs (-2 and -9) and the *ex vivo* mechanical properties of the vessel wall. It was found that histological remodelling occurred in the dissected medial wall characterized by an increase in MMP expression and degradation of the elastic tissue structure. Heterogeneous mechanical properties were measured between the dissected and non-dissected regions and corresponded to the local tissue histology. Ultimately, this article serves to further validate that adverse tissue remodelling leads to a mechanically impaired aortic wall. Furthermore, this case study identifies characteristics of

pathological medial remodelling that is uniquely focal, which provides insight in interpreting regional tissue behaviour by echo (Chapter 6).

A.2 Article

Histopathological and biomechanical properties of the aortic wall in 2 patients with chronic type A aortic dissection

Emmott, A.,[a,b] El-Hamamsy, I.,[b,c] Leask, R.L.[a,b]

[a]Department of Chemical Engineering, McGill University, Montreal, Quebec, Canada

[b]Research Centre, Montreal Heart Institute, Université de Montréal, Montreal, Quebec, Canada

[c]Division of Cardiac Surgery, Montreal Heart Institute, Université de Montréal, Canada

Address for Correspondence :

Richard L. Leask, PhD, PEng, Department of Chemical Engineering, McGill University, 3610 University St., Montreal, Quebec H3A 0C5, Tel: 1-514-398-4270, Fax: 1-514-398-6678, E-mail: richard.leask@mcgill.ca

A.3 Abstract

Type A aortic dissection is an acute condition that requires urgent surgical intervention. However, in a subset of patients, aortic dissections go undiagnosed and become chronic, thereby allowing the dissected wall to undergo a distinct remodelling process from that of the surrounding intact wall. Here, we observe the biomechanical and histological changes in the aortic wall of two patients with chronic Type A aortic dissection. Partial or complete disruption of the elastic structure of the medial layer was observed in the dissected wall of both patients; however, aortic stiffness in the region of dissection covaried with a change in collagen content. A ~50% increase in viscous energy loss was observed in the region of dissection of both patients which suggests an impaired elastic recoil and Windkessel function of the proximal aorta. MMP expression (2 and 9) differed between the dissected and intact wall and was distinct between the two patients. Our observations suggest that an active remodelling process occurs in the dissected aortic wall resulting in a vastly different biomechanical behavior.

A.4 Introduction

Thoracic aortic aneurysms (TAAs) are associated with an increased risk of acute aortic events, especially in patients with familial forms of TAAs. Acute type A aortic dissection represents a life-threatening condition requiring emergency surgical intervention to remove the primary intimal entry tear. In a subset of patients, the dissection goes unnoticed and becomes chronic. Though there is a growing understanding of the pathology and mechanical properties of aneurysmal aortic walls [37, 141], little is known about the characteristics of chronically dissected aortic walls. Moreover, although a few studies have reported the expression of matrix metalloproteinases (MMPs) in cases of chronic aortic dissection [162, 163], no study has reported the disparate mechanical properties of the chronically-dissected wall. Herein, we present two cases of patients with familial TAA who presented with a chronic dissection of the proximal thoracic aorta. Independent of surgical correction of the dissection, both cases qualified for aortic resection based on a diameter criterion of ≥5.5 cm [138]. For each case, tissue samples from the intact aneurysmal wall and the chronically dissected wall were harvested and analyzed for both histological and biomechanical properties.

A.5 Case Description and Findings

Case 1: A 35 year-old male with no known medical history presented for routine screening because of a family history of TAA and dissection. Echocardiographic examination showed a tricuspid aortic valve (TAV) and an 8 cm aortic root with ascending aortic aneurysm. He successfully underwent aortic valve-sparing surgery and had an uneventful postoperative course. At the time of surgery, a large chronic dissection (Stanford Type A) located posteriorly, distal to the sinotubular junction, was discovered and tissue samples from both

the chronically dissected aortic wall and the intact aneurysmal wall were obtained and analyzed.

Case 2: A 37 year-old male with Marfan syndrome who had previously been lost to follow-up, was referred for surgical management of an aortic root and ascending aortic aneurysm. CT and Echocardiographic examination showed a bicuspid aortic valve (BAV) and an 8.0 cm aortic root with concomitant ascending aortic aneurysm and dissection (Stanford Type A) located on the anterior wall, distal to the sinotubular junction (**Figure A.S.1**). The absence of pericardial or pleural effusion reflect the chronic state of the aneurysm, which was further confirmed on surgical examination. The patient underwent an aortic valve-sparing operation with replacement of the ascending aorta and hemiarch. The postoperative course was uneventful and the patient was discharged home on day 6.

Histopathological Characteristics and MMP Expression

Histological analysis of the non-dissected aneurysmal aortic tissues (**Figure A.1-A&C**) revealed an intact wall structure, containing continuous intimal and medial layers. Within the media, a mostly contiguous network of elastic fibers and smooth muscle cells (SMCs) was evident with some elastic fiber fragmentation and collapsed lamellae. Some mucopolysaccharide deposition on the medial side of the internal elastic lamina was also evident. Case 2 had less SMCs and more collagen than Case 1. In contrast, the dissected aortic wall presented with either partial (Case 1) or total depletion (Case 2) of the elastic structure of the tissue (**Figure A.1-B&D**). Increased collagen staining was observed in the regions of elastic fibre disruption in Case 1 (**Figure A.1-B**) with considerable

mucopolysaccharide deposition in Case 2 (**Figure A.1-D**). For comparison, aortic tissue obtained from a non-aneurysmal transplant donor was stained with Movat's pentachrome which revealed full intact elastic lamellae (**Figure A.S.2-A**)

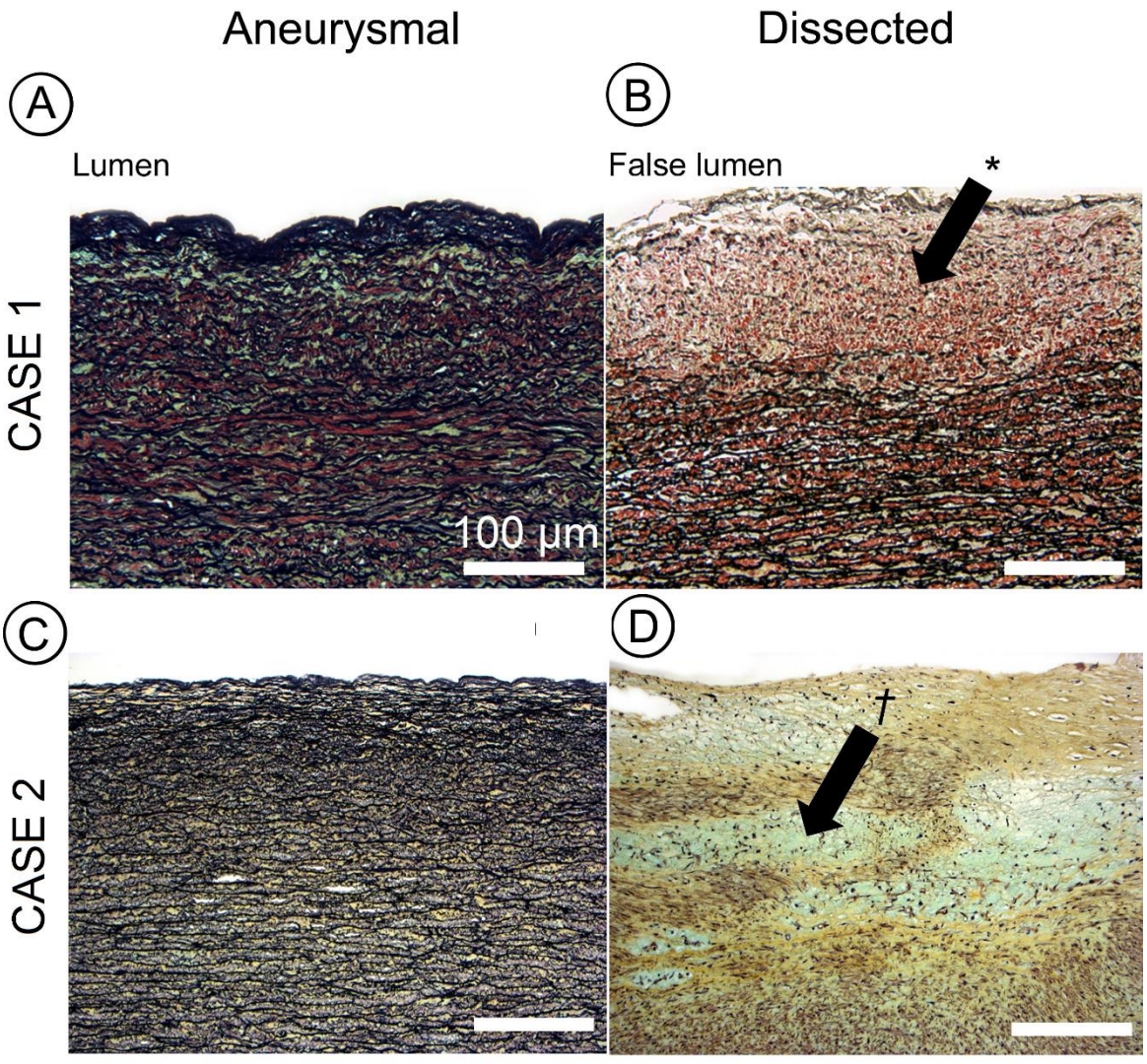

Figure A.1. Ascending aortic tissue composition and structure in 2 cases of chronic dissection using Movat pentachrome staining shows: A&C) undisrupted elastic lamellae (black fibres) with alternating layers of SMCs (red) in the non-dissected regions of the

aneurysms in Case 1 and 2 respectively but, B&D) a disrupted matrix on the luminal side of the dissected region in Case 1 and 2, respectively. *Disrupted elastic fibres; †Increased mucopolysaccharide deposition. Scale bar is 100 μm.

Gelatin zymography of homogenized whole-tissue lysate of the tunica media revealed a differential pattern of expression between the two cases (**Figure A.2**). Using the method and reagents described by Toth & Fridman [164], 5 μg lystate per well were run on a 0.1% gelatin (w/v) SDS-PAGE gel and incubated for 18 hrs at 37°C, followed by Coomassie staining. For Case 1, there was a stark increase in both latent and mature MMP-9 while MMP-2 decreased in the region of dissection. While, for Case 2, no MMP-9 was detected in the tissue and an increase in latent MMP-2 was observed in the region of dissection (no mature band was detected). Aortic tissue was processed and analyzed by zymography for the aforementioned transplant donor (**Figure A.S.2-B**).

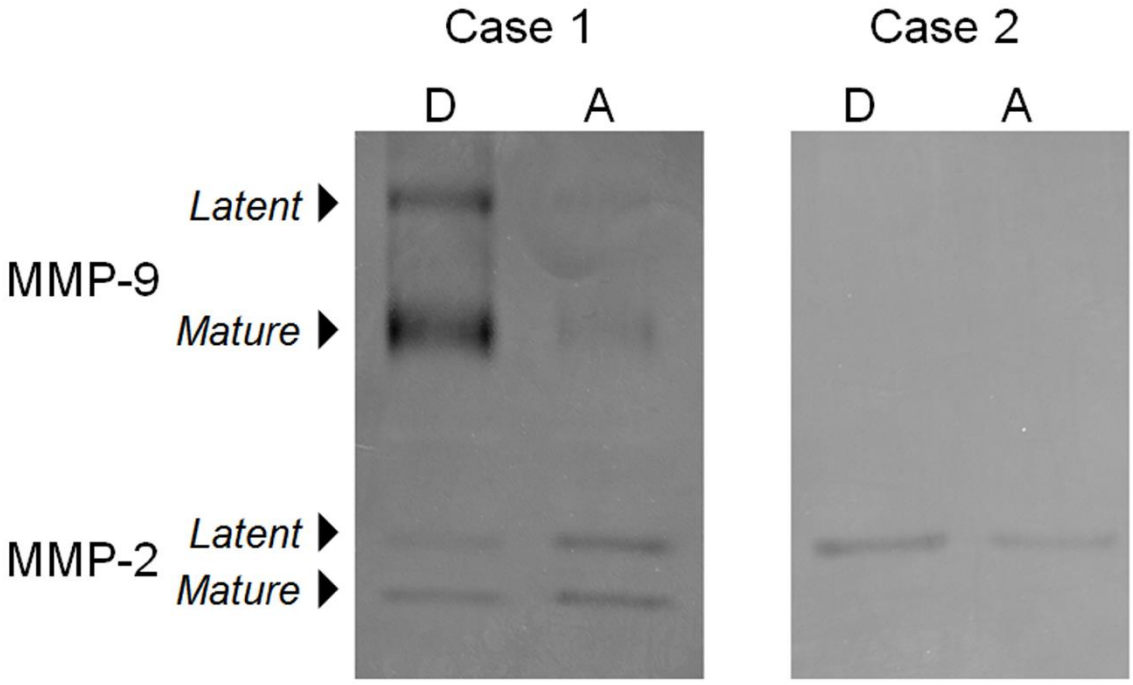

Figure A.2. MMP-2 and -9 expression by gelatin zymography in 2 cases of chronic dissection. Images are inverted to show dark bands corresponding to MMP activity. All lanes contained 5 μg/well of tissue lysate as determined by a bicinchoninic assay. D-dissected aneurysmal wall; A-aneurysmal wall.

Biomechanical Properties

From the excised aortic tissues, 1.5x1.5cm^2 samples were obtained from the aneurysmal and dissected regions of the tissue (**Figure A.3-A&B)** and then stretched bi-axially (**Figure A.3-C)** to determine aortic stiffness and viscous energy loss. For both cases, 5 *ex vivo* thickness measurements per region were taken with a constant force digital micrometer (Mitutoyo Litematic VL-50A, Mitutoyo, Japan), and the values are expressed as the MEAN±STDEV. For Case 1, the mean thickness of the aneurysmal wall was larger than that of the dissected

wall (2.17±0.25mm versus 1.82±0.25mm, respectively). However, for Case 2, the mean thickness of the intact aneurysmal wall was smaller than that of the dissected wall (2.36±0.13mm versus 3.00±0.40mm, respectively). The mechanical properties of the tissues were determined by equibiaxial testing (EnduraTEC ELF 3200, Bose, MN) and the stress-strain relation (**Figure A.3-D**) was analyzed to determine aortic stiffness by incremental modulus of elasticity (*i.e.*, the slope of the stress-strain curve at a defined strain) and viscous energy loss, where an increase in the latter may suggest an impaired Windkessel function due to a loss of elastic recoil energy [94]. Notably, the tissue specimens used for biomechanical testing contained no intraluminal thrombus.

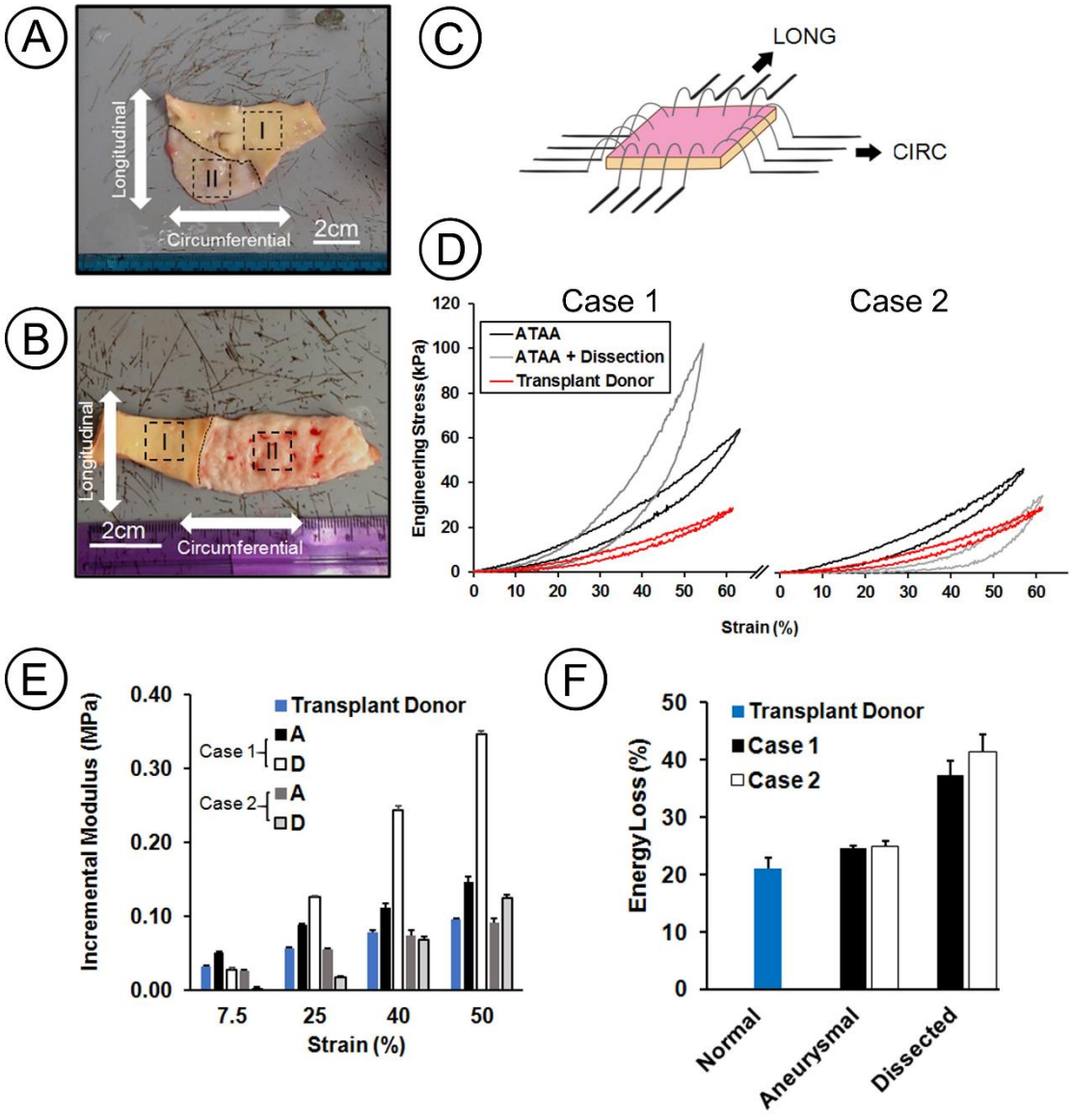

Figure A.3. *Ex vivo* mechanical testing of the resected aneurysm. A&B) Image of the resected aneurysms containing dissections: I) non-dissected aneurysmal testing region and II) chronically dissected testing region for Case 1 and 2, respectively. C) A graphic of the biaxial testing orientation. D) The resultant stress-strain relation in the circumferential axis for both the non-dissected and dissected regions. E) Incremental modulus (i.e., stiffness) at 7.5, 25, 40 and 50% strain in the circumferential direction. F) Regional viscous energy loss

(average of the circumferential and longitudinal axes) is increased in the region of dissection. Error bars are SEM from 3 stretching cycles. A-aneurysm; D-dissected aneurysm.

For Case 1, biomechanical analysis revealed marked tissue stiffening between physiological and supra-physiological strain values (25-50%) in the dissected region when compared to the aneurysmal tissue (**Figure A.3-E**). However, at sub-physiological strain (7.5%) there was greater tissue compliance (lower incremental modulus of elasticity) in the region of dissection compared to the intact aorta. In Case 2, the region of dissection was less stiff than the parent aneurysm at all reported strains below 50%. Finally, for each case, viscous energy loss (averaged for both axes) was increased by approximately 50% in the dissected tissue over the aneurysmal tissue, while the latter is similar in magnitude to the energy loss of non-pathological transplant donor tissue (**Figure A.3-F**).

A.6 Discussion

These cases document the histological and biomechanical properties of aortic wall remodelling following aneurysmal dilatation and chronic dissection. To our knowledge, this is the first report examining the biomechanical properties of chronically dissected ascending aortas with local comparisons of histology and MMP expression. Our findings suggest that intimal disruption followed by chronic medial remodelling results in regional tissue changes compared to the aneurysmal aorta. Altered MMP expression, which may serve to degrade matrix proteins or activate latent TGF-β [165, 166], a potent cytokine that can alter SMC function, suggests an altered state of reorganization of the aortic wall in the region of chronic dissection. With only two cases it is difficult to conclude any global trends from our MMP

data, however, the results do agree with the pattern reported by Lemaire *et al.*, who implicated MMP-9 in tissue remodelling associated in patients with degenerative aneurysm with TAV (*e.g.*, Case 1) while MMP-2 was implicated in aortic wall remodelling associated with BAV (*e.g.*, Case 2) [73].

Indeed, increased collagen deposition in the media, along with increased elastin fragmentation, and SMC disarray, result in increased tissue stiffness at higher strain levels, **Figure 3**. This was confirmed with Masson's trichrome staining of 7 μm sections (not shown) which revealed a ~55% increase (Case 1) and ~10% decrease (Case 2) in medial collagens in the regions of dissection when compared to the intact aneurysm (**Figure A.S.3**). This change in collagen content co-varied with stiffness between regions.

Increased wall stiffness has been associated with higher risk of aortic rupture [141], suggesting that the chronically dissected aortic wall represents the most vulnerable portion of the aorta. Indeed, regional variations in wall stiffness can result in a concentration of stress, thereby creating a potential area of focal weakness at the interface between these boundaries [155]. Furthermore, the observed increase in energy loss in the regions of dissection covaries with elastic fibre fragmentation and a disorganized tissue structure which may impair the healthy elastic recoil function of the aorta. In Case 2, the significant mucopolysaccharide deposition, which is associated with high water content, most likely contributes to this viscous behaviour.

The only partial depletion of elastic fibres in the dissected aortic media and increased MMP expression (both latent and mature) in Case 1 may indicate that this patient was operated

closer to the time of initial intimal tear. However, with different underlying pathologies unique to each of the 2 patients, no formal conclusion in the time between dissection and surgery can be drawn. Furthermore, prior to surgery, both patients took a beta-blocker to control blood pressure (Case 1: 50 mg/day Metoprolol; Case 2: 100 mg/day Labetolol). Beta-blockers have been reported to decrease the rate of aortic dilation in patients with MFS [167] and may have a modest influence on the biomechanical properties of the aorta [168].

In conclusion, these cases illustrate the chronic changes that occur in the aortic wall following an acute type A aortic dissection. Whether these changes represent an acute tissue remodelling or more chronic pathological adaptation remains to be determined through additional studies of aortic tissues.

A.7 Supplementary Materials

The following appeared as supplementary material made available with the published article:

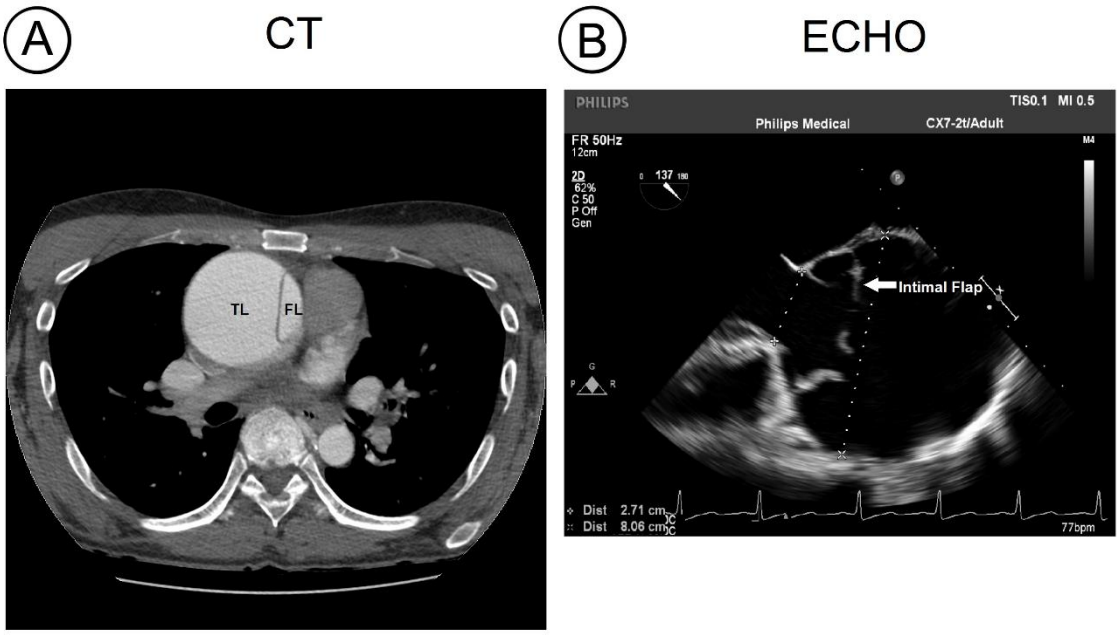

Figure A.S.1. Pre-operative imaging of the aortic root/dissection for Case 2: A) Short-axis CT image of the aortic root containing the dissection (TL-True Lumen; FL-False Lumen). B) Long-axis echo image of the aortic root and ascending aorta containing the intimal flap. Note: no suitable pre-operative images of the dissection were available for Case 1.

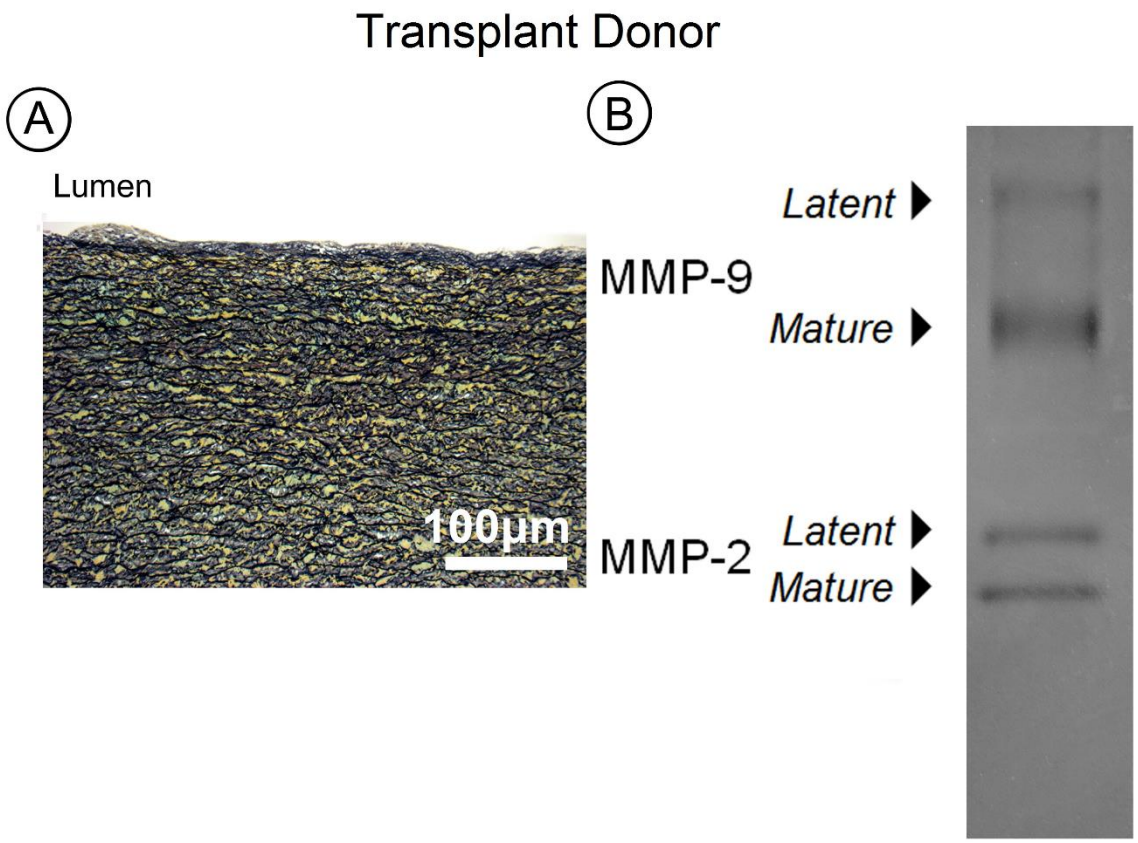

Figure A.S.2. Transplant donor A) tissue histology by Movat pentochrome and B) MMP expression by gelatin zymography. Scale bar is 100µm.

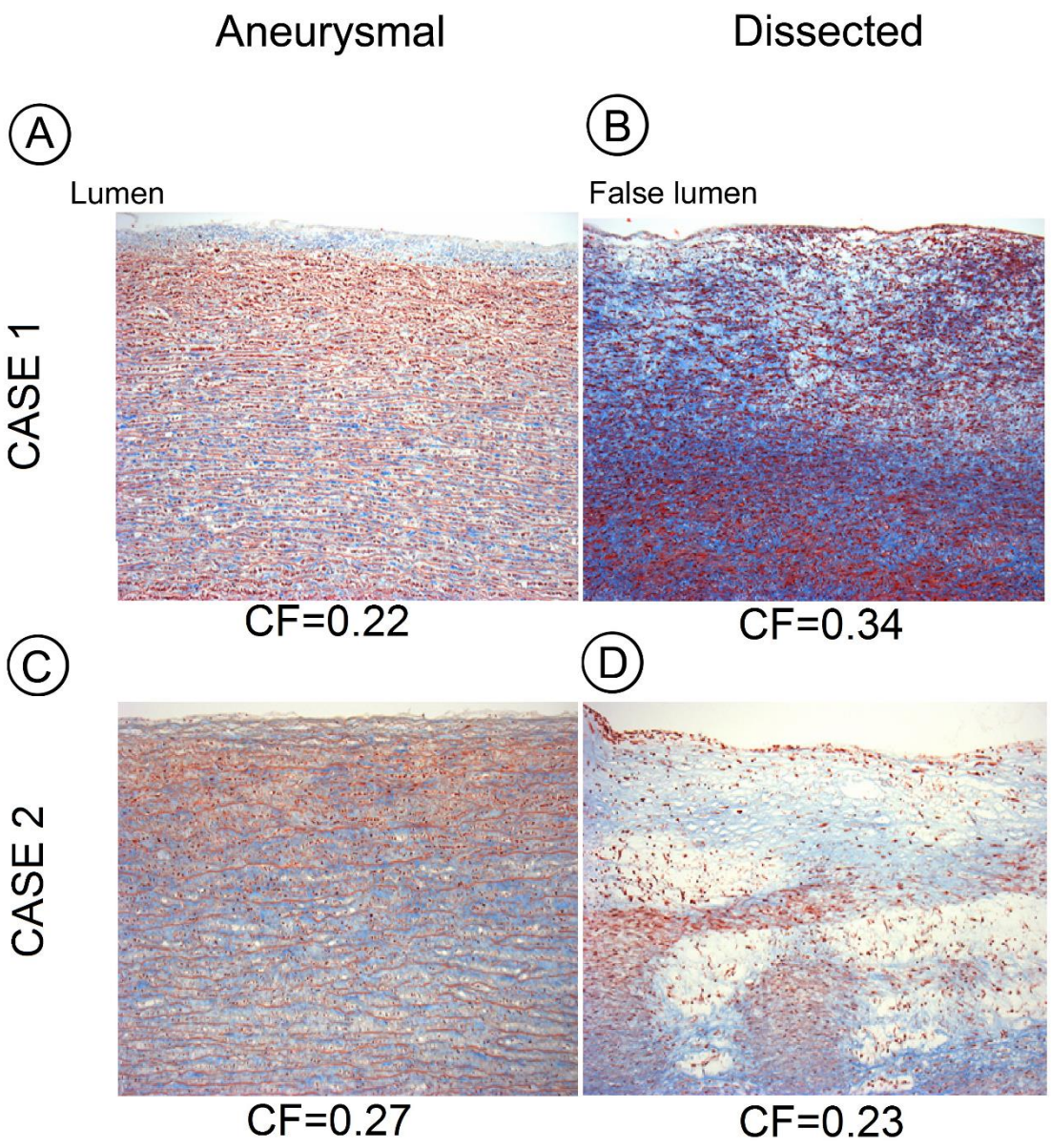

Figure A.S.3. Ascending aortic collagen quantification in 2 cases of chronic dissection using Masson's trichrome staining. Collagens are stained in blue and their relative fraction occupying the field of view was quantified using ImageJ™. Case 1 – aneurysm (A) and dissected aneurysm (B); Case 2 – aneurysm (C) and dissected aneurysm (D). CF=collagen fraction of field-of-view by ImageJ™.

Appendix B: Supplemental Figures

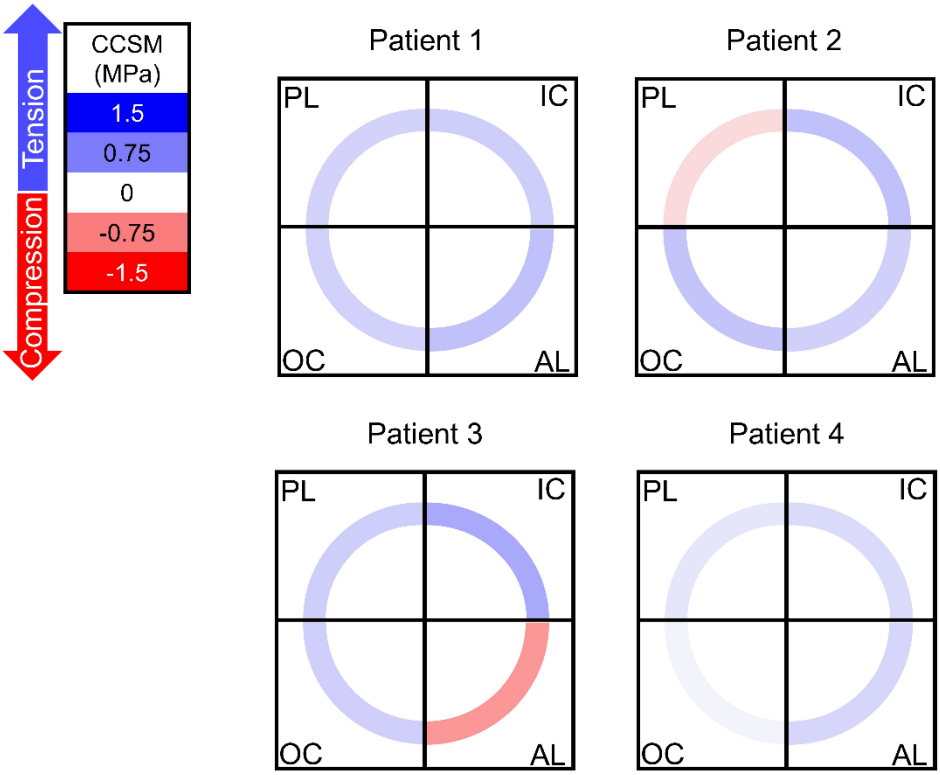

Figure B.1-A. Regional CCSM heat diagrams, Patients 1-4. IC – inner curvature; AL – anterolateral wall; OC – outer curvature; PL – posterolateral wall.

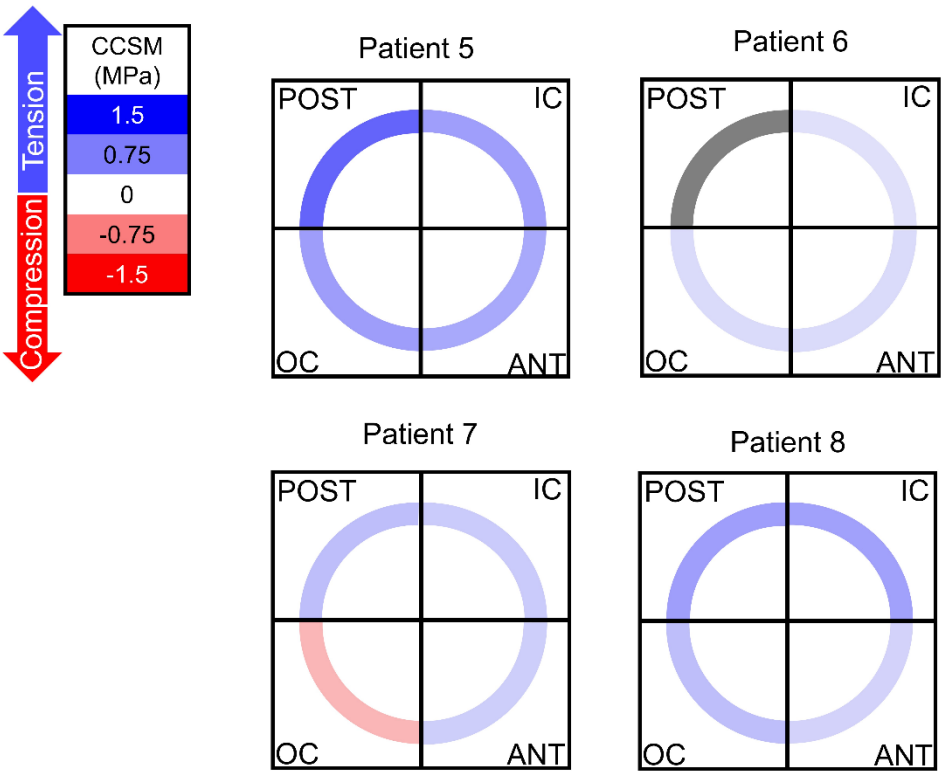

Figure B.1-B. Regional CCSM heat diagrams, Patients 5-8. IC – inner curvature; AL – anterolateral wall; OC – outer curvature; PL – posterolateral wall.

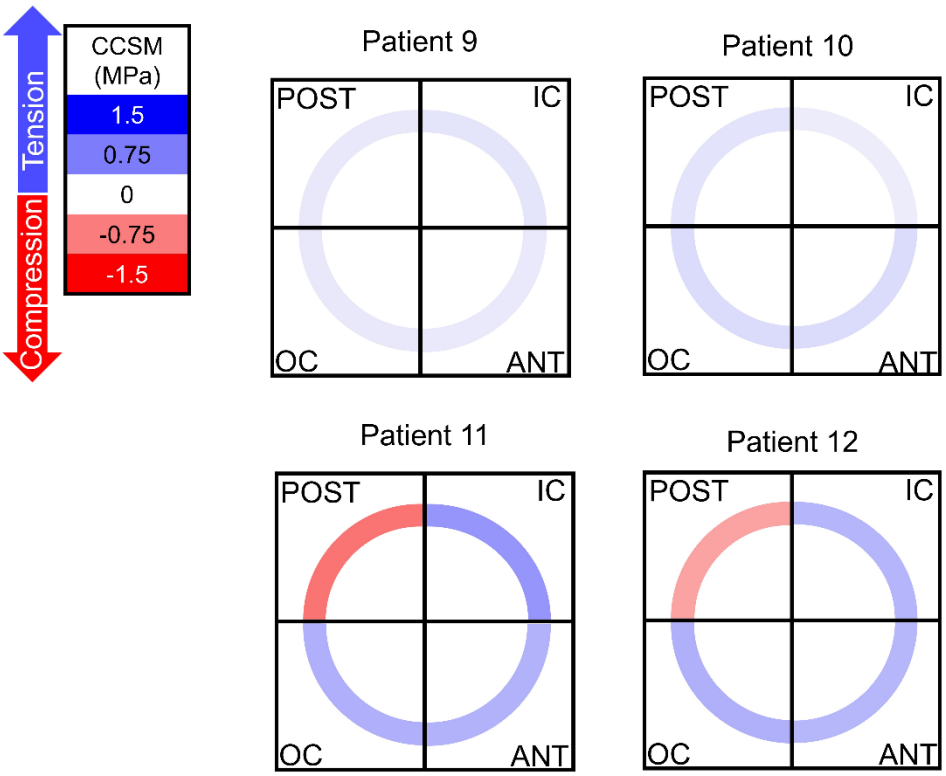

Figure B.1-C. Regional CCSM heat diagrams, Patients 9-12. IC – inner curvature; AL – anterolateral wall; OC – outer curvature; PL – posterolateral wall.

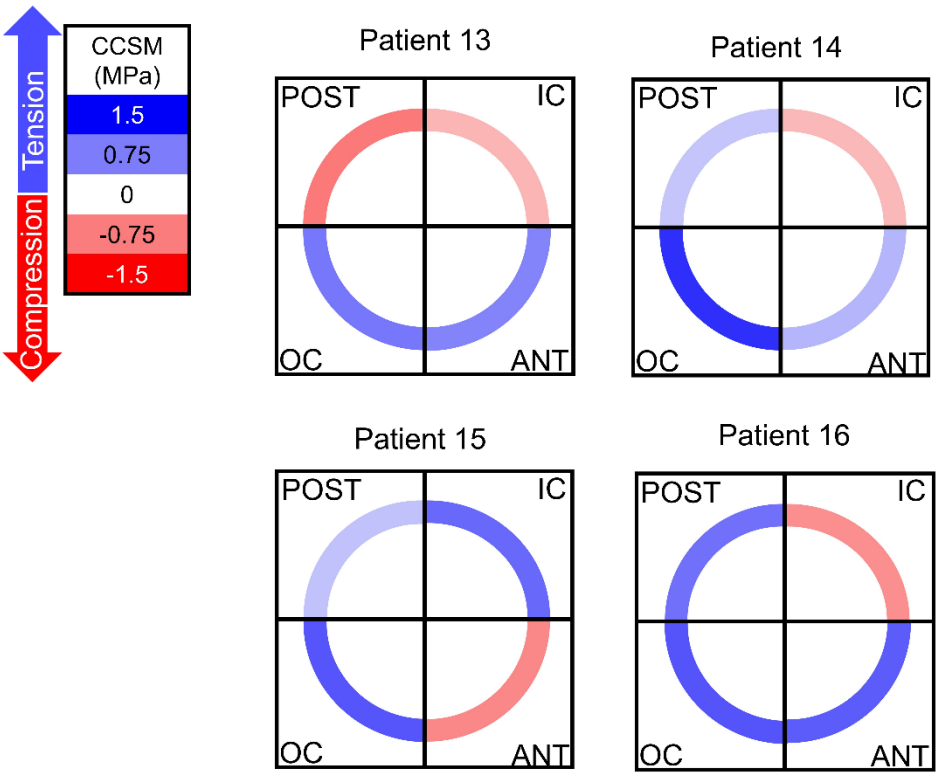

Figure B.1-D. Regional CCSM heat diagrams, Patients 13-16. IC – inner curvature; AL – anterolateral wall; OC – outer curvature; PL – posterolateral wall.

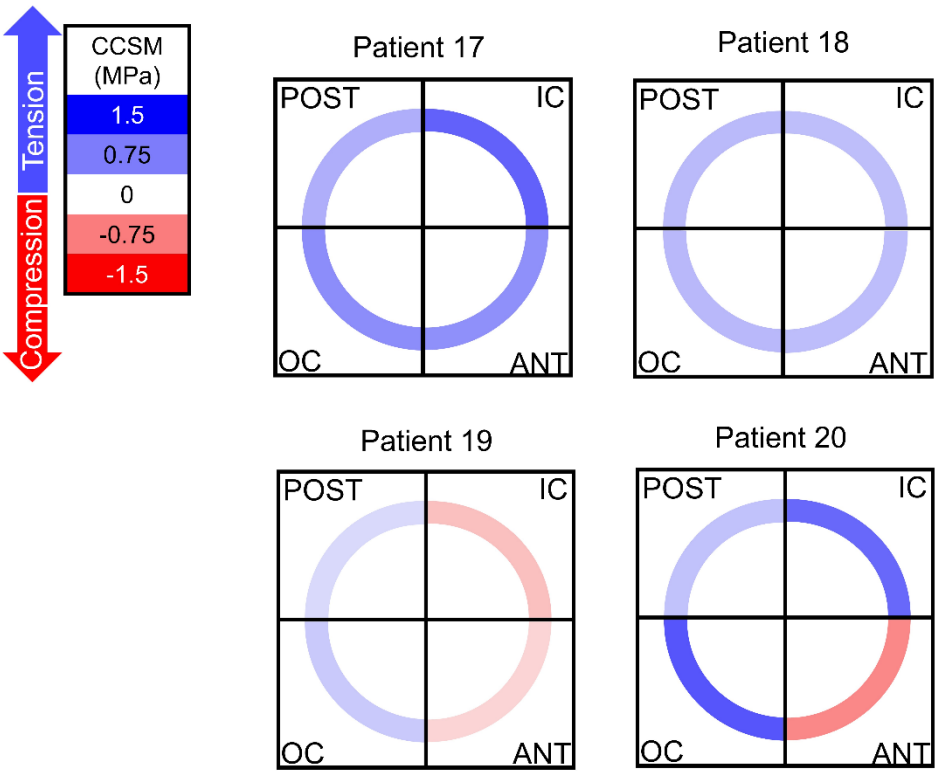

Figure B.1-E. Regional CCSM heat diagrams, Patients 17-20. IC – inner curvature; AL – anterolateral wall; OC – outer curvature; PL – posterolateral wall.

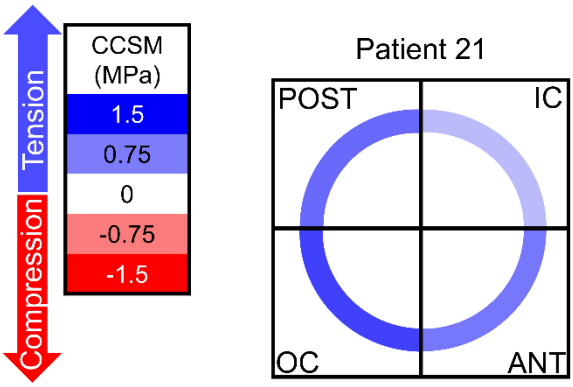

Figure B.1-F. Regional CCSM heat diagrams, Patient 21. IC – inner curvature; AL – anterolateral wall; OC – outer curvature; PL – posterolateral wall.

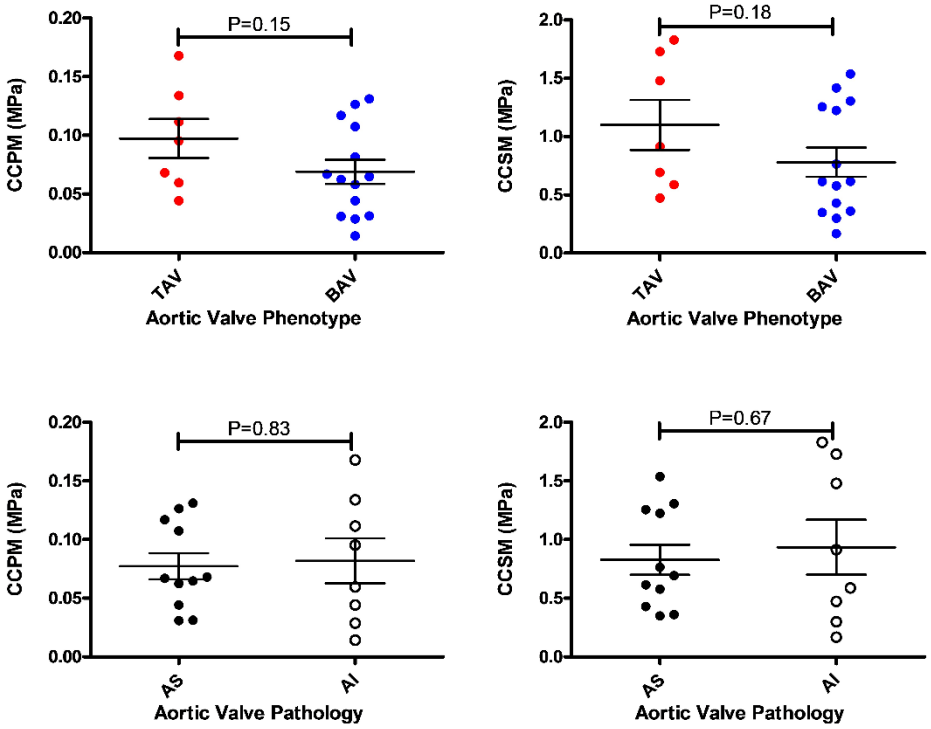

Figure B.2. CCPM and CCSM by aortic valve morphology (BAV/TAV) and aortic valve pathology (AS/AI). TAV (red) – tricuspid aortic valve; BAV (blue) – bicuspid aortic valve; AS (solid black) – aortic stenosis; AI (black outline) – aortic insufficiency.

Appendix C: Ethics Approval Forms

McGill

Faculty of Medicine
3655 Promenade Sir William Osler #633
Montreal, QC H3G 1Y6

Faculté de médecine
3655, Promenade Sir William Osler #633
Montréal, QC H3G 1Y6

Fax/Télécopieur: (514) 398-3870
Tél/Tel: (514) 398-3124

June 13, 2017

Dr. Richard Leask
Department of Chemical Engineering
M. H. Wong Building
3610 University Street
Montreal, QC H3A 2B2

RE: **IRB Study Number A06-M62-04B**
Aneurysms of the ascending aorta: linking hemodynamics to local tissue stiffness, structure and biochemistry

Dear Dr. Leask,

Thank you for submitting an application for Continuing Review for the above-referenced study.

The study progress report was reviewed and full Board re-approval was provided on June 12, 2017. The ethics certification renewal is valid until **June 15, 2018.**

The Investigator is reminded of the requirement to report all IRB approved protocol and consent form modifications to the Research Ethics Offices (REOs) for the participating hospital sites. Please contact the individual hospital REOs for instructions on how to proceed. Research funds may be withheld and / or the study's data may be revoked for failing to comply with this requirement.

Should any modification or unanticipated development occur prior to the next review, please notify the IRB promptly.

Regards,

Roberta Palmour, PhD
Chair
Institutional Review Board

cc: A06-M62-04B

McGill Faculty of Medicine

Institutional Review Board
- CONTINUING REVIEW FORM -

The completed form is to be submitted electronically to submit2irb.med@mcgill.ca. The continuing review form must be received at least **one (1) month** before the expiration of the last ethics approval. If you require additional information, please visit the IRB website at: http://www.mcgill.ca/medresearch/ethics/ or by calling 514-398-3124.

Principal Investigator	Richard L. Leask
Faculty and Department	Chemical Engineering
Study Coordinator, if applicable	
Address:	3610 University St. Dept. Chemical Engineering, McGill, H3A 0C5
E-mail	richard.leask@mcgill.ca Telephone: x4270
Study Title	Geometric and biomechaical data for Modelling of LVOT and Proximal coroanry Arteries
Grant title, if different from study title.	1) Bicuspic aortic valve aortopathy: linking eccentric flow with tissue remodelling (H&S) 2) Thoracic aortic aneurysms and dissections (TAAD): Mechanobiology, Surgical Aortic
IRB Study Number	A06-M62-04B Date of last approval 06/17/2016
Has there been a change or addition to the financial support for this study?	○ YES ◉ NO
If yes, please specify the changes/additions.	

Status of the Protocol

- ☑ Active enrolment
- ☐ Recruitment complete
- ☐ Recruitment on hold
- ☑ Data analysis
- ☐ Secondary Analysis only
- ☐ Inactive/dormant**

When did this study begin?

RECEIVED
McGill University
MAY 3 - 2017
FACULTY OF MEDECINE
IRB

**If the study is inactive/ dormant (i.e., there are no participants enrolled in the study and no study activity is occurring), please specify the reason:

If the study is is actively enrolling participants, or if enrolment is complete, please answer the following questions:

Study sample size:	300
Total number enrolled in the study:	240

Number of participants that have completed this study: 240

Total number of participants withdrawn: 0

Projected date of completion of study enrolment: 05/30/2019

Projected date of study completion: 05/30/2021

Please provide a brief description of what has occurred since the IRB's last ethics approval.

Has the study revealed any new findings or knowledge relevant to the potential benefits and/or study risks that may influence participants' willingness to continue in the study? ○ YES ◉ NO ○ N/A

Has this new information been communicated to participants? ○ YES ○ NO ◉ N/A

If applicable, please describe the findings.

Has an amendment(s) to the protocol been submitted to the IRB in the past year? ○ YES ◉ NO

What is the version date of the most recent IRB- approved protocol?

Has the consent form(s) been revised in the past year? ○ YES ◉ NO ○ N/A

Have consent form modifications been reported to the IRB? ○ YES ○ NO ◉ N/A

Version date/s of the most recently approved consent form(s): January 29, 2103: MUHC-Royal Victoria Hospital

Have any adverse events occurred since the last approval? ○ YES ◉ NO ○ N/A

If yes, how many at McGill sites? 0

DATE OF I.R.B. APPROVAL
JUN 12 2017
Faculty of Medicine
McGill University

Have the adverse events been reported to the IRB? If no, submit all adverse events with this form. ○ YES ○ NO ◉ N/A

Have there been any publications? ◉ YES ○ NO

If yes, append list: Chung J, Lachapelle K, Wener E, Cartier R, De VB, Obtaining the biomechanical behavior of ascending

SIGNATURES

Principal Investigator: Richard L. Leask — Date: 04/4/17

IRB Chair: Roberta Palmour — Date: June 12, 2017